UNIVERSITA' CATTOLICA DEL SACRO CUORE
PIACENZA

Scuola di Dottorato per il Sistema Agro-alimentare

Doctoral School on the Agro-Food System

cycle XXII

S.S.D: BIO/04

Molecular biology of anthocyanin production in plants

Candidate: **GIORGIA CARLETTI**
Matr. n.: 3580175

Academic Year 2008/2009

UNIVERSITA' CATTOLICA DEL SACRO CUORE
PIACENZA

Scuola di Dottorato per il Sistema Agro-alimentare

Doctoral School on the Agro-Food System

cycle XXII

S.S.D: BIO/04

Molecular biology of anthocyanin production in plants

Candidate: GIORGIA CARLETTI
Matr. n.: 3580175

Coordinator: Ch.mo Prof. Gianfranco PIVA

Tutor: Prof. Adriano Marocco

Academic Year 2008/2009

TABLE OF CONTENT

1. ANTHOCYANINS OVERVIEW

Anthocyanins (from Greek: anthos = flower + kyanos = blue) are secondary metabolites produced in plants. They are water-soluble vacuolar pigments that may appear red, purple or blue according to pH. The base pigments are the anthocyanidins which are then glycosylated to form the anthocyanins (Figure 1). In all types of anthocyanins, except for one report of *C*-glycosylation (Saito *et al.*, 2003), only *O*-glycosylation occurs for anthocyanins in plants.

The core of the anthocyanidin is a 15-carbon (C_{15}) structure of two aromatic rings (the A and B rings) joined to a third ring of C_3O_1. Anthocyanidins have two double bonds in the C-ring and hence carry a positive charge (Figure 1).

The core anthocyanidin structure is modified by the addition of wide range of chemical groups, in particular through hydroxylation, acylation, methylation. Most frequently in nature they are glycosides of cyanidin, delphinidin, malvidin, pelargonidin, peonidin and petunidin.

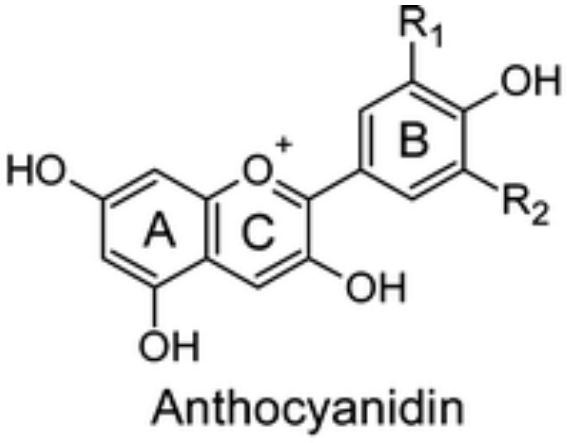

Figure 1. Anthocyanins are glucosides of anthocyanidins, the basic chemical structure of which is shown here.

They are the basis for all pink, red, orange, scarlet, purple, blue and blue-black flower colours.

In fruits, the colourful skins also attract the attention of animals, which may eat the fruits and disperse the seeds (Gould and Lister, 2006).

The anthocyanin biosynthetic pathway is regulated in response to a range of environmental, spatial and developmental/temporal signals. The most evident environmental regulation in flowers is the production of anthocyanins during flower opening, usually to attract pollinators coincident with flower fertility. In some species there is a direct linkage between attainment of fertility and induction of the biosynthetic genes (Weiss, 2000). Anthocyanin biosynthesis may be regulated by both abiotic and biotic environmental stimuli. Light is the principal environmental signal and it is required for full floral colouration in many species (Meng and Wang, 2004). Anthocyanins occur in all tissues of higher plants, including leaves, stems, roots, flowers, and fruits. In these parts they are found predominantly in outer cell layers such as the epidermis and peripheral mesophyll cells.

Anthocyanin biosynthesis

Anthocyanins belong to a parent class of flavonoids synthesized via the phenylpropanoid pathway (Figure 2). The basic skeleton of all flavonoids consists of three aromatic rings and is generated by the enzymes chalcone synthase (CHS) and chalcone isomerase (CHI).

Oxidation of the central ring by flavonoid 3-hydroxylase (F3H) yields a dihydroflavonol (dihydrokaempferol), which can be hydroxylated on the 3□ or 5□ position of the B-ring by flavonoid 3□-hydroxylase (F3□H) and/or flavonoid 3□5□hydroxylase (F3□5□H) yielding precursors of orange (pelargonidin), red–magenta (cyanidin) and purple–mauve (delphinidin) anthocyanin pigments. Some plant species (e.g. rose and carnation) cannot make purple colours because they lack F3□5□H and/or F3□H.

Dihydroflavonols are converted by dihydroflavonol reductase (DFR), leucoanthocyanidin oxidase (LDOX) and a 3-glucosyl transferase (3GT) to yield an anthocyanin 3-glucoside that can be further substituted by 5-glucosyl- (5GTs), rhamnosyl- (RTs), acyl- (ATs) and/or methyltransferases (MTs), resulting in

'decorated' anthocyanins with different colors. Transport of the end product to the vacuole requires a glutathione *S*-transferase (GST) and a specific transporter localized in the vacuolar membrane. Proanthocyanidin (PA) synthesis starts in some species with the reduction of leucoanthocyanidin by a leucoanthocyanidin reductase (LAR).

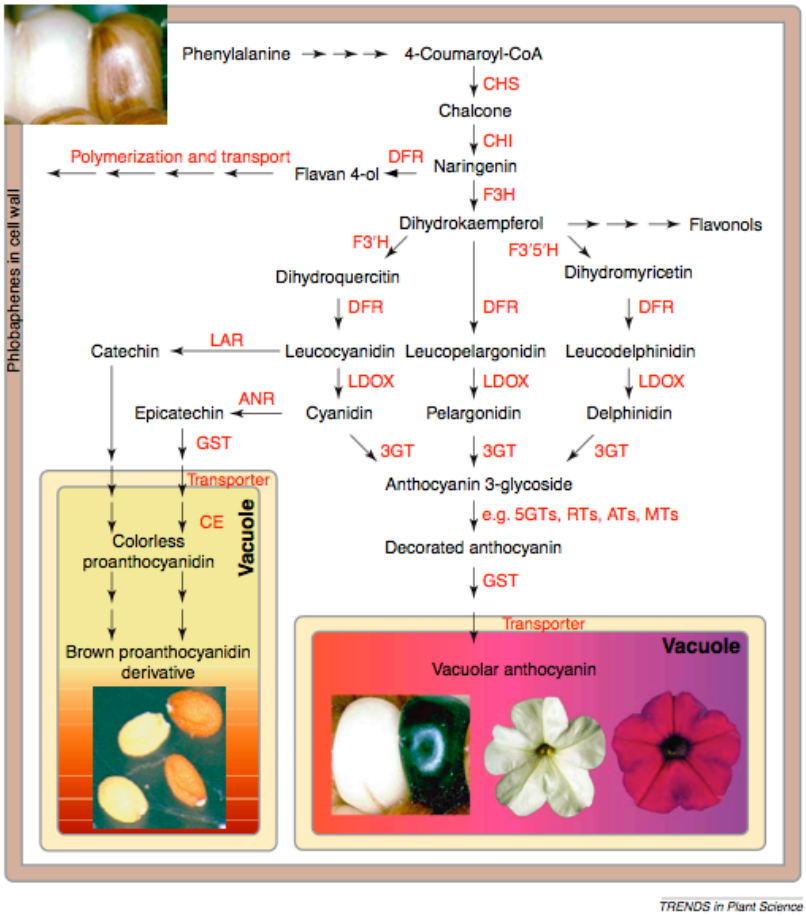

Figure 2. Biosynthesis of flavonoid pigments.

The anthocyanin biosynthetic pathway is well defined at the genetic and enzymatic level with gene sequences available for all the key biosynthetic steps to the primary anthocyanins and also for many of second modification activities.

In plants, anthocyanins are part of the flavonoid biosynthetic pathway, which is one of the most intensively studied (Winkel-Shirley, 2001; Figure 2). As a result, most of the structural genes as well as a number of regulatory genes have now been characterized (Winkel-Shirley, 2001; Broun, 2005), but little is known about the molecular mechanisms involved in the downstream steps of the pathway, including flavonoid accumulation into the vacuole.

Anthocyanin localization and transport

In the cell, anthocyanins are synthesized at the cytosolic surface of the endoplasmic reticulum (ER) by a multienzyme complex, although the association of anthocyanin enzymes with the ER membrane has not been fully established (Saslowsky and Winkel-Shirley, 2001). With regard to transport from the cytoplasmic surface of the ER to the vacuole, Grotewold and Davies (2008) suggested two models, a vesicular transport (VT) model and a ligandin transporter (LT) model. The VT model may be a direct trafficking route from the ER to the vacuole involving vesicle-like structures filled with anthocyanins.

Recently, in Arabidopsis (*Arabidopsis thaliana*) seedlings, anthocyanins were shown to be sequestered in cytoplasmic structures that resemble ER-derived vesicle-like structures (Poustka *et al*., 2007). In *Lisianthus* petals and maize (*Zea mays*) cell suspension, anthocyanins were accumulated as vesicle-like bodies in the cytoplasm, suggesting a transport under this form to the vacuole (Grotewold *et al*., 1998; Zhang *et al*., 2006), although the presence of membranes around such structures remains to be determined. The LT model appears to involve ligandins that bind and escort anthocyanins from the biosynthesis site to the tonoplast, where they are supposed to enter the vacuole through tonoplast transporters.

Why anthocyanins are important?

A lot of research projects focus on study of anthocyanin production and their role in plant, animal and human health.

- **Anthocyanin role in plants**

Anthocyanins play important structural roles in plants, as well as in defence against a variety of biotic and abiotic stresses. Research over the last decade has demonstrated that a wide range of environmental factors that predispose plants to oxidative stress, such as high light, UV radiation, low temperatures, ozone and pathogens, induce the synthesis of phenolic metabolites with antioxidant properties.

Higher plants are naturally exposed to high fluxes of solar radiation and therefore they are subjected to relatively high UV-doses (Caldwell and Flint, 1997). UV-B is the band of lowest wavelength and highest energy that penetrates the ozone layer of the stratosphere. In spite of the relatively low irradiance, UV-B radiation (315-280 nm) could induce severe damage to plants via direct and indirect effects on nucleic acids, proteins and cell membranes (Schmitz-Eiberger and Noga, 2001).

To cope with environmental UV-irradiation conditions, higher plants have evolved a number of protective mechanisms. The accumulation of phenolic compounds that selectively absorb UV radiation in the plant cuticle and epidermis (Krauss *et al.*, 1997) probably represents the most cost-effective strategy for long-term adaptation in the case of regular and prolonged exposure to elevated doses of solar radiation, including its UV-B component (Liakoura *et al.*, 2003). The most common and active antioxidant compounds naturally occurring in foods are flavonoids, possessing activity in both the hydrophilic and lipophilic systems.

They have the ability to act as antioxidants by a free radical scavenging mechanism (Hanasaki *et al.*, 1994) with the formation of less reactive flavonoid phenoxyl radicals (Eq. 1 and Eq. 2); on the other hand, through their known ability to chelate transition metals (Van Acker *et al.*, 1996) these compounds may inactivate iron ions through complexation, thereby suppressing the superoxide-driven Fenton Reaction (Eq. 3 and Eq. 4), which is currently believed to be the most important route to active oxygen species (Afanas'ev *et al.*, 1989).

Eq. 1 $ROO\cdot + Fl\text{-}OH \rightarrow ROOH + Fl\text{-}O\cdot$

Eq. 2 $HO\cdot + Fl\text{-}OH \rightarrow H_2O + Fl\text{-}O\cdot$

Eq. 3 $O_2\cdot^- + Fe(III) \rightarrow O_2 + Fe(II)$

Eq. 4 $Fe(II) + H_2O_2 \rightarrow Fe(III) + HO\cdot + HO^-$

The antioxidant ability of flavonoids resides mainly in their ability to donate hydrogen atoms and thereby scavenge the free radicals. They have been shown to act as a "sunscreen", protecting cells from high-light damage by absorbing blue-green and UV light, thereby protecting the tissues from photoinhibition, or high-light stress reducing the amount of light reaching the cloroplast. This has been shown to occur in

red juvenile leaves, autumn leaves, and broad-leaved evergreen leaves that turn red during the winter (Merzlyak *et al.*, 2008). It has also been proposed that red coloration of leaves may camouflage leaves from herbivores blind to red wavelengths, or signal unpalatability, since anthocyanin synthesis often coincides with synthesis of unpalatable phenolic compounds.

- **Anthocyanin role in animal and human health**

Anthocyanidins and their derivatives, many found in common foods, protect against a variety of oxidants through a number of mechanisms.

They may provide protection from DNA cleavage, estrogenic activity (altering development of hormone-dependent disease symptoms), enzyme inhibition, boosting production of cytokines (thus regulating immune responses), anti-inflammatory activity, lipid peroxidation, decreasing capillary permeability and fragility and membrane strengthening (Acquaviva *et al.,* 2003). For example, red cabbage anthocyanins protect animals against oxidative stress from the toxin paraquat (Igarashi *et al.*, 2000).

Cyanidins, found in most fruit sources of anthocyanins, have been found to function as a potent antioxidant *in vivo* (Tsuda, 2000). In other animal studies, cyanidins protected cell membrane lipids from oxidation by a variety of harmful substances (Tsuda, 1998). Additional animal studies confirm that cyanidin is four times more powerful an antioxidant than vitamin E (Rice-Evans CA, 1995).

The most remarkable aspect of their activities may be their ability to act as either antioxidants or prooxidants in some biological environments. The anti-inflammatory and chemopreventive properties of dietary phenolics are generally believed to be related to their antioxidant properties. The prooxidant action of phenolics may be an important mechanism for their anticancer and apoptosis-inducing properties (Hadi *et al.*, 2000).

The anti-inflammatory and chemopreventive properties of dietary phenolics are generally believed to be related to their antioxidant properties (Elisia and Kitts, 2008). Dietary phenolics were also shown to cause oxidative strand breakage in DNA in the presence of transition metal ions such as copper (Hadi *et al.,* 2007), generate substantial amounts of H_2O_2 in the commonly used media (Lee *et al.,* 2005), and

subsequently exerted antiproliferative effects on cancer cells. Their beneficial effects on health continues to increase, particularly regarding their role in reducing cardiovascular disease risk (Mink *et al.,* 2007), cancer (Rossi *et al.,* 2007) and obesity (Tsuda *et al.,* 2003).

The roles of anthocyanin pigments as medicinal agents have been well-accepted and these pigments are linked to an amazingly broad-based range of health benefits. For example, anthocyanins from *Hibiscus* sp. have historically been used in remedies for liver disfunction and hypertension; and bilberry (*Vaccinium*) anthocyanins have an anecdotal history of use for vision disorders, microbial infections, diarrhea, and diverse other health disorders (Smith *et al.,* 2000). But while the use of anthocyanins for therapeutic purposes has long been supported by both anecdotal and epidemiological evidence, it is only in recent years that some of the specific, measurable pharmacological properties of isolated anthocyanin pigments have been conclusively verified by rigorously controlled *in vitro*, *in vivo*, or clinical research trials (Tsuda *et al.*, 2003). In many other cases, the exact roles of the anthocyanins in human health maintenance versus other phytochemicals in a complex mixture from a fruit extract or whole food have not been completely sorted out. In fact, some reports suggest that anthocyanin activity is potentiated when delivered in mixtures (Hou *et al*., 2004).

For example, visual acuity can be markedly improved through administration of anthocyanin pigments to animal and human subjects, and the role of these pigments in enhancing night vision or overall vision has been particularly well documented (Matsumoto *et al.,* 2001). Oral intake of anthocyanosides from black currants resulted in significantly improved night vision adaptation in human subjects (Nakaishi *et al.,* 2000) and similar benefits were gained after administration of anthocyanins from bilberries (Muth *et al.,* 2000).

Three anthocyanins from black currant stimulated regeneration of rhodopsin (a G-protein-coupled receptor localized in the retina of the eye), and formation of a regeneration intermediate was accelerated by cyanidin 3-rutinoside (Matsumoto *et al.,* 2000). Hou *et al*. in 2004, revealed that anthocyanins inhibit tumorigenesis by blocking activation of a mitogen-activated protein kinase pathway.

Acquaviva R., Russo A., Galvano F., Barcellona M.L., Li Volti G., Vanella A., 2003. Cyanidin and cyanidin 3-O-beta-D-glucoside as DNA cleavage protectors and antioxidants. Cell Biol Toxicol. 19(4):243–252.

Broun P., 2005. Transcriptional control of flavonoid biosynthesis: a complex network of conserved regulators involved in multiple aspects of differentiation in Arabidopsis. Curr Opin Plant Biol. 8:272–279.

Caldwell M.M. and Flint S.D., 1997. Uses of biological spectral weighting functions and the need for scaling for the ozone reduction problem. Plant Ecology. 128:66-76.

Elisia I. and Kitts D.D., 2008. Anthocyanins inhibit peroxyl radical-induced apoptosis in Caco-2 cells. Mol Cell Biochem. 312:139–145.

Gould K.S. and Lister C., 2006. Flavonoid functions in plants. In: Ø.M. Andersen and K.R. Markham, Editors, Flavonoids: Chemistry, Biochemistry, and Applications, CRC Press, Boca Raton, FL: 397–441.

Grotewold E. and Davies K., 2008. Trafficking and sequestration of anthocyanins. Nat Prod Commun. 3:1251–1258.

Hadi S.M., Asad S.F., Singh S., Ahmad A., 2000. Putative mechanism for anticancer and apoptosis-inducing properties of plant-derived polyphenolic compounds. IUBMB Life. 50:167–171.

Hadi S.M., Bhat S.H., Azmi A.S., Hanif S., Shamim U. Ullah M.F., 2007. Oxidative breakage of cellular DNA by plant polyphenols: a putative mechanism for anticancer properties. Semin. Cancer Biol. 17:370–376.

Hanasaki Y., Ogawar S., Fukui S., 1994. The correlation between active oxygen scavenging and antioxidative effects of flavonoids. Free Radical Biology and Medicine. 16:845–850.

Hou D.X., Kai K., Li J.J., Lin S., Terahara N., Wakamatsu M., Fujii M., Young M.R., Colburn N., 2004. Anthocyanidins inhibit activator protein 1 activity and cell transformation: structure-activity relationship and molecular mechanisms. Carcinogenesis. 25(1):29–36.

Igarashi K., Kimura Y., Takenaka A., 2000. Preventive effects of dietary cabbage acylated anthocyanins on paraquat-induced oxidative stress in rats. Biosci Biotechnol Biochem. 64(8):1600-7.

Lee K.W., Hur H.J., Lee H.J., Lee C.Y., 2005. Antiproliferative effects of dietary phenolic substances and hydrogen peroxide. J Agr Food Chem. 53:1990–1995.

Kong J.M., Chia L.S., Goh N.K., Chia T.F., Brouillard R., 2003. Analysis and biological activities of anthocyanins. Phytochemistry. 64(5):923–33.

Krauss P., Markstädter C., Riederer M., 1997. Attenuation of UV radiation by plant cuticles from woody species. Plant Cell Environ. 20:1079–1085.

Liakouraa V., Bornmanb J.F., Karabourniotisa G., 2003. The ability of abaxial and adaxial epidermis of sun and shade leaves to attenuate UV-A and UV-B radiation in relation to the UV absorbing capacity of the whole leaf methanolic extracts. Physiol Plant. 117:33-43.

Matsumoto H., Inaba H., Kishi M., Tominaga S., Hirayama M., Tsuda T., 2001. Orally administered delphinidin 3-rutinoside and cyanidin 3-rutinoside are directly absorbed in rats and humans and appear in the blood as the intact forms. J Agric Food Chem. 49(3):1546–1551.

Matsumoto H., Nakamura Y., Tachibanaki S., Kawamura S., Hirayama M., 2003. Stimulatory effect of cyanidin 3-glycosides on the regeneration of rhodopsin. J Agric Food Chem. 51(12):3560–3563.

Meng X. and Wang X., 2004. Regulation of flower development and anthocyanin accumulation in Gerbera hybrida. J Hort Sci Biotech. 79:131–137.

Merzlyak M.N., Chivkunova O.B., Solovchenko A.E., Naqvi K.R., 2008. Light absorption by anthocyanins in juvenile, stressed, and senescing leaves. J Exp Bot. 59(14):3903-11.

Mink P. J., Scrafford C.G., Barraj L.M., Harnack L., Hong C.P., Nettleton J.A., Jacobs D.R., 2007. Flavonoid intake and cardiovascular disease mortality: A prospective study in postmenopausal women. Am J Clin Nutr. 85:895–909.

Muth E.R., Laurent J., Jasper P., 2000. The effect of bilberry nutritional supplementation on night visual acuity and contrast sensitivity. Altern Med Rev. 5(2):164–173.

Nakaishi H., Matsumoto H., Tominaga S., Hirayama M., 2000. Effects of black currant anthocyanoside intake on dark adaptation and VDT work-induced transient refractive alteration in healthy humans. Altern Med Rev. 5(6):553–562.

Poustka F., Irani N.G., Feller A., Lu Y., Pourcel L., Frame K., Grotewold E., 2007. A trafficking pathway for anthocyanins overlaps with the endoplasmic reticulum-to-vacuole protein-sorting route in Arabidopsis and contributes to the formation of vacuolar inclusions. Plant Physiol. 145:1323–1335.

Rice-Evans C.A., 1995. The relative antioxidant activities of plant-derived polyphenolic flavonoids. Free Radical Res. 22(4):3785-93.

Rossi M., Garavello W. Talamini R. Negri E., Bosetti C., Dal Maso L., Lagiou P., Tavani A., Polesel J., Barzan L., Ramazzotti V., Franceschi S., La Vecchia C., 2007. Flavonoids and the risk of oral and pharyngeal cancer: A case-control study from Italy. Cancer Epidemiol Biomarkers Prev. 16:1621–1625.

Saslowsky D. and Winkel-Shirley B., 2001. Localization of flavonoid enzymes in Arabidopsis roots. Plant J. 27:37–48.

Schmitz-Eiberger M. and Noga G., 2001. UV-B radiation-Influence on the antioxidative defense system in Phaseolus vulgaris leaves. J Applied Botany. 75:210-215.

Smith M., Marley K., Seigler D., Singletary K., Meline B., 2000. Bioactive properties of wild blueberry fruits. J Food Sci. 65:352–356.

Tsuda T., 2000. The role of anthocyanins as an antioxidant under oxidative stress in rats. Biofactors. 13(1-4):133-9.

Tsuda T., 1998. Dietary cyanidin 3-0-beta-D-glucoside increases ex vivo oxidative resistance of serum in rats. Lipids. 33(6):583-8.

Tsuda T., Horio F., Uchida K., Aoki H., Osawa T., 2003. Dietary cyanidin 3-O-□-d-glucoside-rich purple corn color prevents obesity and ameliorates hyperglycemia in mice. J Nutr. 133:2125–2130.

Van Acker A.B.E., Van Den Berg D.J., Tromp M.N.J.L., Griffioen D.H., Van Bennekom W.P., W.J.F. Van Der Vijgh, Bast A., 1996. Structural aspects of antioxidant activity of flavonoids. Free Radical Biology and Medicine. 20:331–342.

Wang H., Cao G., Prior R.L., 1997. Oxygen Radical Absorbing Capacity of Anthocyanins. J Agric Food Chem. 45(2):304–309.

Weiss D., 2000. Regulation of flower pigmentation and growth: multiple signaling pathways control anthocyanin synthesis in expanding petals. Physiol Plant. 110:152-157.

Winkel-Shirley B., 2001. Flavonoid biosynthesis: a colorful model for genetics, biochemistry, cell biology, and biotechnology. Plant Physiol. 126:485–493.

Zhang H., Wang L., Deroles S., Bennett R., Davies K., 2006. New insight into the structures and formation of anthocyanic vacuolar inclusions in flower petals. BMC Plant Biol. 6:29.

2. *MEDICAGO TRUNCATULA* AS A MODEL LEGUME PLANT

What is the role of a model plant in legume species?

The Fabaceae (Leguminosae or legumes), with 650 genera and over 16'000 species, are second only to the Poaceae (grasses) in importance to humans as a source of food, feed for livestock, and raw materials for industry (Graham and Vance, 2003). Seeds and shoots of legumes are a rich source of dietary protein, oil, carbohydrates, fiber, minerals, vitamins, and other beneficial secondary compounds for humans and livestock (Wang *et al.*, 2003)

Legumes can be found all over the world; species as soybean in Asia, beans in America and chickpea in the Near East belong to the legume plant family. The Leguminoseae is one of the largest families of flowering plants, which include some of the most important agricultural species such as common bean, soybean, pea, chickpea, broad bean, pigeon pea, cowpea and lentil. Important forage legumes include alfalfa, white and red clover, and various *Lotus* species. Apart from their use as food and feed, legumes are used in soil conservation, phytoremediation, lumber production, as ornamental herbs and bushes, and for extraction of gums, resins or food additives.

Legumes have the capacity to establish mutually beneficial symbioses with soil bacteria (rhizobia) and fungi (mycorrhiza) that provide the plant with nutrients, such as nitrogen and phosphorus, which are scarce in many soils. These attributes, together with the large, nutritious seeds that are produced by many legumes, have secured a major role for legumes in world agriculture. That allows legume plants to be the object of a lot of research initiatives. Genomic research has and will continue to revolutionize plant biology. Some cultivated legumes are tetraploid (e.g. alfalfa and peanut), many have large genomes (e.g. pea and faba beans) and many are recalcitrant to transformation or difficult to regenerate (e.g. common bean, pea and soybean). Most grain legumes have large seeds, relatively few seeds per plant, and large seedlings, which prevents high-density culture (e.g. chickpea, *Vigna*, pea, beans and soybean). Some legumes, such as soybean, have genome duplications and some are self-incompatible or have a long generation time. As a result, two other species,

Medicago truncatula and *Lotus japonicus*, have been adopted internationally as models for legume research (Handberg and Stougaard, 1992).

The adoption of *Arabidopsis thaliana* as a model species has done much to speed the development of plant genomics and to hasten our increased understanding of basic plant biology. However, Arabidopsis is not an "omniscient" model because this plant does not encompass all of the diverse physiological, developmental, and environmental processes seen throughout the plant kingdom. Thus, to study these other processes and to bring the genomic revolution to crop species, additional genomic resources must be developed in other plants.

Over the past several years, this realization has led to the adoption of the model species concept to the study of legumes. Unlike Arabidopsis, legumes develop important and interesting symbioses with atmosphere nitrogen (N)-fixing rhizobia and with mycorrhizal fungi, as explained before. Compared to Arabidopsis, they exhibit interesting differences in secondary metabolism, pod development, and other processes that cannot be adequately modeled with Arabidopsis model system. *Medicago truncatula* (commonly called barrel medic or simply Medicago) emerged as a model plant for legume genomic and functional genomic research (Cook, 1999).

Medicago truncatula: biological characteristics

M. truncatula is closely related to the majority of crop and pasture legumes (Figure 1), its nearest cousin in this respect being alfalfa *(M. sativa)*, one of the most important forage legume in the world (Choi *et al*., 2004b) (Figure 2).

Choi *et al.,* 2004b

Figure 1. Macrosyntheny among six legume genomes. *M. sativa* in blue, *M.truncatula* in red.

Figure 2. Comparative genetic map of *M. truncatula* and *M. sativa*. The relative separation of genetic markers on each linkage group is correlated with genetic distance. (Choi *et al.,* 2004b)

M. truncatula is an annual species considered to be an autogamous (selfing) species. It is described as an "omni-Mediterrannean" species (Lesins and Lesins 1979) even if it has also become naturalized in other regions of the world following European migrations (Barton and Whitlock, 1997).

M. truncatula has been split into three subspecies mainly on the basis of pod characteristics: ssp *truncatula*, ssp *tricycla* and ssp *longeaculata.* Plant morphology and architecture strongly vary between genotypes and are very dependent upon environmental and cultural conditions (Aitken,1955).

In general a *M. truncatula* plant is made up of a main axis that can organize either in a rosette (the leaves are at the level of the neck with very short internodes) or as an elongated axis; and branches of different orders (e.g. primary, secondary, tertiary, branches), as shown in Figure 3

Figure 3. The picture on the left shows the *Medicago truncatula* plant morphology; on the right is reported the picture of an infiorescence. The inflorescences are small, racemes, bearing 1 to 5 yellow flowers that are 5-8 mm long. Flowers contain 10 ovules and only open after the auto pollen has fertilized the ovules. Residual outcrossing is however possible after the flower opens. *M truncatula* flowers possess a so called "tripping mechanism", a floral characteristic shared by the whole *Medicago* genus (Lesins and Lesins 1979).

M. truncatula has been chosen as a model species for genomic studies in view of its small genome (haploid size 500-550Mbp/1C) and diploid (2x8 chromosomes). It has also short seed-to-seed generation time, it produces a large number of seeds on a plant of relatively small stature, making it amenable to high-density culture (Barker *et al.,* 1990). Medicago is composed by selfing species, it is characterized by high level of biodiversity, a number of available cultivars (Prosperi *et al.,* 2001), and high transformation efficiency which makes it suitable for reverse genetics experiments (Crane *et al.,* 2006). Those characteristics make this close relative of alfalfa (*M. sativa*) a good model system (see Figure 1). It is also a model plant for studying mycorrhizal interactions (Liu *et al.,* 1998) and a well characterized nitrogen –fixing symbiont, *Sinorhizobium meliloti* (Galibert *et al*., 2001).

Current status of *M. truncatula* research

Since 1992, when *M. truncatula* has been proposed as model legume plant, numerous genomic and bioinformatics tools have been developed and are being made available to the research community. In this section an overview of the status of genomics, proteomics, metabolomics and bioinformatics research will be summarized.

Genomics

- ✓ *Sequencing project*

The *M. truncatula* sequencing project was initiated in 2003 from Samuel Roberts Noble Foundation to the University of Oklahoma. The National Science Foundation and the European Union's Sixth Framework Programme provided funding to complete sequencing of the remaining euchromatic genespace. Among the eight chromosomes in Medicago, six are being sequenced by NSF project "Sequencing the

Gene Space of the Model Legume, Medicago Truncatula," and two are being sequenced by partners in Europe.

In the *Medicago* Genome Sequence Consortium (MGSC) the efforts to sequencing project had been divided between U.S. and Europe: the Center for Computational Genomics and Bioinformatics (CCGB) at University of Minnesota and THE Advanced Center for Genome Technology (ACGT) at University of Oklahoma for the sequencing of chromosomes 1, 4, 6, 8; The Institute for Genomic Research (TIGR) for chromosomes 2, 7. In Europe, collaborators include John Innes Center coordinating sequencing of chromosome 3 at the Sanger Center, and the Institut National de la Recherche Agronomique et le Centre National de la Recherche Scientifique (INRA-CNRS) coordinating sequencing of chromosome 5 at Genoscope.

Extensive cytogenetic and sequencing data indicate that the *Medicago* genome is organized into distinct and largely uninterrupted gene- rich euchromatic regions (Figure 4). Thus, members of the Medicago Sequencing Consortium have jointly

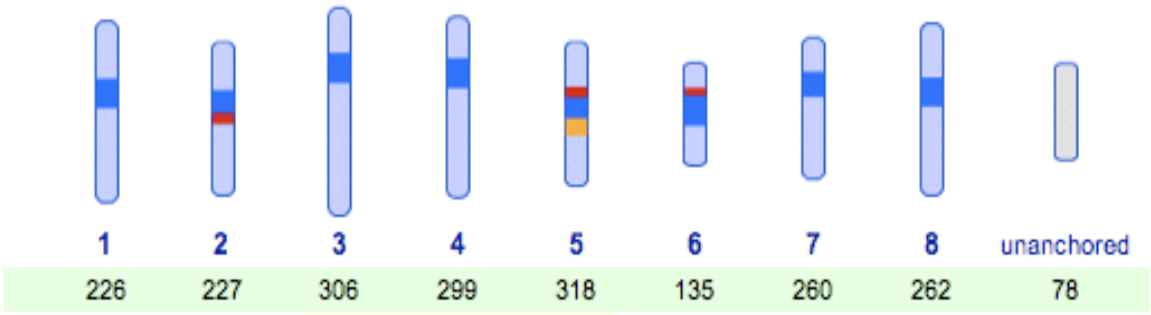

decided that a BAC-by-BAC (Bacterial Artificial Chromosome) approach to Medicago genome sequencing it would have been the best use of resources.
BACs

In making this decision, the Consortium recognized the significant benefit of an anchored BAC-by-BAC approach over shotgun sequencing for comparative genomic analysis with crop legumes.

The Medicago Consortium established that the efforts will be focused on the euchromatic arms of all eight chromosomes. Even before the initiation of the proposed project, 1,000 BACs will be finished or nearing completion at the

Figure 4. Chromosome diagrams show approximate relative sizes as estimated by Kulikova *et al*, 2001. Dark blue regions are condensed, gene-poor heterochromatin. Red: 5S rDNA; orange: 45S rDNA.

University of and a sequencing-ready physical/genetic map is nearing completion by the Sequencing Consortium (Table 1).

Table 1. Estimated Medicago Chromosome Sizes and Sequencing Centers

CHROMOSOME	*CENTER*	*ESTIMATED SIZE*	*PROJECTED BACS*
Chromosome 1	Oklahoma	51 □m / 30 Mbp(a)	156 BACs(b)
Chromosome 2	TIGR	42 □m / 25 Mbp	130 BACs
Chromosome 3	Sanger / JIC	63 □m / 38 Mbp	197 BACs
Chromosome 4	Oklahoma	61 □m / 37 Mbp	192 BACs
Chromosome 5	Genoscope / INRA	39 □m / 23 Mbp	119 BACs
Chromosome 6	Oklahoma	22 □m / 13 Mbp	68 BACs
Chromosome 7	TIGR	43 □m / 26 Mbp	135 BACs
Chromosome 8	Oklahoma	26 □m / 16 Mbp	83 BACs

(a) Size estimates are based on observations of pachytene chromosomes and previous estimates of 600 kbp/□m in euchromatic regions of the *M. truncatula* genome.
(b) BAC projections based on estimated chromosome size, a total euchromatic size of 200 Mbp, an average 100 kbp non-overlapping coverage by each BAC and proportional distribution of previously sequenced BAC clones.

- ✓ *Genetic and physical map*

In 2006 the University of Minnesota developed a genetic map of *M. truncatula* and a physical finger print contigs (FPC-based) map was developed previously at the University of California at Davis (UCD).

The *M. truncatula* Consortium published his experimental approaches to develop Medicago physical map. Medicago FPC-physical map and 150,000 BAC-end sequences (BES) utilize the physical map and BES as a basis to develop a draft sequencing minimum tiling path.

The Consortium extended and joined contigs by identifying additional gap-spanning BACs using overgo primers and hybridization of original BAC libraries, BES-based markers, and long-range PCR with genomic DNA. BAC sequences should be joined into pseudomolecules that run all the way from FISH-characterized telomeric markers to FISH-based markers defining boundaries with pericentromeric regions, characterized by sequence data indicating low gene densities and high

repeat densities. Gaps should consist of scaffolds held together by paired BAC-ends, FPC contigs, or FISH-based estimates of physical gap sizes.

In 2007 the *M. truncatula* Consortium revealed the situation of Medicago genome (Figure 5):

1. Sequence-ready physical map anchored to the genetic and cytogenetic map, consisting of a minimum number of physical contigs — with an ultimate target of ~100 total contigs and covering essentially the entire Medicago genome.
2. Completed sequence of approximately 1,000 BACs, already in-progress, plus 760 new BACs, together constituting the euchromatic regions of 12 chromosome arms.
3. Preliminary, computer-based descriptions for all identifiable genome features (protein coding genes, RNA-coding genes, transposable elements, etc.) throughout the 12 chromosome arms.
4. Uninterrupted sequence assemblies (pseudomolecules) for the euchromatic regions of 12 chromosome arms, and where gaps exist, experimental determination of sequence orientation and gap size.
5. Displays at each of the sequencing center's web sites showing immediate results of sequencing and annotation plus centralized access to BAC sequencing status, map anchoring, BAC-end sequences, gaps and overlaps, overall project statistics, and feature predictions, including Ensembl interface, at the CCGB, University of Minnesota.

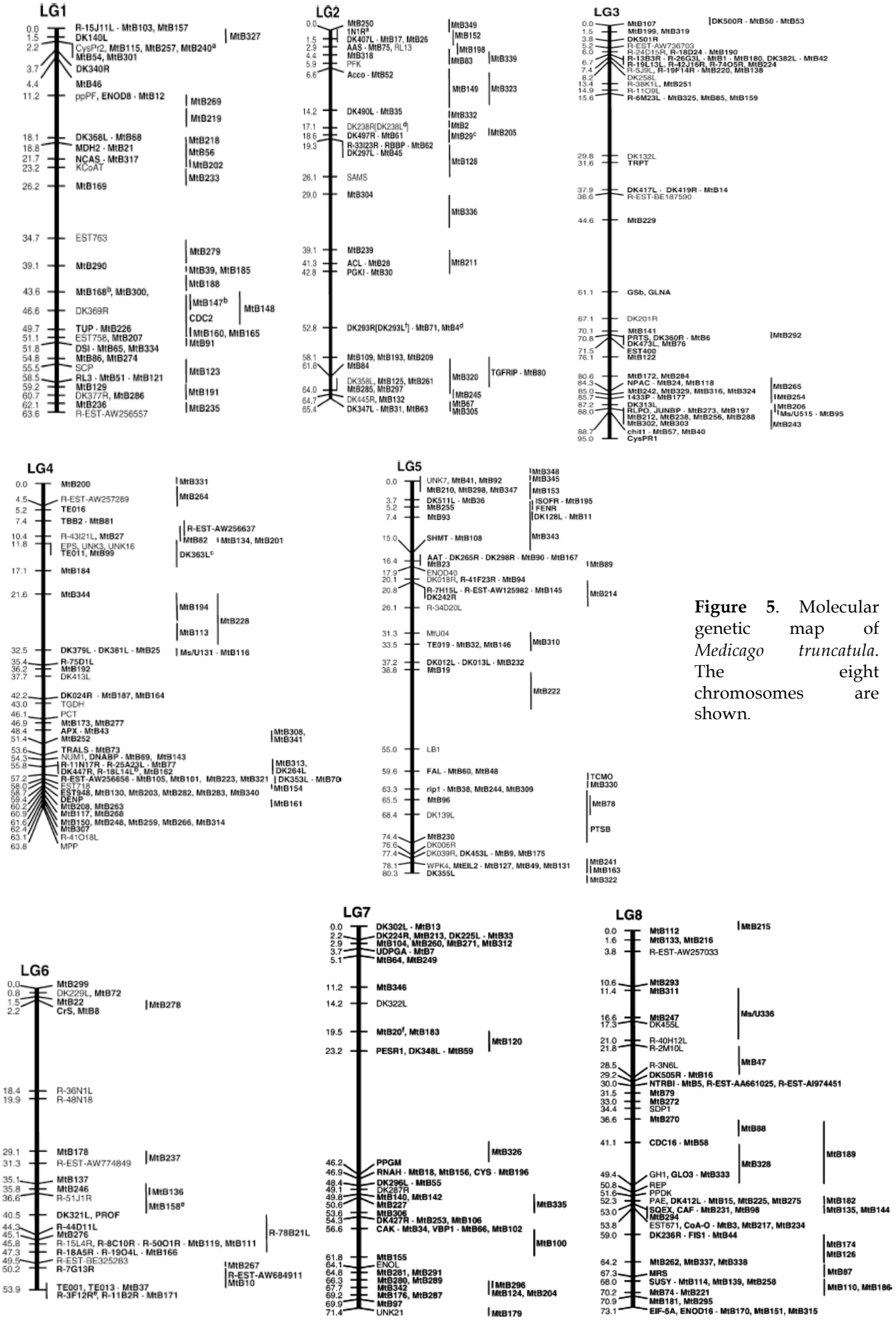

Figure 5. Molecular genetic map of *Medicago truncatula*. The eight chromosomes are shown.

To summarize (see Table 2 and Table 3), the initial goal of the project was to generate an approximately one-fold whole genome shotgun sequence data of the 500 megabase genome from a plasmid-based genomic library and obtain target shotgun clones for additional primer walking-based sequencing.

However, preliminary results from the shotgun approach suggest that the *M. truncatula* genome is highly repetitive. As previously predicted, estimates are that approximately 80% of the genome is highly repetitive and that approximately 80% of the gene-rich regions represent only 20% of the total genome. To reduce the amount of redundant sequence, the strategy has been modified to sequence BAC clones from an *M. truncatula* BAC library. More than 1,000 BACs will be identified based on DNA markers or gene content and will be sequenced to working draft coverage (four- to five-fold) utilizing a BAC-based shotgun sequencing approach.

The whole genome shotgun approach has already resulted in the sequencing of the *M. truncatula* chloroplast genome, since the total genomic DNA preparation not only contains the nuclear genome, but also a significant level of the chloroplast DNA. The DNA sequence of the *M. truncatula* chloroplast genome has now been completed and consists of one contiguous 124,039 base pair circle. Artificially linearizing the sequence at the histidine tRNA prior to the *psbA* gene allows the *Medicago* chloroplast genomic sequence to be co-linear with the *Arabidopsis*, tobacco, and most other chloroplast genomes. The semi-automated annotation of the *M. truncatula* chloroplast genome using Web-Artemis has been completed, and can be viewed at:

http://www.genome.ou.edu/medicago_chloroplast/med_chloro_art.html.

Table 2. BAC clones in M2.0 assembly

chromosome	Chr1	Chr2	Chr3	Chr4	Chr5	Chr6	Chr7	Chr8	unanchored	Total
phase 1	73	16	21	94	8	39	19	58	39	367
phase 2	24	36	11	33	44	26	42	35	11	262
phase 3	129	175	274	172	266	70	199	169	28	1482
OU	212	83	95	286	74	132	111	254	71	1318
TIGR	13	140	0	13	9	3	142	5	2	327
GENOSCOPE	1	0	0	0	234	0	0	0	2	237
SANGER	0	1	211	0	0	0	5	1	3	221
OTHER	0	3	0	0	1	0	2	2	0	8
Total BACs	226	227	306	299	318	135	260	262	78	2111

Table 3. Assembly of the *M. truncatula* genome

chromosome	Chr1	Chr2	Chr3	Chr4	Chr5	Chr6	Chr7	Chr8	unanchored	Total
BACs	226	227	306	299	318	135	260	262	78	2111
Singletons	6	2	7	6	2	3	10	6	72	114
Contigs	44	37	55	52	27	34	39	56	2	346
Scaffolds	39	33	44	39	14	29	33	48	3	282
Gaps (between scaffold)	44	34	50	44	15	31	44	53	75	390
Sequence (bp)	23975187	22539060	29247656	31006788	34139045	14478879	25393341	26415466	7538850	214734272
Pseudomolecule(bp) no 100,000 Ns	26870187	24469060	33177656	34961788	35789045	16893879	28128341	29950466	9448850	239689272
Pseudomolecule(bp) with 100,000 Ns	31270187	27869060	38177656	39361788	37289045	19993879	32528341	35250466	16948850	278689272
Scaffold avg (bp)	667,502	735,535	771,648	891,193	2,739,187	561,892	807,498	600,564	353,091	795,199
Scaffold N-50 (bp)	543,021	520,800	633,189	643,598	2,225,571	423,029	632367	453,829	321,201	710,733

✓ *EST resources and Genome Annotation*

A powerful tool to gain insight into an undescribed genome is to partially sequence random cDNA to generate a collection of expressed sequence tags (EST) (Adams *at al.*,1991). ESTs serve many purposes such as being employed for microarray design, for analyses of gene expression, for generating molecular markers, for physical mapping and for annotation of genes in genomic sequence.

The *Medicago* Genome Initiative (MGI) is an EST sequence database of the model legume *M. truncatula*. The database is available to the public and results from a collaborative research effort between the Noble Foundation and the National Center for Genome Resources (NCGR) to investigate the genome of *M. truncatula*. The *M. truncatula* research community has generated more than 189,000 ESTs from 32 different cDNA libraries. These ESTs separate into more than 170,000 tentative consensus sequences and more than 19,000 singletons. Greater than 36,000 unique sequences have been identified. A breakdown of the types of genes identified, based on Gene Ontology assignments, can be found in Figure 6.

In addition to MGI, the TIGR *M. truncatula* Gene Index (http://www.tigr.org/tdb/mtgi/) and the NSF-sponsored *M. truncatula* Consortium (http://www.medicago.org/) are two additional databases of particular interest to the legume research community. The genome annotation is carried out by the International Medicago Genome Annotation Group (IMGAG), which involves participants from TIGR, INRA-CNRS, MIPS, UMN, Ghent University and NCGR.

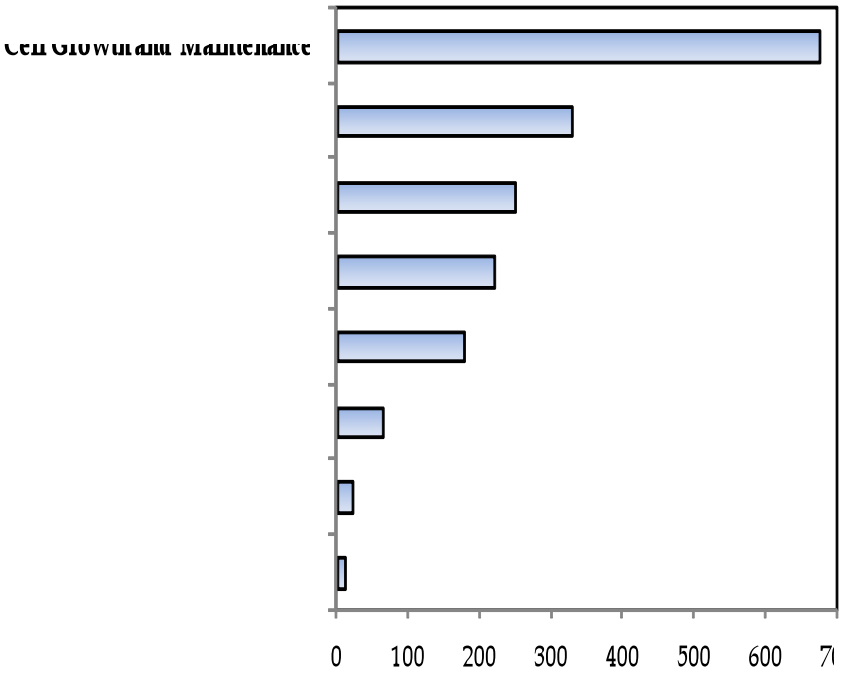

NOBLE Foundation web site

Figure 6. Gene Ontology assignments of the *M. truncatula* expressed sequence tags

To monitor gene expression in *M. truncatula* research community has at disposal the GeneChip® Medicago Genome Array. The GeneChip Medicago Genome Array is a 49-format, 11-micron array design and contains 11 probe pairs per probe set. The sequence information for this array was selected from data sources including the TIGR *M. truncatula* gene index, gene predictions from the International Medicago Genome Annotation Group (IMGAG), gene predictions from the symbiotic organism *S. meliloti* genome, and *M. sativa* EST information made available by TIGR. The array contains over 61,200 probe sets: 32,167 *M. truncatula* EST/mRNA-based and chloroplast gene-based probe sets; 18,733 *M. truncatula* IMGAG and phase 2/3 BAC prediction-based probe sets; 1,896 *M. sativa* EST/mRNA based probe sets; and 8,305 *S. meliloti* gene prediction-based probe sets.

Functional genomics tools

Since Medicago adoption by the international community as a model species, a number of useful tools and resources for functional genomics have been developed,

including a variety of different kinds of mutant populations, such as EMS, fast-neutron deletion, and transposon insertion mutants (Tadege *et al*., 2005).

Functional genomics platforms have been developed to characterise the function of genes by systematically disrupting them and analysing the phenotypic consequences. Three complementary types of platforms have been generated, based on the mode of disruption of gene function: fast neutron deletion, retrotransposon (Tnt1) insertion and chemical mutagenesis (treatment with ethylmethanesulphonate (EMS).

Proteomics

Custom and commercial transcriptome based approaches have been established in *Medicago* research however transcript profiles do not always provide a complete story due to limited correlations in transcript and protein levels (Gygi *et al*., 1999).

Thus, proteomics has become a critical complement to mRNA data and a better systems biology view of plant and legume biology. A large number of groups have published protein reference maps for specific *Medicago* tissues that include roots, stems, flowers, seed pods and cell suspension cultures (Lei *et al.,* 2005; Mathesius *et al*., 2001; Watson *et al.,* 2003). Additional organ specific proteome analyses have been reported for specific stages of seed filling and seed development (Gallardo *et al.,* 2003) and for somatic embryogenic tissue culture cells (Imin *et al.,* 2004). A major factor that accentuates *M. truncatula* as a model plant is its ability to associate with nitrogen fixing rhizobium bacteria and mycorrhizal fungi. Unlike in *Arabidopsis,* this enables the study of plant symbioses in *Medicago*. Proteomics of roots inoculated with mycorrhizal fungi *Glomus mosseae* or nitrogen fixing bacteria, *Sinorhizobium meliloti* (Bestel-Corre *et al.,* 2002), and the study of *S. meliloti* and *M. truncatula* symbiosome membrane protein profile (Catalano *et al.,* 2004) have also been published. The effect on *Medicago* roots upon infection by a pathogen, *Aphanomyces euteiches* has been analyzed (Colditz *et al.,* 2004). In 2003 Watson *et al.,* published a map of six organ-/tissue-specific proteomes of *M. truncatula* (Figure 7).

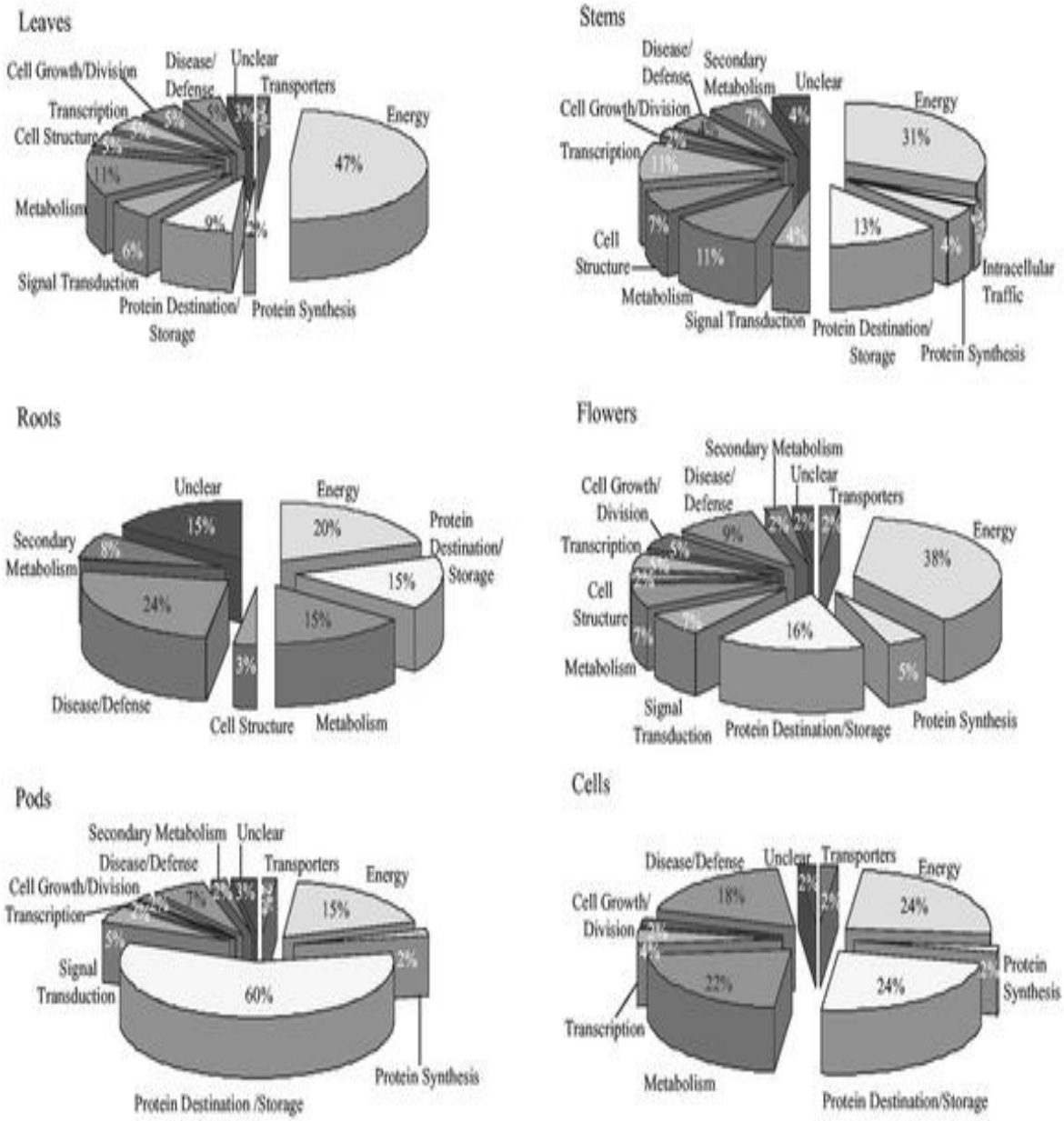

Watson *et al.*, 2003

Figure 7. Summary of the distribution of tissue specific identified protein classes as determined using the protein function database Pfam (http://www.sanger.ac.uk/Software/Pfam/) and classification schema previously reported for Arabidopsis (Bevan *et al.*, 1998).

Bioinformatics

A bioinformatics platform is essential to the storage, analysis and interpretation of Medicago functional genomics data generated from high throughput transcriptomics, proteomics and metabolomics experiments. From NOBLE Foundation (www.noble.org) research, different tools are available such as:

- computational models for the study of gene expression regulatory mechanisms in *M. truncatula,* integrated informatics in functional genomics of Legume transporters,
- a comparative Legume Gene Expression Atlas (which genes are expressed in which tissues and under what conditions) for the major organ systems of the reference legume, *M. truncatula,*
- integration and mining of heterogeneous data from high-throughput "omics" platforms, such as Affymetrix microarrays and x-MS platforms (gene expression and metabolite levels),
- integration of metabolic profiles with gene expression patterns in intact *M. truncatula* tissues in order to assist in functional annotation of genes.

Researchers have also developed database systems and data analysis tools for the genomics studies: a Database for Transcription Factor Prediction in *M. truncatula* and *Medicago truncatula* Mutagenesis Database.

In 2003, Lamblin *et al.* have developed a MtDB (*M. truncatula* Database), containing only the transcriptome information (146,000 ESTs and their computed assembly as 26,000 unigenes). Its parsed homology search results and a set of unique and elaborate queries for data mining. MtDB contents are updated as new sequences are released. MtDB is intended to provide a data mining environment that integrates features of NCBI, TIGR, NCGR, INRA-Mt (EST finished sequences, Unigene cluster, BLASTX analysis reports) while incorporating new attributes requested by the user community such as complex Boolean searches and comparative assessment between sequence assembly algorithms' results.

Medicago truncatula as model for plant-microbe interaction

M. truncatula is also being explored as a model for the genomics research involving study of plant-microbe interactions (Dénarié *et al.*, 1993). The most well characterized interaction involves *S. meliloti*: a nitrogen-fixing bacterium (rhizobium). The Rhizobium–Fabaceae association is a mutualistic relationship. The free-living soil bacteria colonize the roots of a host-plant, and are confined in specialized structures known as nodules (Figure 8).

They are thus protected against competition with other soil bacteria and are provided with carbohydrate compounds by the plant. In return, some of the bacterial cells, modified as bacteroid, fix nitrogen and provide ammonium to the plant that cannot itself reduce atmospheric nitrogen (nitrogen fixation ability is restricted to prokaryotes) (Figure 9). In the absence of bacteria, in poorly fertilized soils, plant growth and seed production lessen dramatically. In the absence of the plant, the bacteria reproduce very slowly and compete with other soil bacteria for limited carbohydrates resources. There is therefore a clear reciprocal benefit, in term of fitness, for the two partners in maintaining this cooperation, even though the bacteroid stage in the indeterminate nodules of Medicago represents a dead-end of individual bacteria (Sutton & Paterson, 1980).

In June 2009, Rodriguez-Llorente *et al.,* have presented an analysis of the 'Symbiosis Interactome' using novel computational methods in order to address the complex dynamic interactions between proteins involved in the symbiosis of the model bacteria *S. meliloti* with model plant *M. truncatula.* They have identified 263 potential novel symbiosis components, and have demonstrated experimentally the participation of novel proteins involved in this important process.

Figure 8. *Medicago truncatula* roots with nodules. Rhizobium invades the root cells. Inside the root, rhizobia colonize expanded cells of cortex, and then bacteria differentiate into Nitrogen-fixing "bacteroids". On the left is microscopic picture of dissected nodules on the root. The effectiveness of a given nodule may be checked by cutting it open: an effective nodule should be pink (or purple) in color, while immature or ineffective ones are either green or white inside. Rhizobia inside the nodules, differentiated into "bacteroids", fix inert atmospheric N2 for the plants, and supply it in the water-soluble form for the plants.

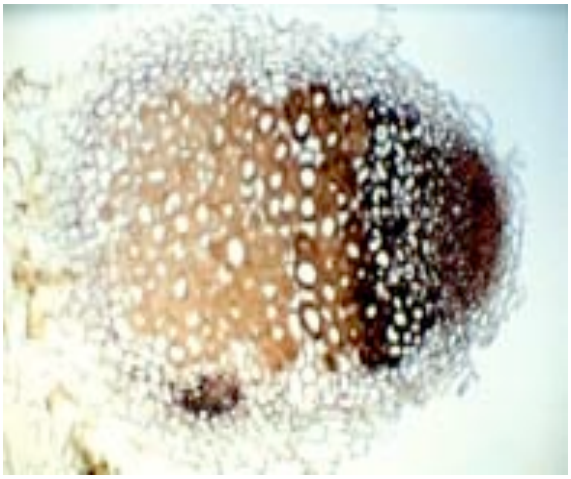

Figure 9. Nitrogen-fixing *Medicago truncatula* nodule, showing distinct cell types and regions of nigrogenase activity (www.noble.org).

Adams M.D., Kelley J.M., Gocayne J.D., Dubnick M., Polymeropoulos M.H., Xiao H., Merril C.R., Wu A., Olde B., Moreno R.F. *et al.*, 1991. Complementary DNA sequencing expressed sequence tags and human genome project. Science, 252(5013):1651-6.

Barker D.G., Bianchi S., Blondon F., Dattée Y., Duc G., Essad S., Flament P., Gallusci P., Génier G., Guy G., Muel X., Tourneur J., Dénarié J., Huguet T., 1990. *Medicago truncatula*, a model plant for studying the molecular genetics of the Rhizobium-legume symbiosis. Plant Mol Biol Reporter, 8:40-49.

Barton N.H., Whitlock M.C., 1997. The evolution of metapopulation; in: Hanski I.A., Gilpin M.E. (eds): Metapopulation Biology - Ecology, Genetics and Evolution.

Bestel-Corre G., Dumas-Gaudot E., Poinsot V., Dieu M., Dierick J.F., Van T.D., Remacle J., Gianinazzi-Pearson V., Gianinazzi S., 2002. Proteome analysis and identification of symbiosis-related proteins from *Medicago truncatula* Gaertn. by two-dimensional electrophoresis and mass spectrometry. Electrophoresis, 23:122-37.

Catalano C.M., Lane W.S., Sherrier D.J., 2004. Biochemical characterization of symbiosome membrane proteins from *Medicago truncatula* root nodules. Electrophoresis, 25:519-31.

Choi H.-K., Mun J.-H., Kim D.-J., Zhu H., Baek J.-M., Mudge J., Roe B., Ellis N., Doyle J., Kiss G.B., Young N.D., Cook D.R., 2004b. Estimating genome conservation between crop and model legume species. Proc Nat Acad Sci USA, 101:15289-15294.

Colditz F., Nyamsuren O., Niehaus K., Eubel H., Braun H.P., Krajinski F., 2004. Proteomic approach: identification of Medicago truncatula proteins induced in roots after infection with the pathogenic oomycete Aphanomyces euteiches. Plant Mol Biol, 55:109-20.

Cook D.R.,1999. Medicago truncatula – a model in the making! Curr Opin Plant Biol, 2:301–304.

Crane C., Wright E., Dixon R.A., and Wang Z.-Y., 2006. Transgenic *Medicago truncatula* plants obtained from Agrobacterium tumefaciens-transformed roots and Agrobacterium rhizogenes-transformed hairy roots. Planta, 223:1344-1354.

Dénarié J., Debellé F., Truchet G., Promé J-C., 1993. Rhizobium and legume nodulation : a molecular dialogue. In New horizons in Nitrogen Fixation ed. Palacios, R., Mora, J. and Newton, W.E. 19-30.

Galibert F., Finan T.M., Long S.R., Puhler A., Abola P., Ampe F., Barloy-Hubler F., Barnett M.J., Becker A., Boistard P. *et al.*, 2001. The composite genome of the legume symbiont Sinorhizobium meliloti. Science, 293:668–672.

Gallardo K., Le Signor C., Vandekerckhove J., Thompson R.D., Burstin J., 2003. Proteomics of Medicago truncatula seed development establishes the time frame of diverse metabolic processes related to reserve accumulation. Plant Physiol, 133:664-82.

Graham, P.H., and Vance, C.P., 2003. Legumes: importance and constraints to greater use. Plant Physiology, 131:872-877.

Handberg K., and Stougaard J., 1992. Lotus japonicus, an autogamous, diploid legume species for classical and molecular-genetics. Plant Journal, 2:487-496.

Imin N., De Jong F., Mathesius U., Van Noorden G., Saeed N.A., Wang X.D., Rose R.J., Rolfe B.G., 2004. Proteome reference maps of Medicago truncatula embryogenic cell cultures generated from single protoplasts. Proteomics, 4:1883-96.

Lesins K.A., Lesins I., 1979. GenusMedicagoLeguminosae, Dr. W. Junk, The Hague.

Kulikova O., Gualtieri G., Geurts R., Kim D.J., Cook D., Huguet T., de Jong J.H., Fransz P.F., Bisseling T., 2001. Integration of the FISH pachytene and genetic maps of Medicago truncatula. Plant J, 27(1):49-58.

Lei Z., A.M. Elmer B.S. Watson R.A. Dixon P.J. Mendes and L.W. Sumner. 2005. A two-dimensional electrophoresis proteomic reference map and systematic identification of 1367 proteins from a cell suspension culture of the model legume Medicago truncatula. Mol Cell Proteomics, 4:1812-25.

Liu H., Trieu A.T., Blaylock L.A., Harrison M.J., 1998. Cloning and characterization of two phosphate transporters from *Medicago truncatula* roots: regulation in response to phosphate and to colonization by arbuscular mycorrhizal (AM) fungi. Mol Plant Microbe Interact, 11:14–22.

Mathesius U., Keijzers G., Natera S.H., Weinman J.J., Djordjevic M.A., Rolfe B.G., 2001. Establishment of a root proteome reference map for the model legume Medicago truncatula using the expressed sequence tag database for peptide mass fingerprinting. Proteomics, 1:1424-40.

Prosperi J.M., Auricht G., Génier G., Johnson R., 2001. Medics (Medicago L.). Plant Genetic Resources of Legume in the Mediterranean (eds N. Maxted and S.J. Bennett), Kluwer Academic Publishers. 99–114.

Rodriguez-Llorente I., Caviedes M.A., Dary M., Palomares A.J., Cánovas F.M. and Peregrín-Alvarez J.M., 2009. The Symbiosis Interactome: a computational approach reveals novel components, functional interactions and modules in Sinorhizobium meliloti. BMC Syst Biol, 3:63.

Tadege M., Ratet P., and Mysore K.S., 2005. Insertional mutagenesis: a Swiss Army knife for functional genomics of *Medicago truncatula*. Trends in Plant Science, 10:229-235.

Wang T.L., Domoney C., Hedley C.L., Casey R., Grusak M.A., 2003. Can we improve the nutritional quality of legume seeds? Plant Physiol., 131(3):886-91.

Watson B.S., Asirvatham V.S., Wang L., Sumner L.W., 2003. Mapping the proteome of barrel medic (*Medicago truncatula*). Plant Physiol, 131:1104-23.

This thesis describes a molecular study of flavonoid biosynthesis in *M. truncatula* plants and in detail two different functional genomics approaches to analyse a metabolic pathway.

In **Chapter 3** the molecular and biochemical characterization of five *M. truncatula* mutants affected in flavonoid metabolism is described. The work begun with the phenotype analysis and quantification of total anthocyanins. Flavonoids localization in immature seeds was checked, while in mature seeds the amount of tannins was quantified. Then the expression profiles of genes encoding the key enzymes and the transcription factors involved in flavonoid biosyntesis were investigated. After the biochemical and molecular characterization, the mutant genotypes have been treated by UV-B radiation to induce an oxidative stress. The molecular and physiological responses to UV-B damages have been investigated in relation to anthocyanin contents. Part of this work has been developed during a stage in the laboratory of Seed Biology at the INRA Versailles-Grignon.

Chapter 4 reports on the isolation and molecular characterization of a new *Myb* transcriptional factor in *M. truncatula* involved in anthocyanin biosynthesis and accumulation. The gene expression has been investigated in different tissues and over time at different development stages. The *Myb* gene has been over-expressed by cloning the coding sequence under the control of 35S promoter and then transforming *M. truncatula* and *A. thaliana* plants. The localization of the Myb protein in plant tissues and in cells has been checked through promoter analysis using GFP and GUS reporter gene. This work has been developed in collaboration with Centro di ricerca per le produzioni foraggere e lattiero-casearie, Consiglio per la Ricerca e Sperimentazione in Agricoltura (CRA), Lodi.

3. CHARACTERIZATION OF *M. truncatula* MUTANTS AFFECTED IN FLAVONOID BIOSYNTHESIS AND THEIR RESPONSE TO UV-B STRESS

INTRODUCTION

Flavonoids are plant secondary metabolites responsible for the characteristic pigmentations of most flowers, fruits and seeds (Nielsen *et al*., 2005, Castellarin *et al*., 2006). They are a broad class of low molecular weight, plant phenolic characterized by the flavan nucleus (Figure 1).

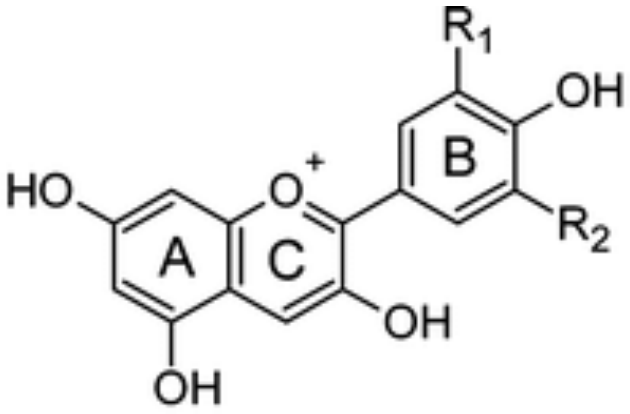

Figure 1. The flavan-3-ol nucleus.

They are synthesized by the phenylpropanoid pathway in which the amino acid phenylalanine is converted to 4-coumaroyl-CoA that, combined with malonyl-CoA, yelds the true backbone of flavonoids.

Over 6000 different flavonoids have been reported (Harborne and Williams, 2000) and subdivided into different classes that comprise seven major subgroup: the chalcones, aurones, flavones, flavonols, flavandiols, anthocyanins and proanthocyanidins, according to the oxidation level of the C-ring. Additionally, the stereochemistry, position and nature of substitutions (hydroxyl, methyl, galloyl, glycosyl), combination, degree of polymerization and linkages between the basic units allow for the multitude of compounds characterized in plants (Figure 2).

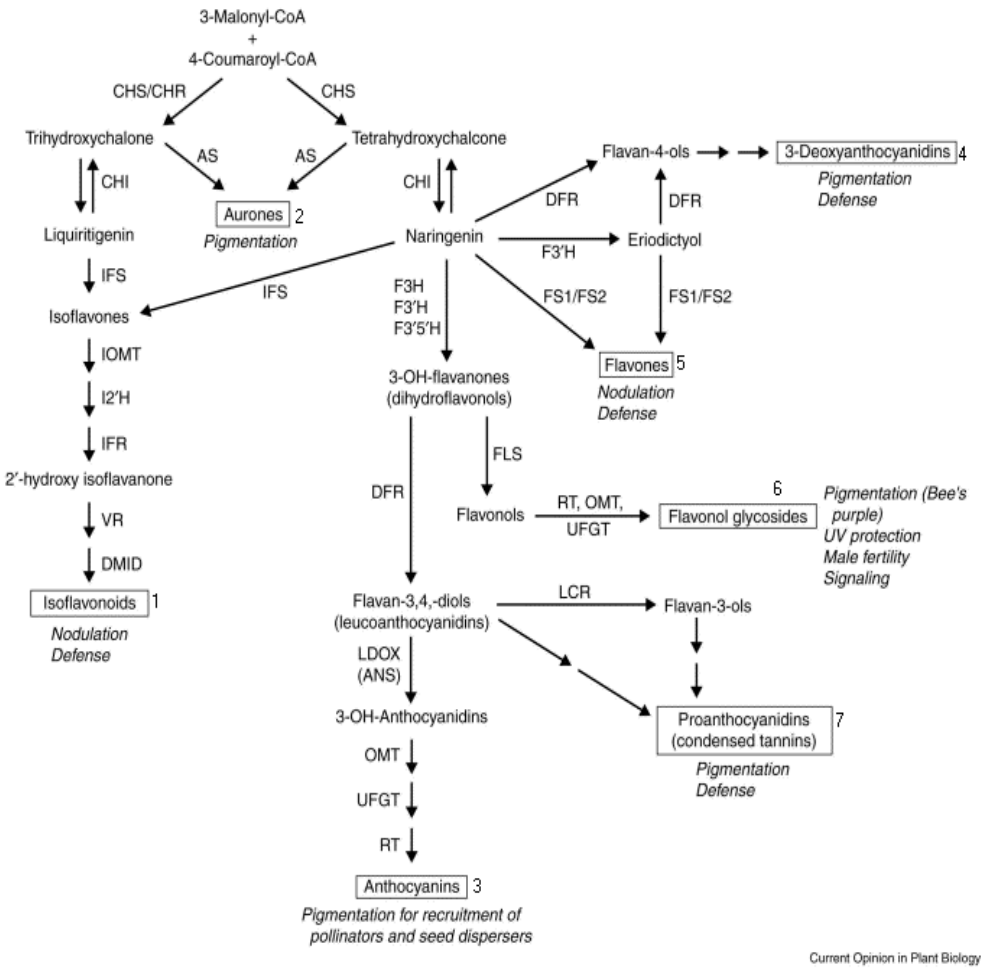

Figure 2. Flavonoid metabolic pathway. The seven major subgroups are highlight and the main functions of them are shown.

Their synthesis is localized within the cytosolic compound as others secondary metabolites, they are considered highly reactive and potentially toxic in the cytoplasm (Smith *et al.,* 2003). Most of the flavonoid enzymes are recovered in the "soluble" cell fraction; immuno-localization experiments suggest that they are loosely bound to the endoplasmic reticulum, possibly in a multi-enzyme complex (Winkel-Shirley, 2001), whereas the pigments themselves accumulate in the vacuole (anthocyanins, glycosylated flavonols and proanthocyanidins) or the cell wall (phlobaphenes and methylated flavonols) (Grotewold, 2004).

To avoid toxicity, flavonoids are sequestered within vacuoles or transported outside the cell by glutathione *S*-transferase (GST) (Schröder *et al*., 2007). In the detoxification pathway, exogenous compounds are conjugated with glutathione by GST protein. The glutathione conjugates are recognized and sequestered to the vacuoles or exported to the

cell wall by ATP-dependent, proton-gradient-indipendent transporters, named ATP-binding cassette (ABC)-type transporters (Martinoia *et al.,* 1993).

Flavonoid functions

Flavonoids are implicated in several biological and physiological functions such as visual signal to attract pollinating insects (Tanaka *et al*., 2008), seed dormancy and dispersal (Debeaujon *et al*., 2000), UV protection (Giuntini *et al*., 2008), signalling to symbiotic microorganisms (Harrison 2005; Cooper, 2007), and control of auxin transport (Santelia *et al*., 2008; Peer *et al*., 2004). Also in animal kingdom flavonoids are particularly interesting. For example isoflavones (a class almost exclusive of Leguminosae) possess estrogenic, antiangiogenic, antioxidant and anticancer activity (Galluzzo and Marino, 2006; Yao *et al.,* 2004; Androutsopoulos *et al.,* 2009). In fact, they reduce susceptibility to mammary cancer in rats (Ekambaram *et al*., 2008) and help to prevent bone loss caused by estrogen deficiency in female mice (Kaludjerovic and Ward, 2009).

Flavonoids and particularly proanthocyanidins (also known as condensed tannins, CTs) have diffuse effects on ruminant nutrition. The principal agronomic benefit of CTs is due to their ability to prevent the "bloating" characteristics of forage legumes though the bind of the leguminosae proteins in the rumen. Decreasing the protein degradation during ensiling of forage legumes, they improve the nitrogen nutritional value of the feed, avoid protein degradation, prevent bloat and increase the animal's nitrogen intake (Min *et al*., 2005). Most dietary flavonoids occur in food as *O*-glycosides (Hammerstone *et al.,* 2000). The most common glycosidic unit is glucose, but other examples include glucorhamnose, galactose, arabinose and rhamnose.

Most of the beneficial health effects of flavonoids are attributed to their antioxidant and chelating abilities. It is known their capacity to transfer electrons free radicals, chelate metal catalysis (Ferrali *et al.,* 1997), activate antioxidant enzymes (Elliott *et al*., 1992), reduce alpha-tocopherol radicals (Hirano *et al.,* 2001) and inibit oxidases (Cos *et al*., 1998).

The best strategy for study metabolic pathways is still to resort to the "functional genetics" by the analysis of mutants showing an altered metabolic profile. Several mutants of different plant species contributed to the discover of flavonoid metabolic pathway. In

this thesis five *M. truncatula* mutants showing an altered flavonoid biosynthesis have been described. Besides the molecular characterization of those mutants, their response to oxidative stress (UV-B) was also investigated. Reading this chapter it is possible to understand how each mutant reacts to UV-B radiation and if the different responses observed are correlated to the different amounts of anthocyanins found in leaves. These mutants can be useful tools for future study on biotic or abiotic stress responses or for functional genomic assays.

MATERIAL AND METHODS

Genotypes and growing conditions

Seven genotypes of *M. truncatula* - two wild-types, Jemalong 2HA (wt_Jem) and JRC1 (wt_JRC1) and five mutants (mut_735, mut_204, mut_150, mut_115, mut_137) - have been investigated in this study. Mutants were produced using two different mutagenesis methods: i) mut_735 was obtained by EMS (Ethylmethane Sulphonate) treatement of wild-type Jemalong 2HA and screened by TILLING method at the Plant Genetic Institute, Perugia, Italy; ii) mut_204, mut_150, mut_115, mut_137 were obtained by fast neutron mutagenesis of wild-type JRC1 at John Innes Center, in Cathie Martin's laboratory. Mut_204, mut_150, mut_115, mut_137 are not allelics.

For molecular and biochemical analysis three plants per genotype were seeded in a pot containing loam soil. After germination, plants were acclimated in a growth chamber to a photoperiods of 16 hours, light by 7000 lux of light radiation and 8 hours dark and maintained at 23°C.

Biochemical and molecular analyses have been performed using leaves collected 25 days after leaf emission, a stage corresponding to the maximum flavonoid production in *M. truncatula* leaves.

Plant growth conditions for UV-B exposure experiments

For UV-B exposure experiments, the seven genotypes were grown for 30 days in pots with loam soil, with photoperiod of 16 hours of light at 100 □mol photons $m^{-2}s^{-1}$ of light radiation and 8 hours dark at 23°C. Thereafter, the plants were moved to an exposure chamber equipped with UV-B tubes with the same temperature, humidity and light as before. 30 days-old plants were radiated by UV-B radiation with fluorescence tubes (Philips, TL-d 18W 108, Eindhoven, The Netherlands)). The leaves were harvested after 4 and 14 h of radiation and after 24 h of recovering. For each genotype, three biological replications were done. The UV-B experiments have been performed in collaboration with the Institute of Plant Biology, Biological Research Center (BRC), Szeged, Hungary (dott. Eva Hideg).

Absorbance analysis

Twenty mg of fresh *M. truncatula* leaves were manually grounded in liquid nitrogen. After an addition of 150 µl of methanol, samples were manually homogenised and incubated overnight at 4°C in the dark to minimize anthocyanins oxidation. The day after, 250 µl of chlorophorm: 1% HCl were added to the samples and gently mixed. After 5 min centrifugation at 5000g, the upper chlorophorm phase was carefully collected and analysed by spectrophotometric assay. Anthocyanins absorbance was read in a range between 530nm and 657nm. The percentage of anthocyanins was expressed according to cyanidin-3-glucoside chloride (Extrasynthèse, http://www.extrasynthese.com/). All measurements were repeated three times.

HPLC-DAD-MS/MS assay

Sample preparation

Leaves were treated for 5h with acidic methanol (1% HCl v/v) with shaking in the dark. The methanol was removed by rotary evaporation, and the red residue was suspended in a small volume of water. The aqueous solution was then extracted three times with EtOAc and the remaining aqueous fraction was partially purified by adsorbing to a disposable SPE C18 cartridge (Varian Inc, Palo Alto, CA, USA). MeOH-1% HCOOH v/v was used to elute the anthocyanins. The methanolic elute was evaporated and the residue was finally redissolved in a small volume of mobile phase (solvent A). An aliquot was used to quantify anthocyanins by spectrophotometric analysis and the remaining amount was 0.45 µm filtered and subjected to HPLC-MS analysis.

Individual anthocyanins identification by HPLC-DAD-MS/MS

Separation of anthocyanins was conducted in collaboration with dott. Paolo Rapisarda at the Centro di Ricerca per l'Agrumicoltura e le Colture Mediterranee, Acireale, Catania, Italy, on a Merck Chromlith Performance RP-18e column (100-3 mm) using a Ultra Fast HPLC system coupled to a photodiode array (PDA) detector and a Finnigan LXQ ion trap equipped with an electrospray ionization (ESI) interface, in a series configuration (Thermo Electron Corporation, San Jose, CA). A binary gradient composed of (solvent A) water containing 7% formic acid and (solvent B) methanol was used for separation. The gradient was run as follows: from 5% to 40% of B in 20 min, isocratic for 7 min, followed by re-equilibrating the column to initial conditions. MS conditions were: spray voltage (KV) 5.50, capillary temperature (°C) 275, capillary voltage (V) 27. MS full-scan acquisition (m/z 250-2000) was first performed in a positive mode. Then, chosen peaks were isolated in the ion trap and fragmented by an MS-MS full scan acquisition. The UV-Vis absorption chromatogram was detected at 520 nm.

Vanilline assay

Intact immature seeds were incubated as described by Aastrup *et al*. (1984) in a solution of 1% (w/v) vanillin and 6N HCl at room temperature for 20 min. Vanillin turns red upon binding to flavan-3,4-diols (leucoanthocyanidins) and flavan-4-ols (catechins), which are present either as monomers or as terminal subunits of proanthocyanidins (Deshpande *et al*., 1986).

RNA extraction and reverse transcription

The RNA isolation was performed using TRIZOL® Reagent (Invitrogen, USA) and according to the manufacturer's protocol. The yields and concentration of the isolated RNA was determined by measuring the optical density in a biophotometer (Biophotometer, Eppendorf, Germany) at 260 nm. RNA purity was evaluated by the absorbance *ratio* A260/A280 nm while RNA integrity by 1% agarose (Seakem® LE Agarose, CAMBREX, USA) gel electrophoresis. Reverse transcription (RT) was performed using BIO-RAD iScript™ cDNA Synthesis Kit starting from 1µg of total RNA and following the manufacturer's instruction.

Primer design

31 pair of gene-specific primers corresponding to the enzymes and transcription factors involved in flavonoid biosynthesis were designed and synthetized by MWG-Biotech AG, Germany. For PCR assays (RT-PCR and qPCR) primers were designed (Primer3 Input 0.4.0) to obtained PCR fragments of 400-900bp of cDNA (Table 1), whereas for qPCR assay the primers designed have given maximum products of 150bp (Table 2). The annealing temperature used for RT-PCR assay is 57°C for each couple of primers, while for qPCR the annealing temperature used is 60°C for each primer pair.

Table 1. Primers used for RT-PCR assays

Gene	*ID*	*Primer f or*	*Primer rev*
acti n (ACT)	TC106785	5'-TTCTCCTCTTCGATCCATTTTC-3'	5'- ACGACCAGCAAGATCCAAAC-3'
phenylalanine ammonia lyase (PAL)	TC106669	5'-GAAGTGAAACGTATGGTGGAGG-3'	5'-GAACAATTGAAGCTAAACCGGAAC-3'
chalcone synthase (CHS)	TC106552	5'-GCAGTGAAAGCTATAAAAGAATGGG-3'	5'-CTTTGAAACAATCCCAGGAACATC-3'
chalcone isomerase (CHI)	TC100522	5'-GAAGAATATGGCTGCATCAATCAC-3'	5'-CCAGGTGGAAAATTAATAGGCTTG-3'
fl avonoid 3'-hydroxylase (F3'H)	TC99759	5'-GCTCAAGTTCAACAAGAATTGGAC-3'	5'-CTTCATCCATGTTCATTTTTCCAG-3'
fl avonoid 3',5'-hydroxylase (F3',5'H)	TC99191	5'-TCACAAAAATATGGACCCGTAATG-3'	5'-GTCATGAGCTCAACAACCATATCC-3'
fl avanone 3-dioxygenase (F3H)	TC94828	5'-TTTCAAGTTGTTGATCATGGTGTG-3'	5'-TCGTTTTAGGCCAAGAGTTAGGTC-3'
dihydrokaempf erol 4-reductase 1 (DFR1)	AY389346	5'-GTCATTTGTTAGAACTGCCAGGTG-3'	5'-AAGAAAAGGACCAACAACAAGAGG-3'
dihydrokaempf erol 4-reductase 2 (DFR2)	AY389347	5'-TGACCTTGGGGAAGAGGGTAG-3	5'-TCTCCCATGTGCTTTAGGGTTCT-3'
leucoanthocyanidin dioxygenase (LDOX)	CR538722	5'-TTGCAGCAATGGATTCAGAAATG-3'	5'-TTTGGATCTTTAATGCTTTTGACATA-3'
UDP-glucose:anthocyanin 3-O-glucosyltransf erase (3-GT)	CT863710	5'- TGTTCTGCACCACCATGATT-3'	5'- AACAACGTCCTTGGTTTTGG-3'
anthocyanin 3-O-rhamnosyltransf erase (3-RT)	CT030165	5'-GCTACAGATCGGCGAAGAAA -3'	5'- TGTACCATTACCCCCACCAT-3'
anthocyanin acyltransf erase (AAT)	AC171168	5'-TTTCACCACCACCAAGTTCA-3'	5'- ATTTGAATGGCCATGAGAGG-3'
UDP-glucose:anthocyanin 5-O-glucosyltransf erase (5-GT)	AC146585	ACAGGCAGCGATGCTTACTT-3'	5'- GCTCTCAACGCTTTTGGTTC-3'
anthocyanidin reductase (ANR)	AY184243	5'- CTCGAAGGGACTGGTCATGT-3'	5'-TGCTGGGGAAATCATCAAAT-3'
leucoanthocyanidin reductase (LAR)	BN000703	5'-CGATGTGGACAGAGCAGATCC-3'	5'-CGGCTATTCCTAGAAGATCGTCT-3'
fl avonol synthase (FLS)	CX539858	5'-AGGGTACAAACAATAGCTCATC-3'	5'-CAGGGTTGTTAGGCCAAAAAC-3'
fl avone synthase II (FSII)	DQ354373	5'-CCAATGGTTTGTCCCAATAAGC-3'	5'-GGGTTTGGGAAGAGGATAGAG-3'
isofl avone synthase (IFS)	AY939826	5'-CAAACCCATGAAGCTACTTCC-3'	5'-TCAATGATAGGATCATACTTATTG-3'
isofl avone-O-methyltransf erase (IOMT)	BF637366	5'-ATGTATGCCTTTGTAGATTC-3'	5'-TGGAATCACTAGCCAAAGCATC-3'
glutathione S-transf erase (GST)	TC103187	5'-GTTCAATTAATGCAGCATGTCCTC-3'	5'-CAGCCAAAGTGAACTTATCACCAG-3'
producti on of anthocyanin pigment 1 (PAP1)	AC172742	5'- ATGAAGTTGATTAAGGAAAGGGTA-3'	5'-CTAAAGATCCCAAAGAGAATCATAA-3'
producti on of anthocyanin pigment 2 (PAP2)	BF635572	5'-ATGTATCGGTGCTCTAAATATATG-3'	5'-GAGGTTTAGGTTTAATAATTTCATG-3
anthocyanin 2 (AN2)	AC152405	5'-TCAGAGATCTGGATTGAATAGATG-3'	5'-GTTCCACAAACTGTCACACCAC-3'
anthocyaninless 2 (ANL2)	AC148764	5'-TCTGGTAGTGATAACATGGATGG-3'	5'-TTTGGTAACGACGTAATTGGACG-3'
enhancer of glabra 3 (EGL3)	AC135317	5'-AACTCGTCGTCCATGTGCTTC-3'	5'-TCTTCATCCATGTCGTCTTGATT-3'
glabra 3 (GL3)	AC135317	5'-CTAAGATATCTCTTCCACCTCC-3'	5'-CACACCTACTCTCTTCACCCA-3'
transparent testa glabra 1 (TTG1)	BI267010	5'- CGCCACACATTCTTCTCTCCAG-3'	5'-ACTATCCATCAAAATCGTGGCC-3'
pericarp (MYBP)	AC145329	5'- CAAGATGCATGCTTCTTTTGGC-3'	5'-CAAAGCATCCATGATAATATCATTA-3'
purple leaf (MYBPL)	AC119408	5'-GGGATTGATCCCAGAACTCA-3'	5'-AGCTTTCCCGTCTTGGTTTT-3'
MYB15	AC149493	5'- GTGGTCAGCAATAGCAGCAA-3'	5'-AACCCAAAAACCCATTCCAT-3'
MYB4	AC121235	5'-CATCAAACTCCATAGTCTTCTTG-3'	5'-GCAAACCCAAACTACAAACAAAAC-3'

Table2. Primer sequences used for qPCR assays

Gene	ID	Primer for	Primer rev
acti n (ACT)	TC106785	5'-TTCGGCATTTTCCTTCCCAAAG-3'	5'-TATTTAAGAGTCAAAATACCCCTC-3'
fl avonoid 3'-hydroxylase (F3'H)	TC99759	5'-GGGAATTGAGTGGTCCTGAG-3'	5'-AGGCTTGAAAGCTTCAGCAA-3'
fl avonoid 3',5'-hydroxylase (F3',5'H)	TC99191	5'-CCTGGAACATCATTGGCTTT-3'	5'-CAACCCAGGTTTCTCTTCCA-3'
dihydrokaempf erol 4-reductase 1 (DFR1)	AY389346	5'-TGTCCCTATGGAAGGCTGAC-3'	5'-TTCATTCTCAGGGTCCTTGG-3'
dihydrokaempf erol 4-reductase 2 (DFR2)	AY389347	5'-TTCAAAAACCCTGGCAGAAC-3'	5'-GGTGGCATTGAAGGCATAAT-3'
isofl avone-O-methyltransf erase (IOMT)	BF637366	5'-ATCCACAATCATGGCAAACC-3'	5'-TCCATTGTGTGCGAGGTAAC-3';
glutathione S-transf erase (GST)	TC103187	5'-GTTCAATTAATGCAGCATGTCCTC-3'	5'-CAGCCAAAGTGAACTTATCACCAG-3'
UDP-glucose:anthocyanin 3-O-glucosyltransf erase (3-GT)	CT863710	5'-TCCTGTGCTTCAAGATGAAGAAA-3'	5'-CTGGAAGGTTGATGATGTTGAG-3'
UDP-glucose:anthocyanin 5-O-glucosyltransf erase (5-GT)	AC146585	5'-AACAATCCACCATGCCTCACCG-3'	5'-AAACTCTGCATGGTATTCTAAGC-3'
producti on of anthocyanin pigment 2 (PAP2)	BF635572	5'-GGCTTGCATCCACAAGTATG-3'	5'-TCGGCGAAACTTTCTCTGTT-3'
MYB15	AC149493	5'-AGATGCCGGTTTATTAAGATGTG-3'	5'-TAATTTTGCTGCTATTGCTGACC-3'
MYB4	AC121235	5'-TTCTTGGTAACAAATGGTCTTTG-3'	5'-AGATGAAGAGTTTGAGATTGTG-3'
anthocyanin 2 (AN2)	AC152405	5'-TCAATGACCATCTATTTCCTAGTA-3'	5'-AGAGATCTGGATTGAATAGATGC-3'

RT-PCR amplification

The RT-PCR reaction was conducted in a final reaction volume of 20 µL containing 30 ng of cDNA, 0.3µM of primer forward and 0.3µM of primer reverse (MWG-Biotech AG, Germany), 1X Buffer containing 1.5mM of $MgCl_2$ (GeneSpin, Italy), 0.2mM of dNTPs and 0.3U/µL of Taq Polymerase (GeneSpin, Italy). The PCR amplification profile was: 3 minutes initial denaturation at 94°C, followed by 35 cycles of 94°C for 40 sec, 57°C for 40 sec, 72°C for 50 seconds, and a 7 min final extension at 72°C. The amplified PCR products were separated in 1% agarose gel (Seakem® LE Agarose, CAMBREX, USA) and stained with ethidium bromide (0,5µg/ml). The length of PCR products was determined by comparison with the gene marker Superladder-Low 100bp Ladder (Thermo Scientific, USA).

qPCR amplification

The qPCR assay was performed with real-time PCR (Mini-Opticon; Bio-Rad Laboratories, CA) thermal cycler and all the operations during amplification reaction were controlled by MJOpticon Monitor, Version 3.1 software. qPCR reaction was performed using iQ™ SYBR® Green Supermix (containing *Taq* DNA polymerase, dNTPs, $MgCl_2$, and SYBR Green I dye; BIO-RAD). Each reaction mix (25 µL) contained 20 ng of cDNA, 0.4 □mol/L of primers. The amplification profile was: 1 cycle of 3 minutes at 95°C followed by 44 cycles of 10 seconds at 95°C, 25 second of annealing temperature and 72°C for 7 minutes.

A negative control was added to each assay to assess the overall specificity. The expression of each gene was tested through three biological repetition and each sample

was repeated three times to performed technical repetition. The □-actin gene, a stable housekeeping gene, was used for signal normalization.

Bioinformatic analysis

Some genes tested in this thesis were already sequenced and annotated in *M. truncatula* genome. For the others, a comparative mapping approach was adopted with *Arabidopsis thaliana*, *Petunia hybrida* and *Zea mays genomes* and exploiting the information stored in public databases: TIGR (www.tigr.org), Genebank/NCBI (www.ncbi.nlm.nih.gov) and TAIR (www.arabidopsis.org). Sequences were blasted using BLOSUM62 matrix available in BLASTP software (www.blast.ncbi.nlm.nih.gov/Blast.cgi) considering the value of e-10 as homology thresholds.

RESULTS AND DISCUSSION

- **Mutants characterization**

Phenotype description

Leaves of *M. truncatula* ecotypes Jemalong and JRC1 are characterized by particular red spots in the middle of the upper page absent in the inferior page as shown in Figure 3. Those red spots are a visible accumulation of anthocyanins.

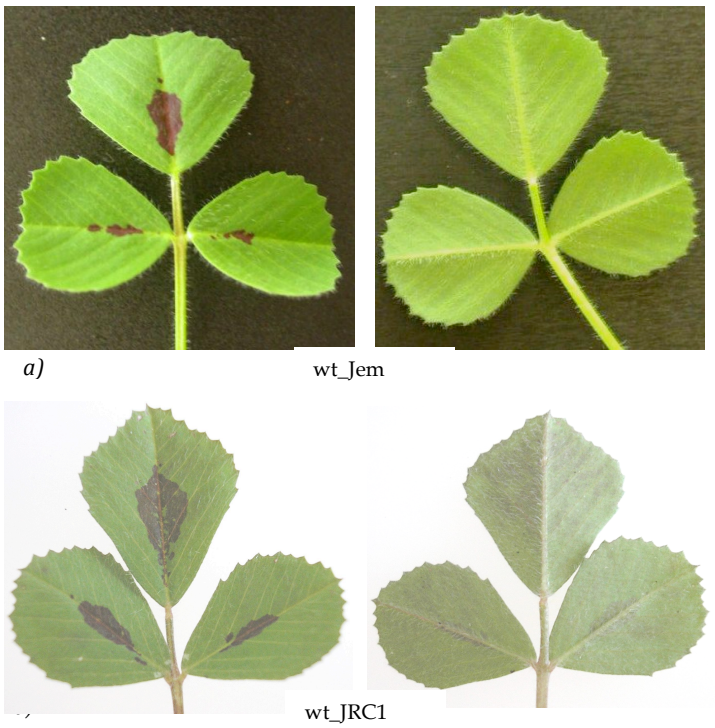

Figure 3. *Medicago truncatula* ecotype Jemalong wild-type leaves: *a)* genotype coming from Italian laboratory of Perugia, Italy; *b)* genotype coming from English laboratory in Norwich, England. The pictures on the left represent the upper page, while on the right it has been reported the inferior page

Mutants described in this paper show two abnormal phenotypes: i) a total absence of red pigmentation on the upper page and the presence of little red lines on inferior page (mut_735); ii) the absence of anthocyanins accumulation on both pages (mut_204, mut_150, mut_115, mut_137) as reported in Figure 4. Mut_735 derives from EMS mutagenesis of Italian wt_Jem; mut_204, mut_150, mut_115, mut_137 were obtained by fast neutron mutagenesis of English wild-type wt_JRC1.

ıut_735

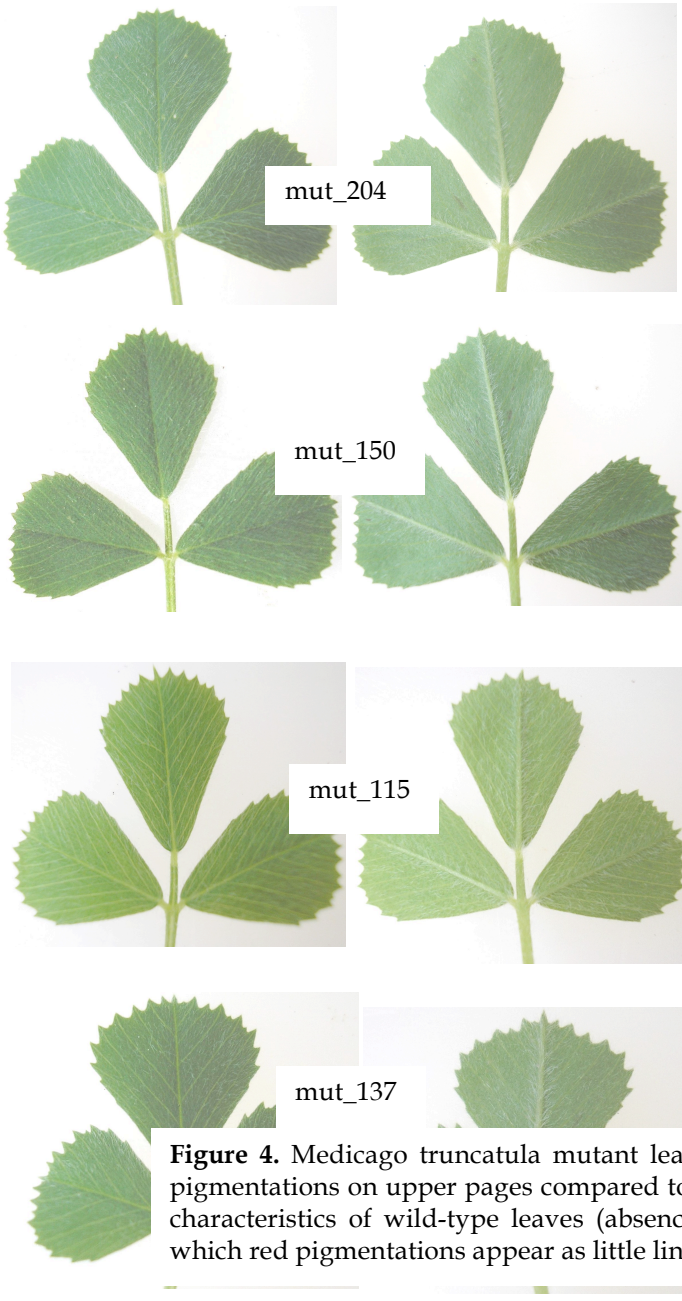

Figure 4. Medicago truncatula mutant leaves.As described in the text, all mutants have lost the re pigmentations on upper pages compared to their wild-types. The inferior pages, instead, keep the sam characteristics of wild-type leaves (absence of visible anthocyanin accumulation), except mut_735 i which red pigmentations appear as little lines

As in *M. truncatula,* anthocyanins can be accumulated in different tissues, the phenotypic analysis has been extended to flowers. In flowers, in fact, it is possible to see dark (blue or purple) pigmentations on the lower part of sepals and on the top of petals produced by anthocyanins accumulation. All genotypes show dark pigmentations on the

flowers except mut_735 where dark spots are absent (Figure 4). In contrast to wt_Jem, flowers of wt_JRC1 do not show large anthocyanin accumulation and the phenotype of its mutants is not homogeneous. About mutants, flowers of mut_204 are similar to wt_JRC1, mut_150 has not blue pigmentations, in mut_115 dark spots are visible on the sepals and mut_137 is very pigmentated, also much more than its wild-type.

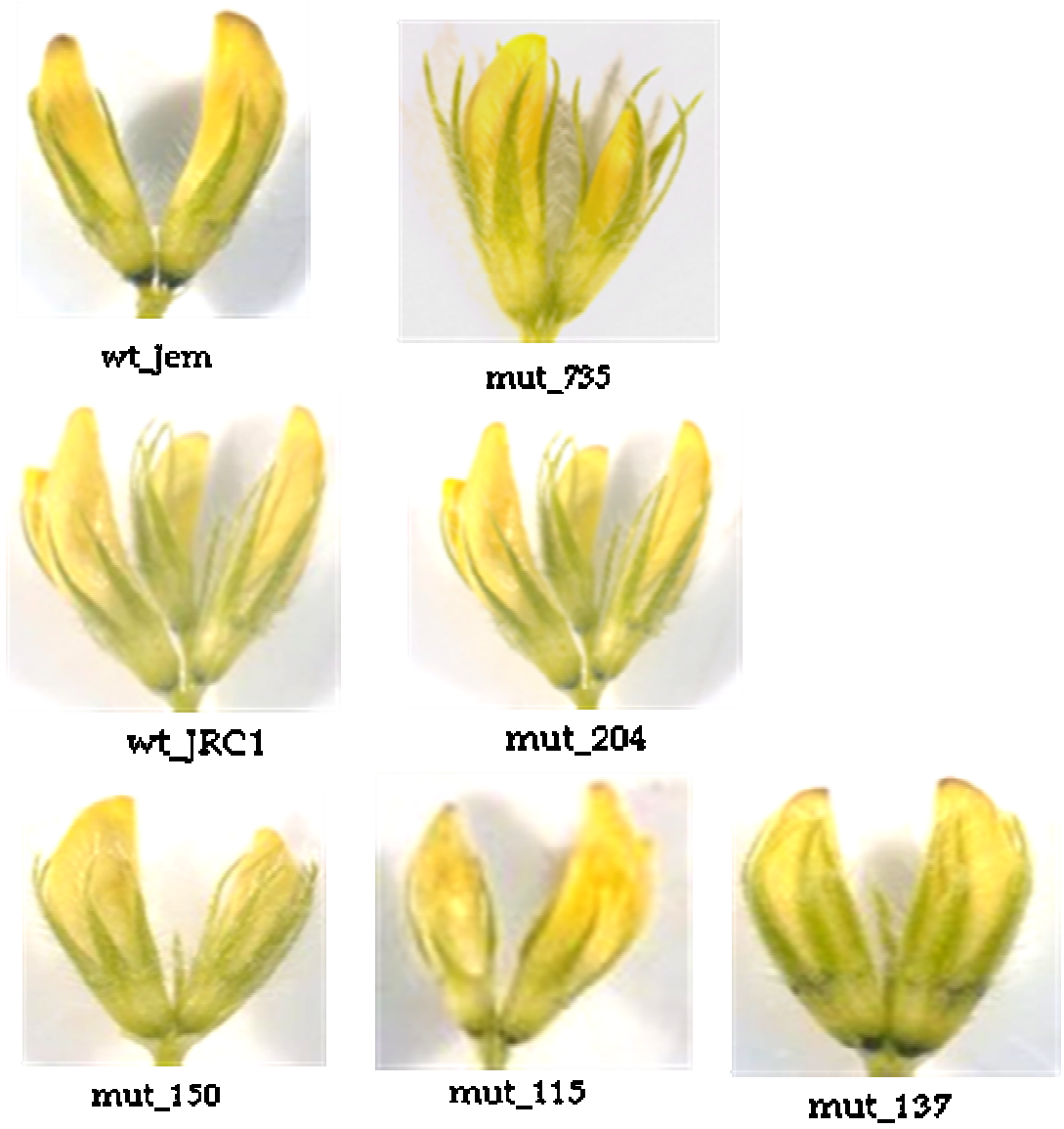

Figure 4. Flower details are shown.

During their life cycle, two wild-types and the five mutant genotypes were monitored and some physiological parameters were recorded such as pigmentation in young, mature and senescent leaves, pigmentation in flowers, flowering and fruit formation time. According to the available literature, in *Medicago truncatula* leaves the maximum peak of

anthocyanin production is between 22 and 26 day after leaf emission. According to this observation, all measurements and analysis reported in this thesis have been done at this stage. In Table 1 and Table 2 a summary of some physiological differences in the genotypes studied is reported.

All genotypes show evidence of anthocyanin accumulation in early developed leaves. At a mature stage (22-26 day after germination (DAG)), the mutant leaves acquire their final phenotype: the anthocyanin accumulation is totally absent in four mutants (mut_204, mut_150, mut_115, mut_137), and present as little lines in one of them (mut_735). At senescent stage (after 40 DAG), all genotypes show a strong reduction of anthocyanin accumulation and also, wild-types loose the characteristic red pigmentations on the leaves.

In this work the starting time of flowering and fruit production have been monitored. Interestingly, all mutants flower and produce fruits earlier their wild-types. Indeed a precocious fruit formation time in all mutants has been registered (the first fruit is visible in mut_150 and the last one in wt_Jem).

Table 1.Physiologica parameters observed in the Italian genotypes (wt_Jem and mut_735).

	wt_Jem	**mut_735**
young leaves *(0-20 days)*	big red spots on the upper page	spots (little lines/points) on both pages
mature leaves *(25 days)*	big red spots on the upper page	spots (little lines) on the lower page
senescent leaves *(after 40 days)*	lack of spots/presence of red points	lack of spots
flowering time *(DAG)*	60	47
flowers	dark spots on the sepals and petals	lack of spots
fruit formation *(DAG)*	64	50

Table 2. Physiological parameters observed in the English genotypes (wt_JRC1, mut_204, mut_150, mut_115, mut_137).

	wt_JRC1	**mut_204**	**mut_150**	**mut_115**	**mut_137**
young leaves *(0-20 days)*	big red spots on the upper page	spots (little lines/points) on both pages	spots (little lines/points) on both pages	spots (little lines/points) on both pages	spots (little lines/points) on both pages
mature leaves *(25 days)*	big red spots on the upper part	lack of spots	lack of spots	lack of spots	lack of spots
senescent leaves *(after 40 days)*	lack of spots/presence of red points	lack of spots	lack of spots	lack of spots	lack of spots
flowering time *(DAG)*	55	53	42	52	43
flowers	dark spots on the sepals	dark spots on the sepals	lack of spots	dark spots on the sepals	dark spots on the sepals and
fruit formation *(DAG)*	60	58	47	57	48

When these mutants arrived in our laboratory, the test for allelism has already been performed by Cathie Martin Laboratory at John Innes in Norwich, England. That test, through the complementation approach, confirmed that the mutation in these mutants was at different loci thus not allelic.

The first trial in our laboratory was dedicated to understand if the absence of red pigmentation on the leaves was due to a strong reduction of anthocyanin production or to an interruption to the anthocyanin transport from cytosol to vacuole. In fact, anthocyanins appear colored only when they are sequestered in the vacuole.

Quantification of total amount of anthocyanins in *M. truncatula* leaves

The total amount of anthocyanins in wild-type and mutant leaves has been extracted and quantified. Total anthocyanin content in *M. truncatula* leaves is presented in Figure 5. For this assay, leaves at 25days after leaf emission have been used, because this is the period of maximum pick of anthocyanin production in *M. truncatula* specie. A link between the presence of red spots on the leaves and the values of total amount of anthocyanins has been observed, challenging the interruption of anthocyanins transport hypothesis.

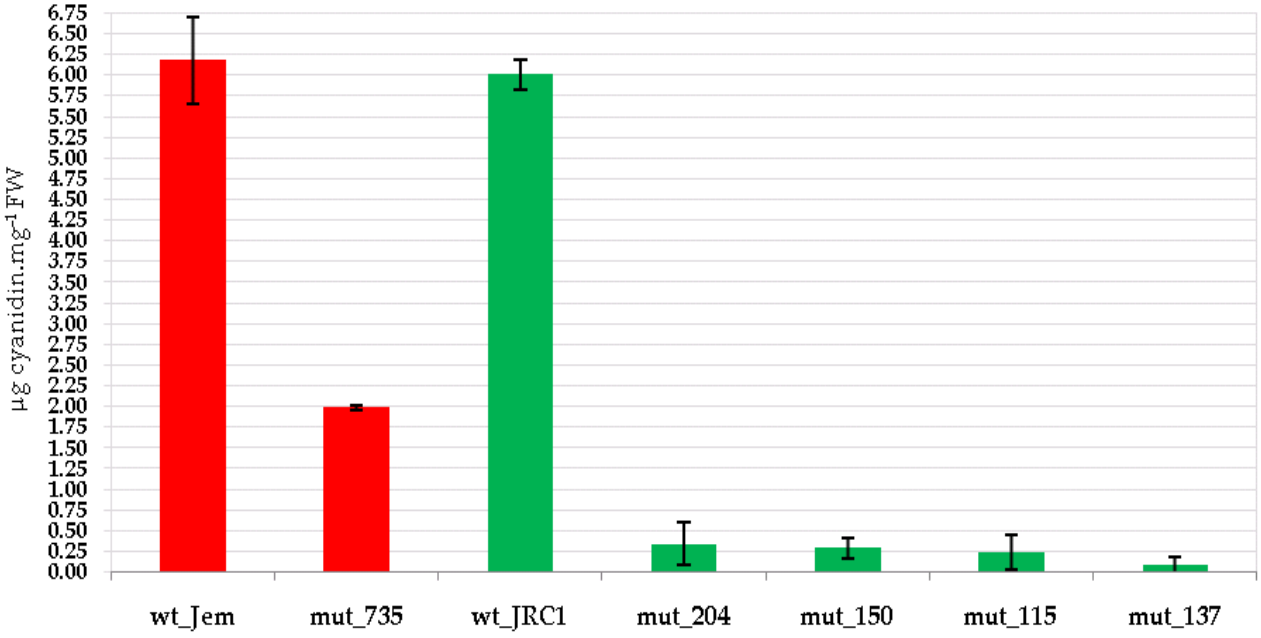

Figure 5. Total amount of anthocyanins in *M.truncatula* leaves in the seven genotypes described in this thesis. Red bars represent the Italian genotypes (wt_Jem and mut_735), while green bars indices English genotypes (wt_JRC1, mut_204, mut_150, mut_115, mut_137).

Accordingly wt_Jem and wt_JRC1 are the only two genotypes with evident pigmentations on the upper page of the leaf, index of major amount of anthocyanins. Mut_735 (with red pigmentations as little lines, see Figure 2) is characterized by a high reduction of anthocyanins respect to the wild-type, while a larger amount compared the other mutants, as already observed during the phenotypic analyses.

HPLC-DAD-MS/MS analysis

Chromatograms of pigmented samples are reported in Figures 6 and 7. Identification of anthocyanins required a combination of MS spectra and UV-Vis spectra for attribution of major peaks (Baldi *et al.*, 1995). Thus, the data are consistent with a cyanidin-3-*O*-feruloyl approximately 12 (peak 1), 14 (peak 2), 15 (peak 3) and 22 (peak 4) minutes. Due to small amount of original samples peak 1 and 3 are here reported as unknown anthocyanins because TIC chromatograms, obtained performing full-scan analysis, produced no useful preliminary information on predominant m/z ratios for further MS-MS isolations.

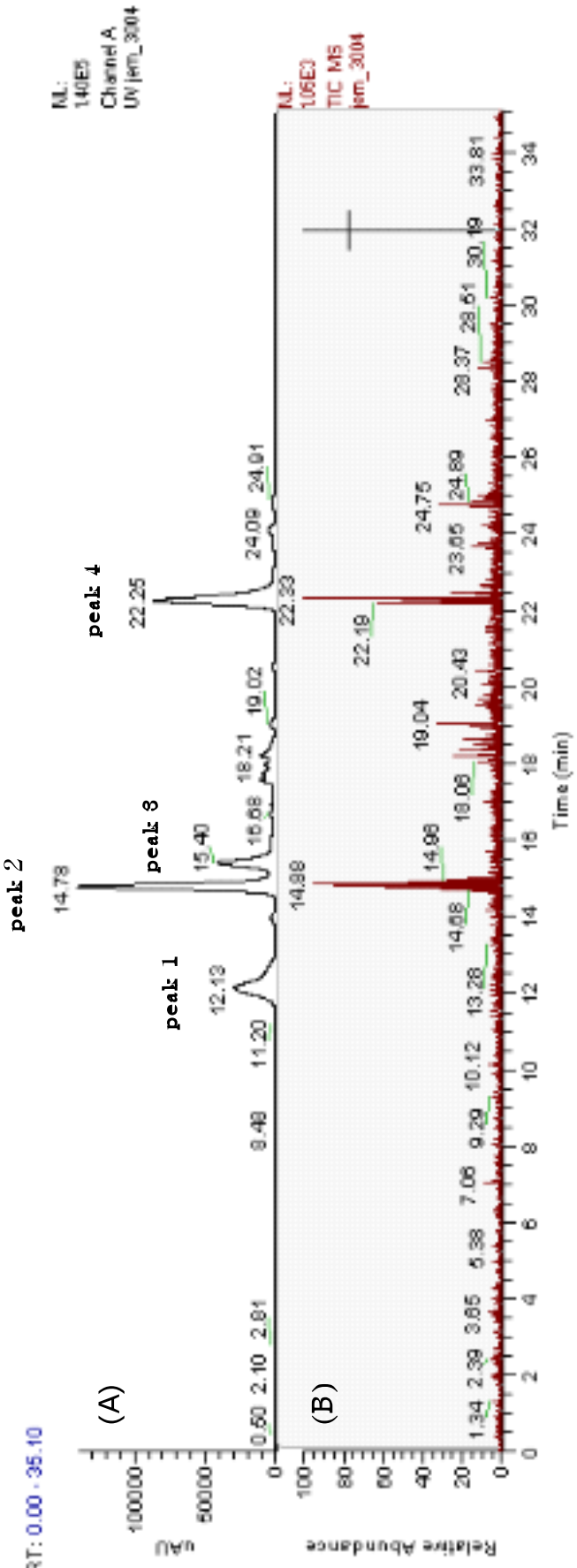

Figure 6. (A) HPLC-UV chromatogram (detection was set at 320 nm) of wt_Jem; (B) TIC chromatogram of wt_Jem.

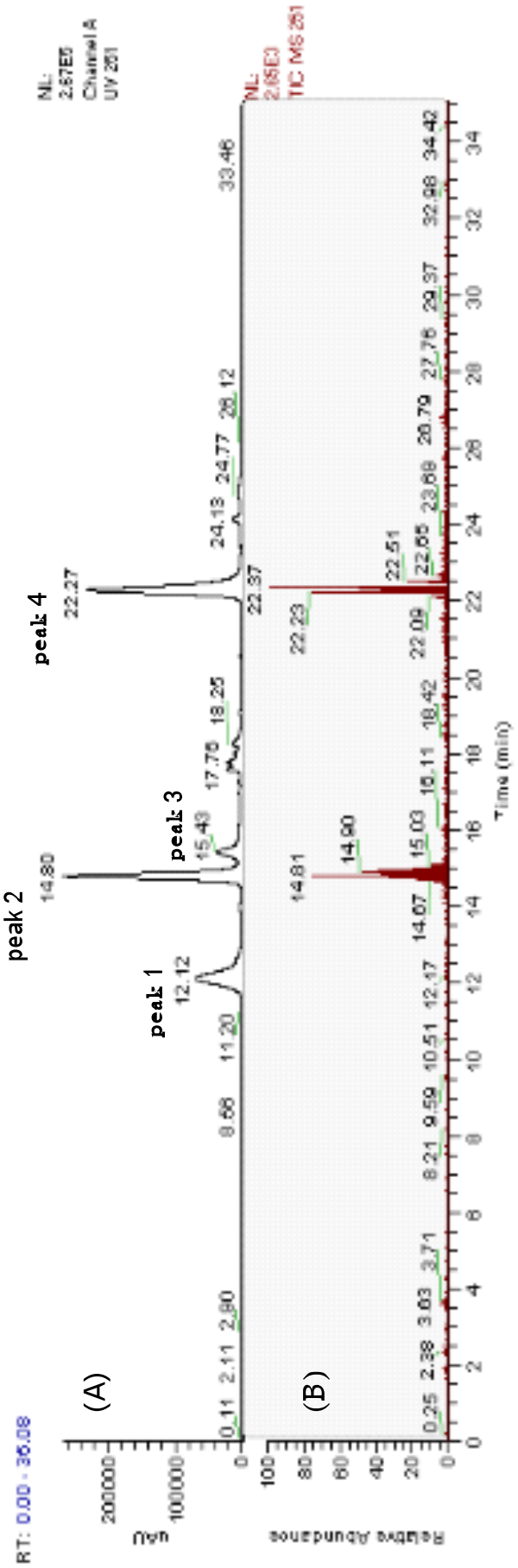

Figure 7. (A) HPLC-UV chromatogram (detection was set at 520 nm) of wt_JRC1; (B) TIC chromatogram of wt_JRC1

Anyway diode array scans revealed that these peaks have UV-Vis absorption pattern consistent with common anthocyanins with maxima at 280 and 520 nm (Figure 8). The two major peak (peak 2 and peak 4) have been investigated. The parent ion observed for peak 2 was m/z = 625 amu with major fragments at m/z = 449 amu and 287 amu. (Figure 8A). The fragment masses of 287 and 449 are equivalent respectively to the mass of cyanidin and cyanidin-3-O-glucoside ions (Dugo *et al.,* 2003). Thus, this anthocyanin is consistent with a cyanidin-3-O-glucoside acylated with an aliphatic acid. Even UV-Vis spectra of this compound is consistent with this identification (Figure 8B) caused by the lack of absorption in the 320-350 nm range. Peak 4 presented a parent ion at m/z 667 amu with major fragments at m/z 491 and 287 (Figure 8A). The 176-amu mass difference is consistent with the loss of a ferulic acid (Wu and Prior, 2005). Indeed, UV-Vis spectra of this compound presents a maximum at 340 nm, typical for an aromatic acylated group. A difference of 204 amu (491-287 amu) corresponds to the acetyl-glucoside group (42+162 amu), as widely reported in literature (Wu and Prior, 2005).

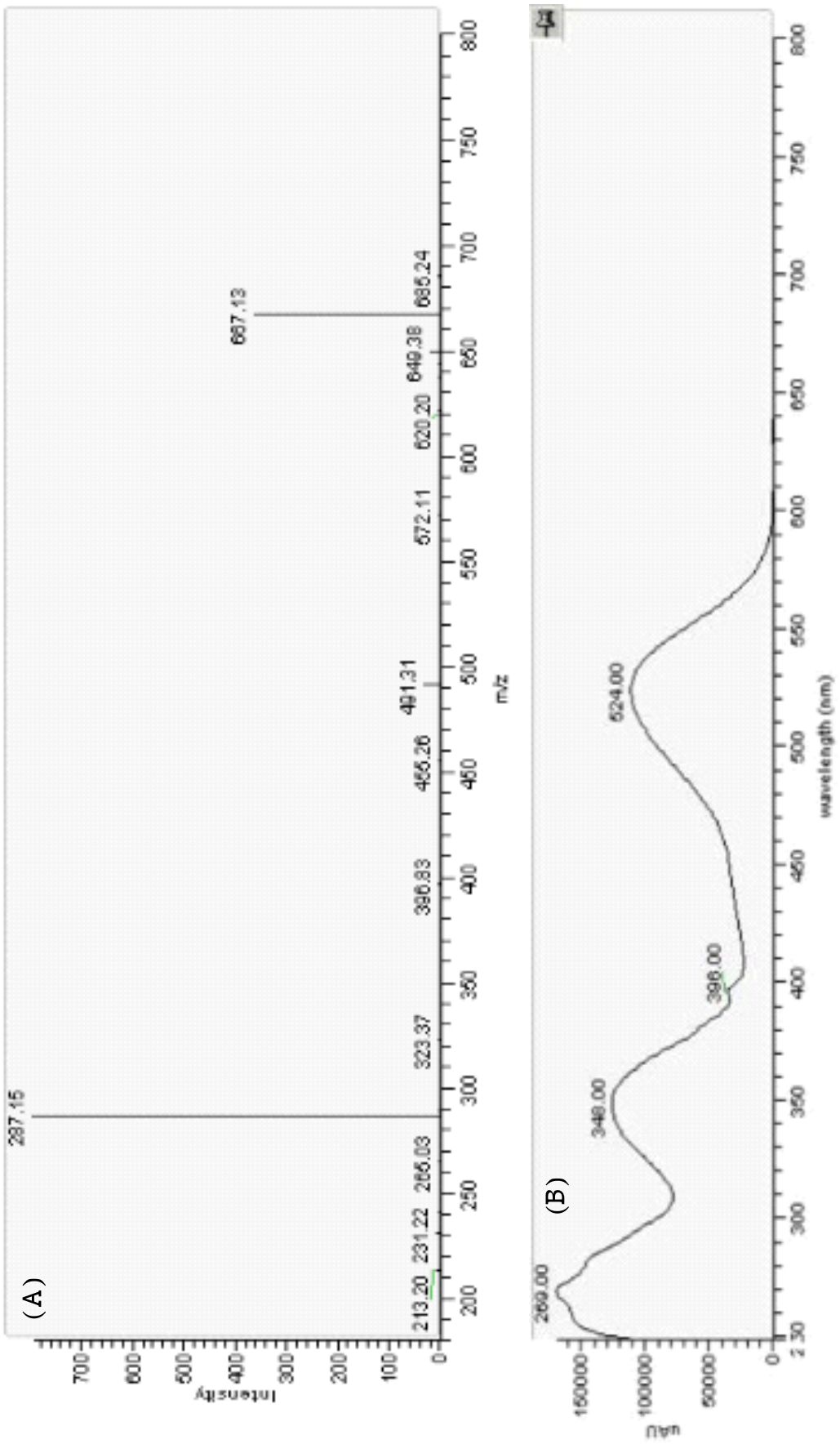

Figure 8. (A) LC-ESI/MS/MS and (B) UV-Vis spectra for peak 4 (parent ion 625 amu).

In order to assess the presence of flavonoids in the *M. truncatula* mutants, the localization of those pigments in immature seeds was also investigated.

Localization of flavonoids in immature seeds

Vanillin assay is a histochemical assay used to localize in tissues two classes of flavonoids: flavan-3-ols and proanthocyanidins (tannins or PAs). Vanillin, in acid environment, reacts with tannins and flavans to create a red product. This method is useful to detect flavonols because they are not coloured in nature. For each genotype analysed, some immature seeds have been tested (Figure 9). No clear differences between mutants and wild-types were observed concerning the localization of flavonoids. This means that the potential mutations in these plants unlikely produce consequences at flavonoids localization level in immature seeds.

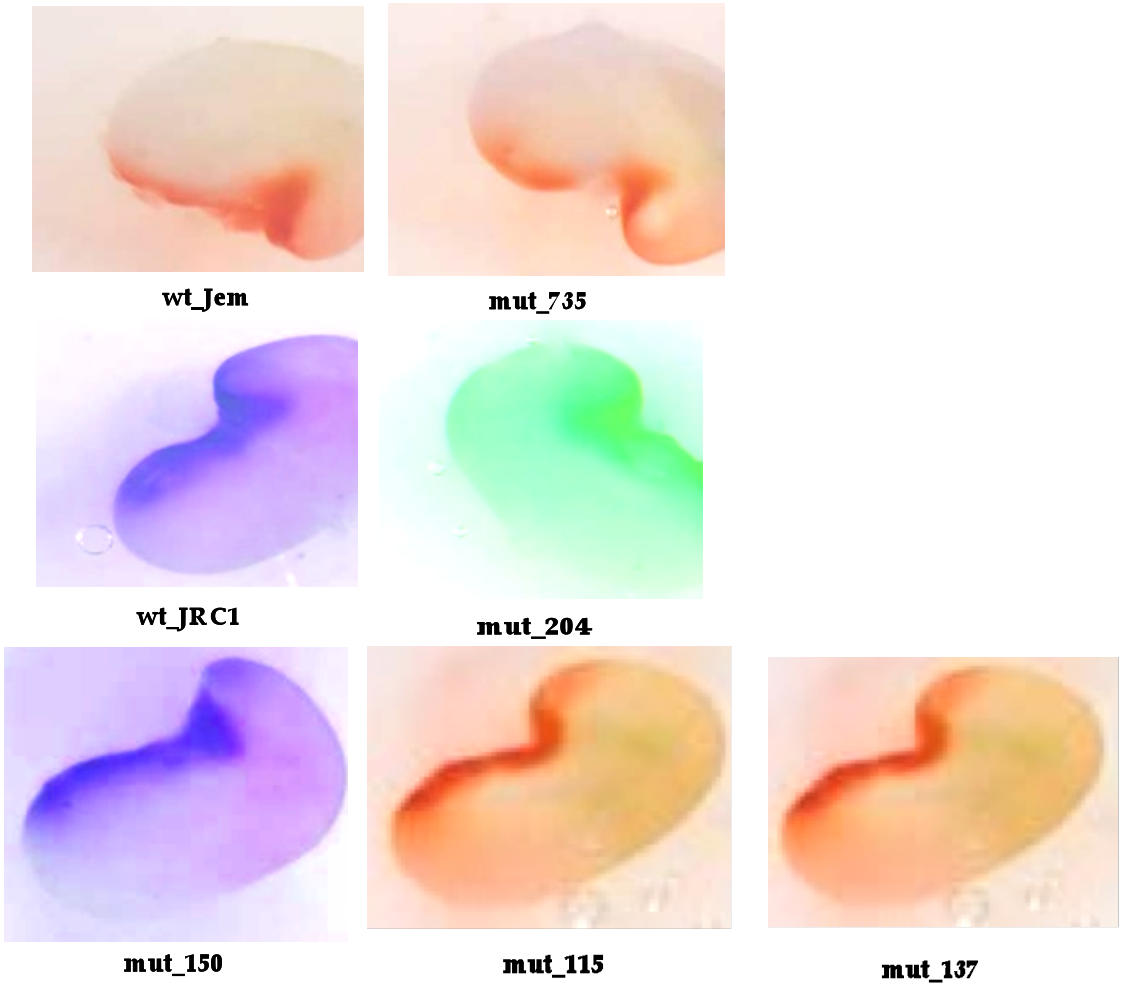

Figure 9. Histochemical detection of flavonoids in *M. truncatula* immature seeds.

From literature (Lepiniec et al., 2006), it is well known that the seed coat of legume mature seeds recover a large amount of tannins, also called proanthocyanidins. They are a class of flavonoids investigated for their positive effect on plant, animal and human health. For that reason, they became targets for genetic modification to improve their amount in forage, forage quality traits and the "plant-healthiness" for human diet. In this work the amount of soluble and insolubile tannins in *M. truncatula* mature seeds was quantified with butanol-HCL (Porter *et al*., 1986) method (Figure 10). In this assay, *Arabidopsis thaliana* (Ara) mature seeds have been used as positive control.

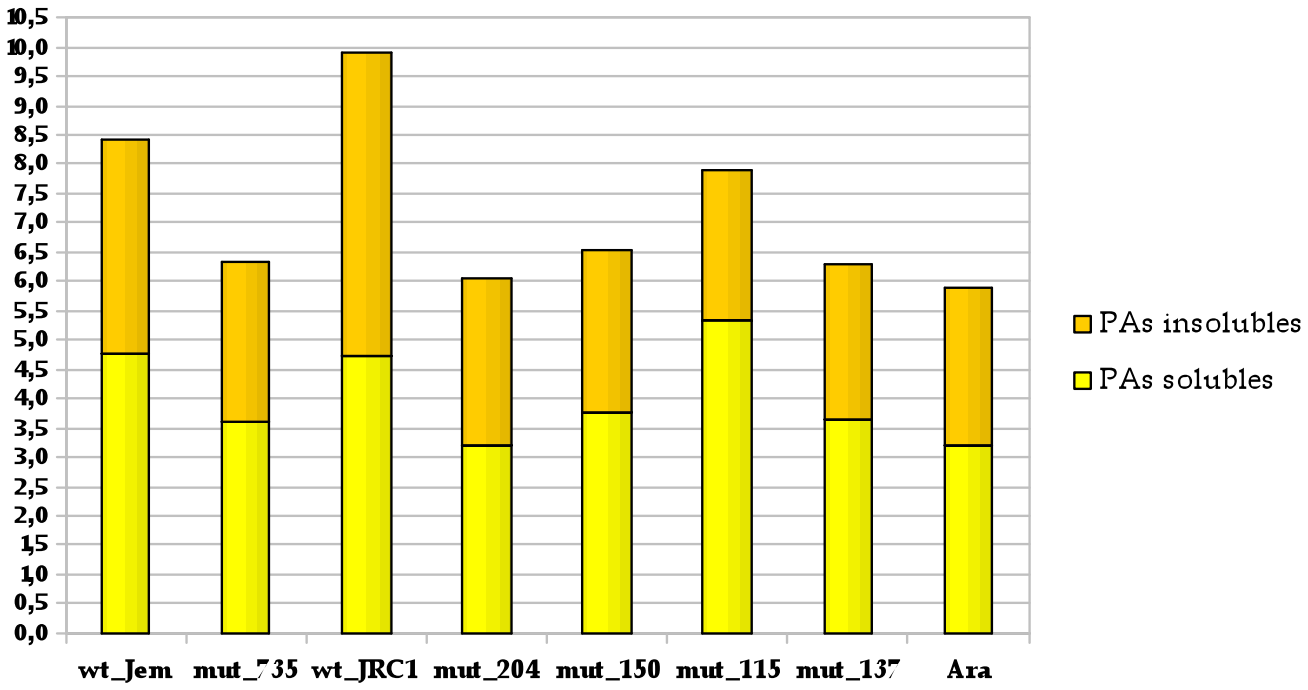

Figure 10. Analysis of soluble and insoluble PAs measured after acid-catalyzed hydrolysis

The seven genotypes (two wild-types and five mutants) investigated do not show significant differences in tannins quantity. However mut_115 is the genotype with the larger amount of soluble tannins (the detectable tannins) also considering the two Medicago wild-types (wt_Jem and wt_JRC1). The comparison between tannin amount in *M. truncatula* and Arabidopsis seeds has never been published before (Figure 11). From this results it seems that in *M. truncatula* mature seeds present a larger amount of tannins compared to Arabidopsis mature seeds.

Expression analysis of genes codifying enzymes involved in flavonoid biosynthesis

To further characterize the two wild-types and the five mutants of *M. truncatula*, the subsequent step has been the gene expression analysis of the enzymes and transcriptional factors involved in flavonoid biosynthesis. Poor information on gene annotation of genes that belong to flavonoid pathway in *M. truncatula* is available in public genebanks. In fact only three genes DFR1, DFR2 and LAR belong to barrel medic. A comparative genomic approaches has been thus requested starting from protein sequences well annotated in other species. Using the Blastp software (based on the homology sequence research), the Medicago sequence have been find and used for the primer design.

This approach allowed to retrieve 28 *M. truncatula* gene sequences linked to this flavonoids metabolic pathway. The total number of Medicago genes tested in this thesis has been 31: 3 annotated in the public genebanks and belonging to *M. truncatula*, 28 obtained using the homology approach. They belong to 5 flavonoid classes: anthocyanins, flavonols, flavones, isoflavones and condensed tannins. In the 31 genes investigated, 21 encode the key enzymes and 10 encode the most common transcription factors involved in flavonoid pathway. Here below, in Figure 11, the RT-PCR assay is reported, showing the expression of these genes in the seven genotypes (two wild-types and five mutants).

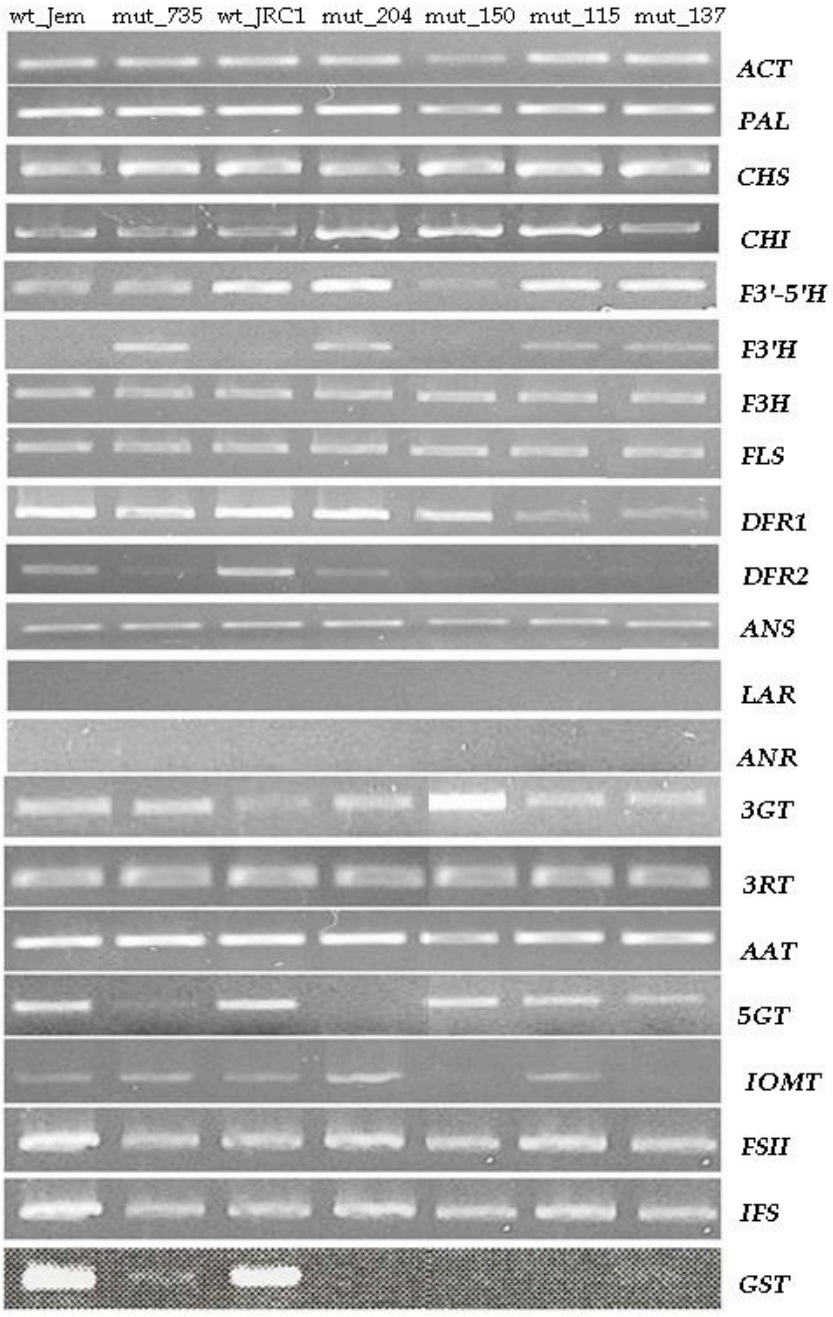

Figure 11. Expression profiles of the genes encoding the key enzymes in flavonoid biosynthesis have been evaluated by RT-PCR for each *M. truncatula* wild-type and mutant genotypes.

RT-PCR results show different possible pathway of reduction of anthocyanins in the five mutants. It seems that the two wild-types and mut_150 lack *F3'H* gene expression. Possibly in the naringenin level of biosynthesis pathway (see Figure 2), the metabolic flow is shifted towards pentahydroxyflavanone intermediate through the activity of F3'5'H enzyme.

DFR2 gene, a common enzyme responsible of anthocyanins accumulation, is expressed in the two wild-types and in mut_204 (that unexpectedly does not show the red pigmentations on the leaves). In other genotypes (with marked reduction of anthocyanins accumulation), the *DFR2* gene expression is very low or absent.

3GT, the first enzyme of anthocyanin biosynthesis after *ANS* action, seems over expressed in *M. truncatula* genotypes with red pigmentations (wt_Jem, wt_JRC1 and mutant).

5GT, the last enzyme of anthocyanin metabolic pathway, is down regulated in mut_735 and absent in mut_204.

It is possible also postulate that in the seven genotypes the production of tannins on the leaves is absent because LAR and ANR, the two enzymes required for tannin biosynthesis, are not expressed (Figure 11).

The expression of GST gene is clearly correlated to anthocyanin accumulation.

The RT-PCR data have been confirmed by qPCR. Only the genes that, through semiquantitative PCR, showed a large difference expression between mutants and wild-types have been tested: *DFR2, DFR1, F3'H, F3'5'H, IOMT, 3GT, 5GT,* and *GST*.

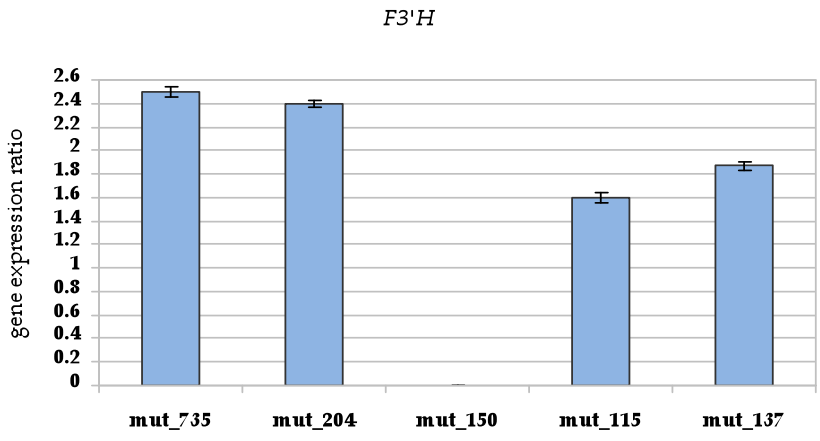

F3'5'H

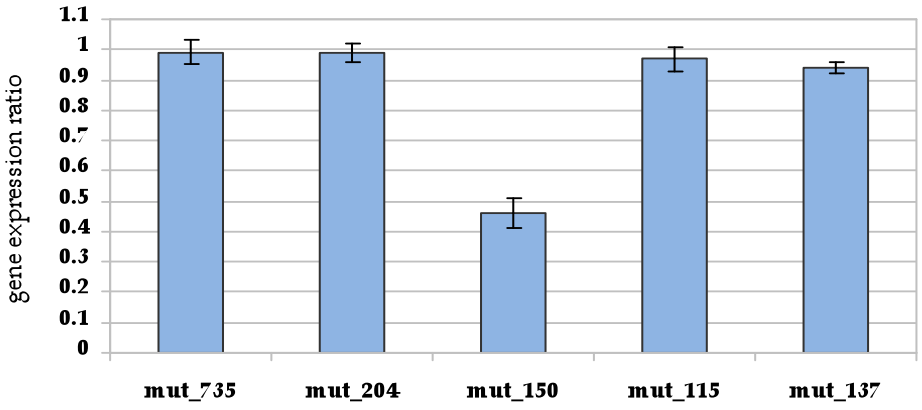

DFR1

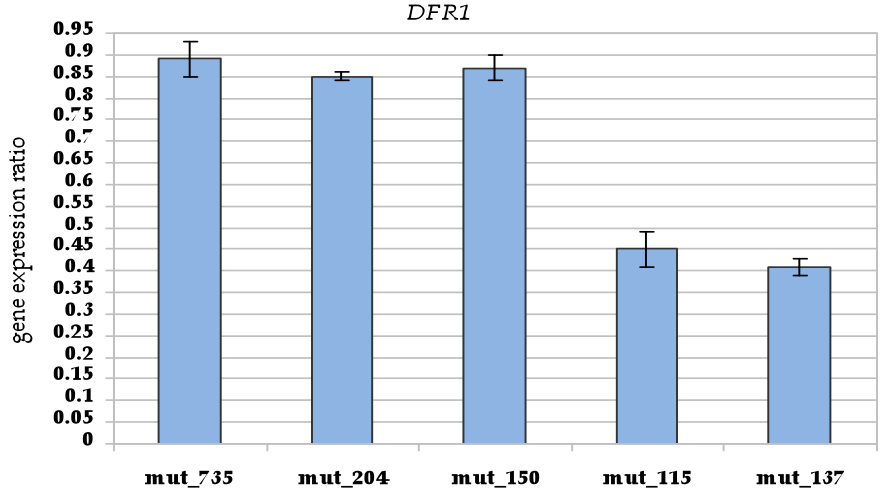

DFR2

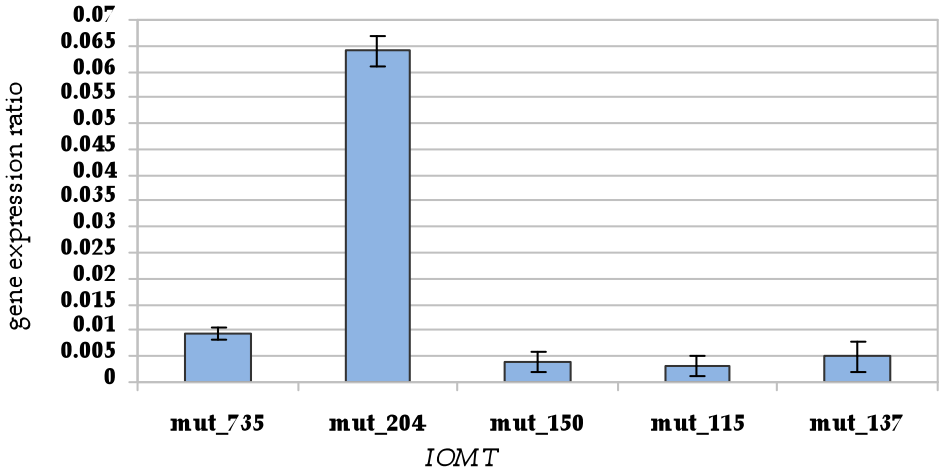

IOMT

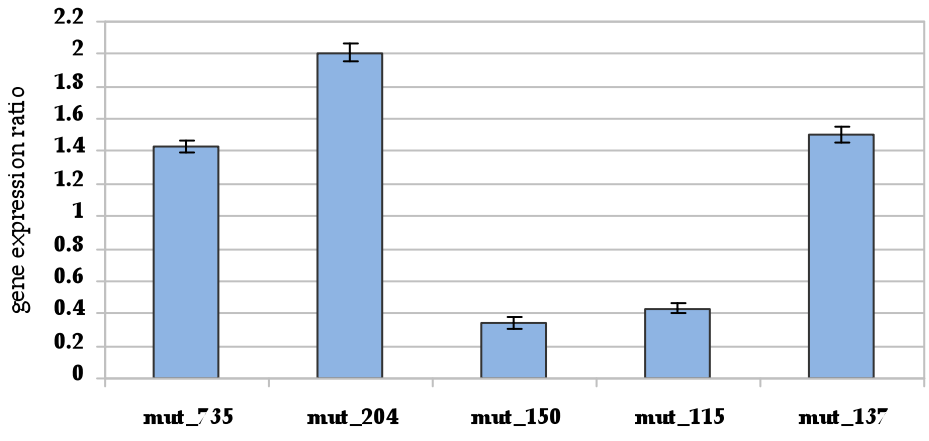

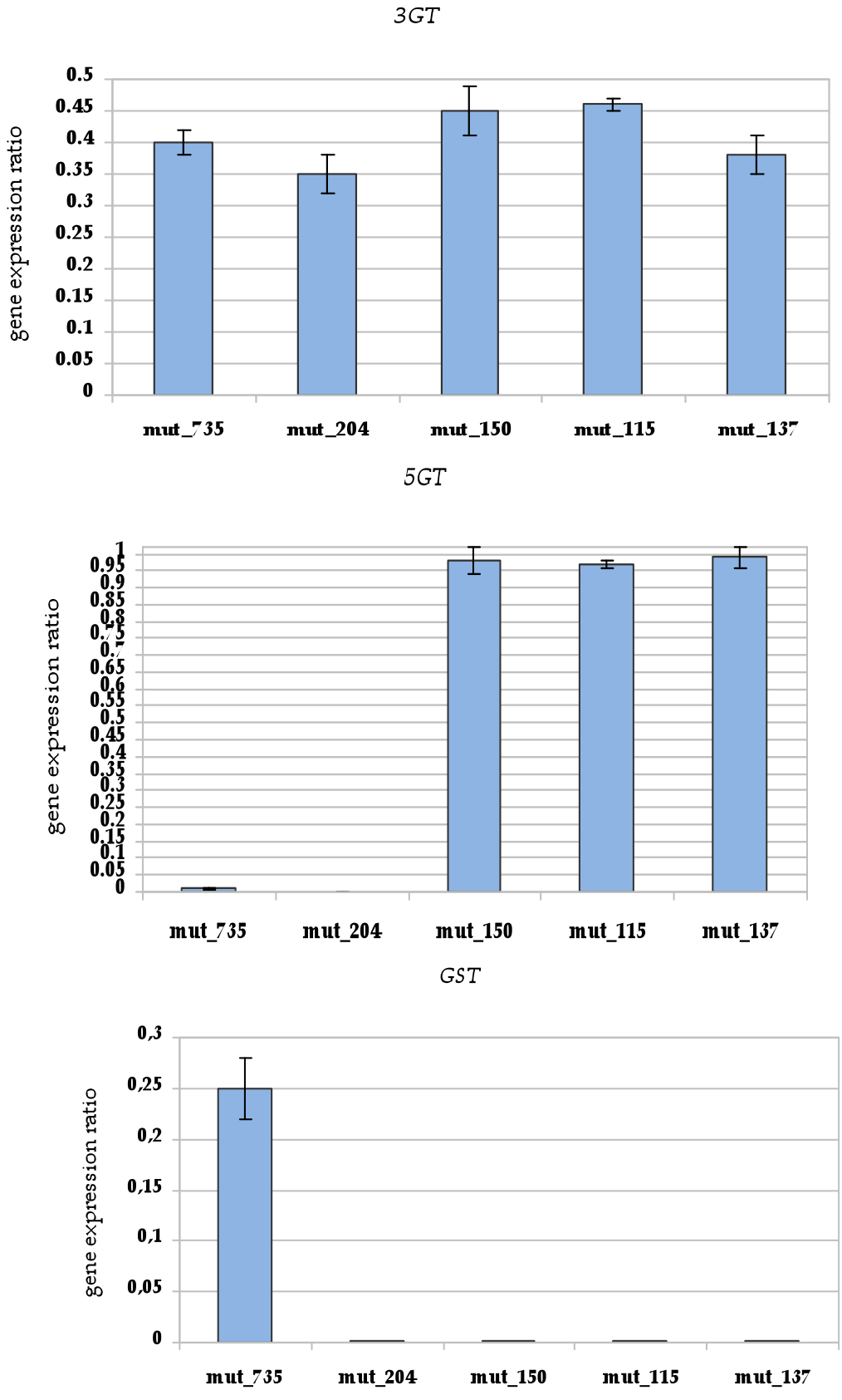

Figure 12. qPCR assay. F3'H, F3'5'H, DFR1, DFR2, IOMT, 3GT, 5GT, and GST gene expression in *M. truncatula* mutants. In each graphic the blue bars represent the value of gene expression ratio between the mutant and the relative wild-type. When the ratio is 1, the expression level of the target gene is the same in the wild type and in the mutant genotype.

In this work -actin gene has been used as reference gene and all the qPCR results have been normalized on -actin 11 gene expression (Kuppusamy *et al.*, 2004).

The expression of that reference gene is the same between the mutants and moreover it is the same between the mutants and the respective wild-type.

DFR1 and *DFR2* gene are well known to be related to anthocyanin biosynthesis. Tissues with high production of anthocyanins show a relevant level of one or both of these genes (Xie *et al.*, 2004).

In our mutants *DFR2* gene is obviously linked to red pigmentation production on the leaves. In fact only the two wild-types characterized by a big accumulation of anthocyanins on the leaves have a relevant *DFR2* gene expression.

3GT and *5GT* are specific genes of anthocyanin biosynthesis. *3GT* is localized at the beginning of the biosynthesis pathway (it is the second gene involved), while *5GT* is the last gene that takes part in anthocyanin metabolic pathway. They behave differently in the *M. truncatula* mutants, since 3GT seems to have a proportional trend with the phenotypic characteristics of mutants, conversely the expression of second gene appears independent of anthocyanins amount.

IOMT, a well known gene involved in isoflavones production and indeed extremely important in Leguminosae family, does not appear to be link with anthocianins. Mut_735, mut_204 and mut_137 show, in fact, higher level of *IOMT* expression compared to the wild-types.

The last expression profile tested with qPCR concerns *GST* gene. Gst protein is the flavonoids carrier, it binds them in the cytosol (where they are produced) and it transports them into the vacuole (where they are stocked). In *M. truncatula* genotypes (two wild-types and five mutants), the expression level of *GST* gene is closely related to estimated amount of anthocyanins as reported in Figure 12. In fact, the gene is expressed in the two wild-types (wt_Jem and wt_JRC1) and in the mutant (mut_735) with higher amount of pigments. It is likely that gst protein is subjected to feedback regulation mode, i.e. if the anthocyanins production is blocked, also the gst carrier production is inhibited.

Expression analysis of genes encoding transcriptional factors involved in flavonoid biosynthesis

To carry out a exhaustive molecular study of these mutants, also the expression profiles of genes coding for transcription factors (TF) has been investigated. In table 3, the ten TF analysed are reported.

Table 3. The main features of the *M. truncatula* genes encoding transcription factors analysed in the present work are shown.

Transcription Factor Gene	Acronimous	Accession number	Original specie	Gene family
TRANSPARENT TESTA GLABROUS 1	AtTTG1	CR940305	*Arabidopsis thaliana*	WD40-like
GLABROUS 3	AtGL3	AC135317	*Arabidopsis thaliana*	myc
ENHANCER GLABROUS 3	AtEGL3	AC135317	*Arabidopsis thaliana*	myc
ANTHOCYANIN 2	PhAN2	AC152405	*Petunia hybrida*	myb
PRODUCTION OF ANTHOCYANIN PIGMENT 1	AtPAP1	AC172742	*Arabidopsis thaliana*	myb
PRODUCTION OF ANTHOCYANIN PIGMENT 2	AtPAP2	CT573509	*Arabidopsis thaliana*	myb
PERICARP	ZmP	AC145329	*Zea mays*	myb
PURPLE LEAF	ZmPL	AC119408	*Zea mays*	myb
MYB15	*AtMYB15*	AC149493	*Arabidopsis thaliana*	myb
MYB4	*AtMYB4*	AC121235	*Arabidopsis thaliana*	myb

AtTTG1 is required for the accumulation of purple anthocyanins in leaves and stems. It is involved in trichome and root hair development. It controls epidermal cell fate specification, affecting also dihydroflavonol 4-reductase gene expression.

AtGL3 encodes a basic helix loop helix (bHLH) domain protein that interacts with the myb protein GL1 in trichome development and it is well known the link of this TF and anthocyanin production.

AtEGL3 encodes a bHLH transcription factor. The protein interacts with TTG1, the myb proteins GL1, PAP1 and 2, CPC and TRY, and it will form heterodimers with GL3.

AtPAP1 (also called myb75) and AtPAP2 (known also as myb90) transcription factors, containing MYB domains, are involved in anthocyanin metabolism and radical scavenging. They are essential for the sucrose-mediated expression of the dihydroflavonol reductase gene.

ZmPL works in the vegetative plant tissues to activate transcription of the structural genes of anthocyanin biosynthesis.

ZmMYBP controls phlobaphene biosynthesis in pericarp tissue. Phlobaphenes are derived from the flavonoid pathway that also gives rise to anthocyanins.

PhAN2 is required for the accumulation of anthocyanins in flowers and vegetative tissues.

AtMYB15 transcription factor is responsive to salt stress, auxin, ethylene, jasmonic acid, cadmium ions and chitin.

AtMYB4 encodes a transcriptional repressor of the cinnamate 4-hydroxylase (C4H) gene which is involved in the biosynthesis of flavonoids.

In figure 13 the expression levels (obtained by RT-PCR) of the genes encoding transcription factors hereby tested are shown. □-actin gene has been considered as reference gene to evaluate the expression of target genes.

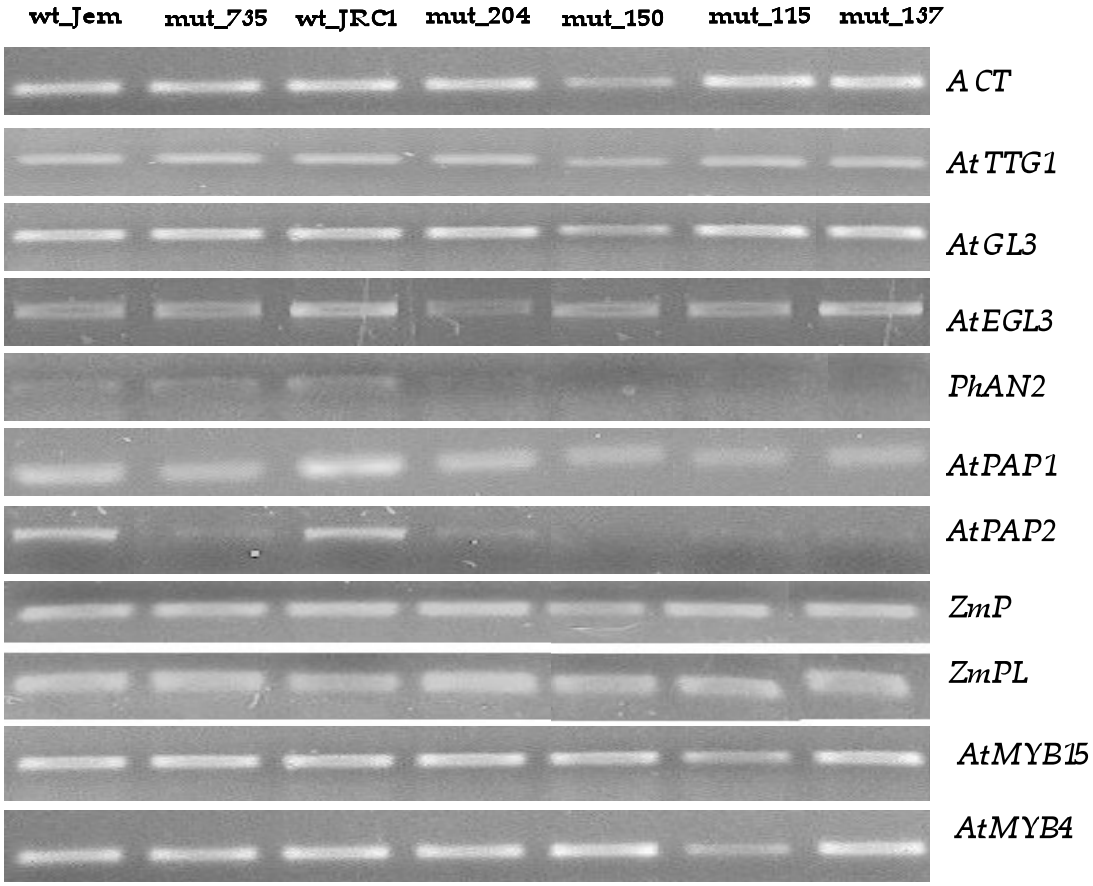

Figure 13. Expression profiles of the most common transcriptional factor genes involved in flavonoid pathway evaluated by RT-PCR.

After RT-PCR analysis (Figure 13), several interesting results have been obtained. The genes homologous to PhAN2 and AtPAP2 are clearly linked to anthocyanin production since their expression is higher in the genotypes with red spots (wt_Jem, wt_JRC1 and mut_735). Also the genes homologous to *AtMYB15* and *AtMYB4* show different expression levels among the seven genotypes. It seems that in wt_Jem, mut_735 and mut_150, the expression level of MYB15 is very low.

Mut_ 150 is the only genotype showing repression of the MYB4 gene. These observations have been confirmed by qPCR as shown here below in Figure 14.

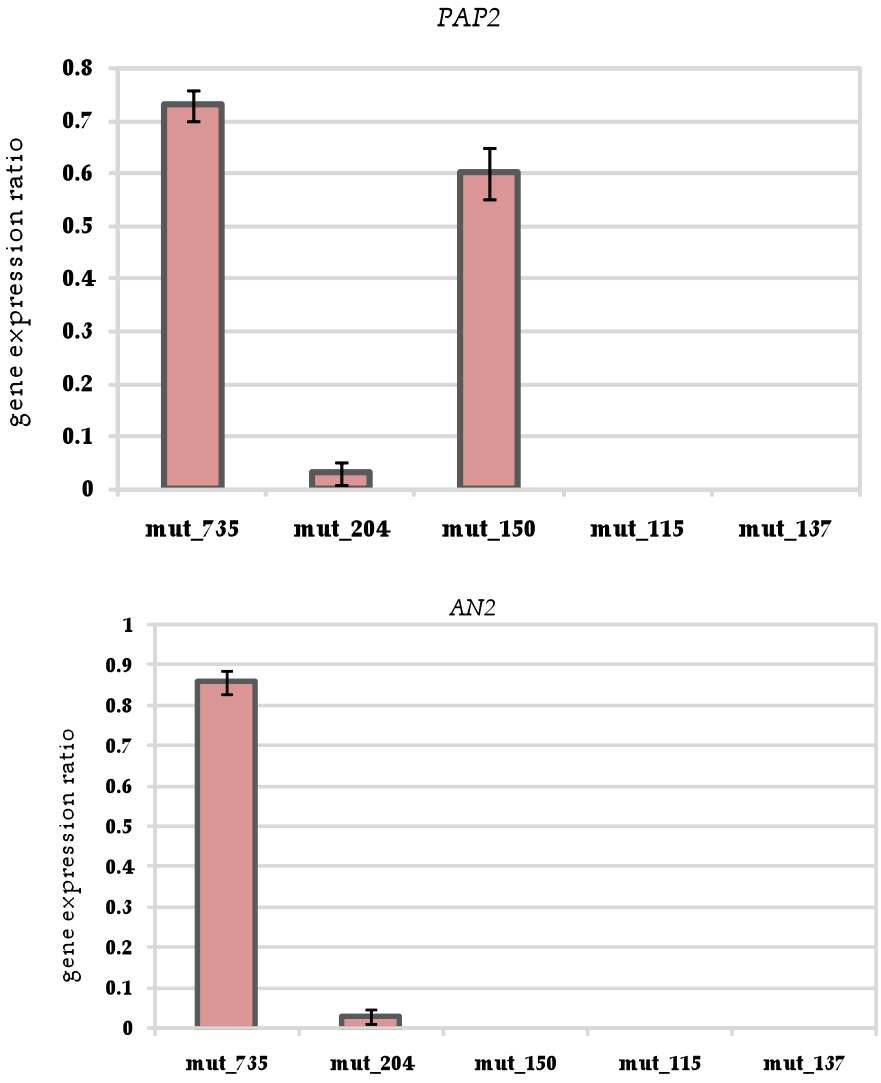

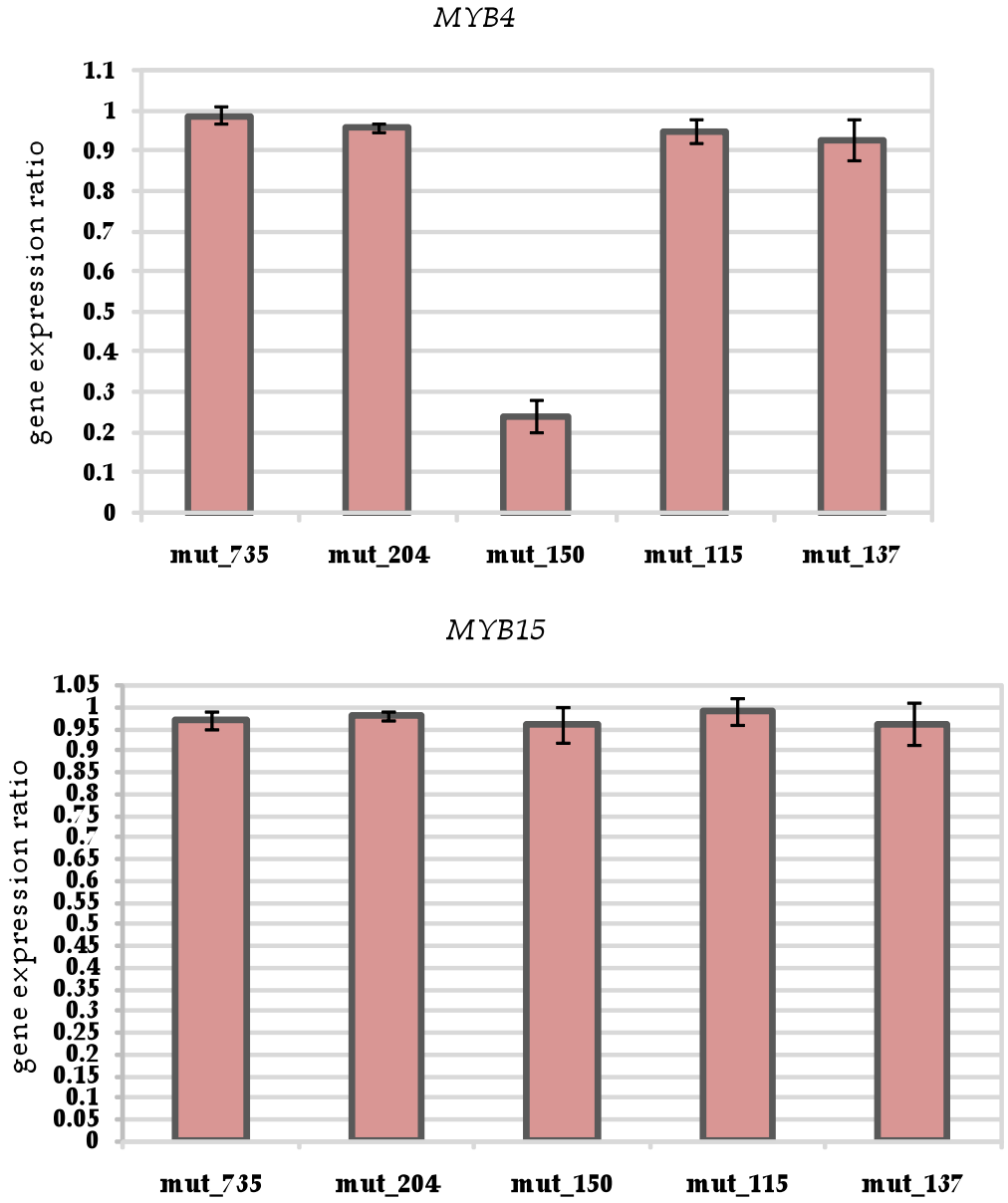

Figure 14. qPCR assay. The *M. truncatula* homologous genes of *PhAN2*, *AtPAP2*, *AtMYB15*, *AtMYB4* were tested by qPCR. In each graphic the pink bars represents the value of gene expression *ratio* between the mutant and the relative wild-type. When the ratio is 1, the expression level of the target gene is the same in the wild type and in the mutant genotype.

- **UV-B treatment and oxidative stress response**

As described in Chapter 1, flavonoids and anthocyanins are implicated in the protection of the cells against damages. They enhance the mechanisms that protect the photosynthetic apparatus of plants from the damaging effects caused by reactive oxygen species (ROS), produced during oxidative stress. In this work the seven genotypes have been irradiated with ultraviolet-B (UV-B) radiations to investigate their photosynthetic behaviour under oxidative stress condition.

Measurement of chlorophyll fluorescence parameters and anthocyanin content

The aim of this experiment is to investigate the effect of UV-B treatment on the chlorophyll fluorescence parameters in relation to anthocyanin content in wild-type and mutant genotypes. The measurement has been performed on leaves 30 DAG-old before, after 4hrs and 14hrs of UV-B treatment and after 24hrs of recovering period.

Three chlorophyll fluorescence parameters have been estimated: maximum fluorescence yield in the light-acclimated state (Fv/Fm); photochemical quenching (qP) and non-photochemical quenching (NPQ)..

The Fv/Fm, qP and NPQ parameters measured on seven genotypes of barrel medic before (UT), during (4hrs and 14 hrs) of UV-B treatment and after a recovering period of 24hrs (rec) are presented in Table 4. Mut_735, mut_150, mut_115 and mut_137 have an higher value of Fv/Fm than wild-types and mut_204. Mut_115 and mut_735 have higher values of qP. Non significant differences are detected for NPQ between wild-types and mutants. As expected, the anthocyanin content varies significantly between wild-types and mutants.

As regards UV-B treatment, Fv/Fm is lower at 14hrs after treatment and remain low during the recovering phase. Similarly, the non photochemical quenching is statistically different between 4 and 14 hrs after UV-B treatment. qP values during the UV-B treatment are intermediate between UT and rec phase. A significant increase in anthocyanin content is observed after 4hrs of UV-B treatment.

The interaction Genotypes x Treatment is statistically significant for the three traits ($P<0.001$).

Table 4. Effects of UV-B treatments on chlorophyll fluorescence parameters and anthocyanin contents in leaves of seven genotypes of *M.truncatula*. UT, Untreated; 4 and 14, hrs after UV-B treatment; rec, 24 hrs of recovering period.

Genotypes	Fv/Fm	qP	NPQ	Anthocyanins (μg cyanidin * g^{-1} FW)
wt_Jem	0.786 d	0.372 cd	0.064 cd	30.7 b
mut_735	0.818 a	0.441 b	0.084 ab	8.4 c
wt_JRC1	0.810 b	0.393 c	0.050 de	65.4 a
mut_204	0.796 c	0.258 e	0.061 cd	6.2 cd
mut_150	0.820 a	0.356 d	0.095 ab	1.2 e
mut_115	0.822 a	0.480 a	0.073 bc	4.7 ce
mut_137	0.823 a	0.351 d	0.035 e	2.9 de
Significance	0.001	0.001	0.001	0.001
Treatment				
UT	0.822 a	0.327 d	0.036 b	16.0 bc
4h	0.828 a	0.358 c	0.040 b	20.6 a
14h	0.797 b	0.378 b	0.096 a	18.7 ab
rec	0.796 b	0.452 a	0.092 a	13.0 c
Significance	0.001	0.001	0.001	0.001
Interaction G x T				
Significance	0.001	0.001	0.001	0.001

Within the same coloumn and within each experimental factor, means followed by the same letter are not significantly different at $P< 0.05$ according to Tukey's test.

Expression analysis of *GST* gene involved in anthocyanin transport after UV-B treatment

The expression of the GST gene involved in anthocyanin transport has been tested in the leaves of the seven genotypes treated with UV-B radiations. Figure 15 reports the RT-PCR analysis of GST before and after 14hrs of UV-B treatment.

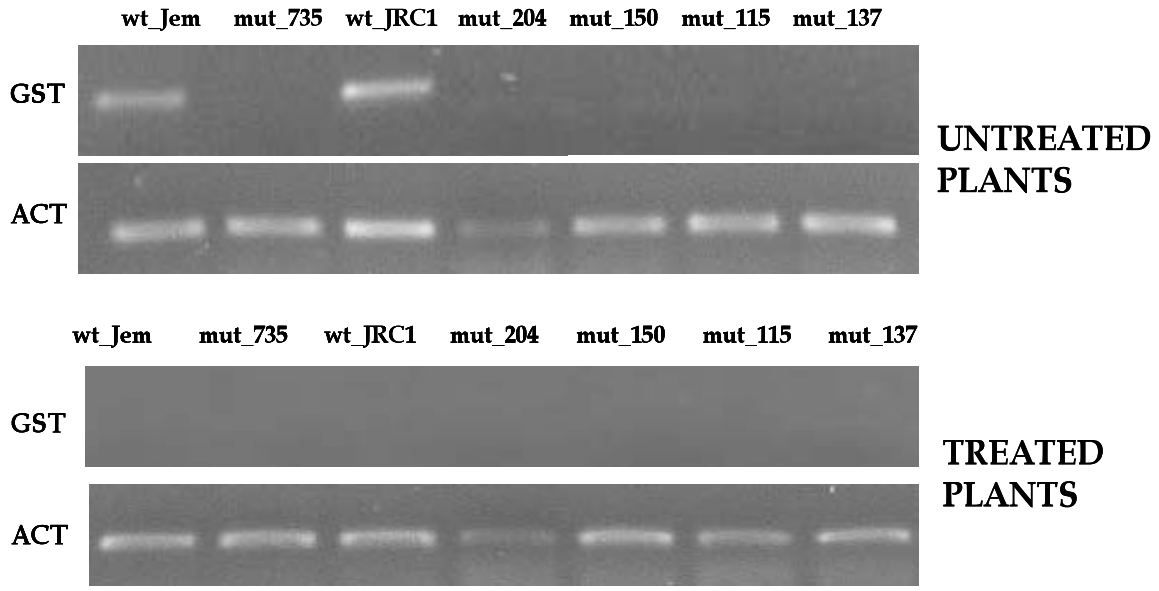

Figure 15. Expression profiles of *GST* gene evaluated by RT-PCR for each *M. truncatula* wild-type and mutant genotypes before and 14hrs after treatment.

In untreated genotypes, the *GST* gene, codifying the vacuolar carrier is expressed only in the two wild-types (plants with big red spots on the leaves) and absent in the mutants, as expected. After 14hrs of UV-B treatment, interestingly, the expression of *GST* gene is absent in all genotypes. This experiment has been performed in three independent biological replications.

The results presented in this chapter, although preliminary, indicate that UV-B light (280-320nm) induces anthocyanin accumulation in some genotypes. The accumulation of phenylpropanoid compounds in response to UV-B light is well known (Harborne and Williams, 2000). The presence of a significant treatment by genotype interaction ($P < 0.001$) indicates that not all genotypes responds similarly to UV-B exposure. In contrast to the situation in Arabidopsis and other species, not all *M. truncatula* plants investigated have shown un increase of anthocyanins in the leaves extract after UV-B treatment. A lack of anthocyanin accumulation in Medicago grown under other stressful environmental conditions (such as high light intensity, cold, outdoors in summer) has been already reported in literature (Ray *et al*., 2003) and may be related, in some cases, to the absence of flavanone 3-hydroxilase expression in the leaves (Charrier *et al*., 1995). The plants used in

this experiment have been maintained in a greenhouse and the higher amount of anthocyanins in the untreated plants (when compared to levels in growth chamber-grown plants, Figure 5) may be attributed to the different environmental conditions, in particular the much higher light intensity in the greenhouse (detailed in "Material and Methods").

Wt_JRC1 does not increase the amount of anthocyanins after treatment, wt_Jem is sensible to UV-B only after 4hrs of exposure and in the mutants, containing low levels of pigments, foliar anthocyanin content is only marginally affected by UV-B exposure.

Analyzing the effects of UV-B radiation on photosynthetic apparatus, the FV/Fm and the non photochemical quenching (NPQ) reveal changes in the seven genotypes. The most important changes are demonstrated after 14hrs of treatment. The Fv/Fm value decreases in all genotypes only 14hrs after UV-B exposure and the NPQ level, also, in this stage increases, as reported in Table 4. This reveals that 14hrs of exposure are important to affect the photosynthetic apparatus in the seven *M. truncatula* genotypes. 14hrs after UV-B exposure the anthocyanin content is not statistically different to the amount at 4hrs after treatment, but the NPQ level is two folds higher than the ratio find after 4hrs of exposure. This observation reveals that in the seven genotypes analyzed, the increase of anthocyanin amount during UV-B treatment is not able to limit the high NPQ production. This consideration could support the hypothesis of a limited significance of anthocyanins in the UV-protection of plants, at least when they occur in low or moderate amounts (Woodall and Stewart, 1998).

After UV-B exposure the amount of anthocyanin has increased in two genotypes only, but at phenotypic level no change in pigmentation between treated and untreated plants has been observed. For this reason, the expression of GST gene has been investigated further. Interestingly, in the seven *M. truncatula* genotypes the anthocyanin accumulation is not correlated with the expression of the GST carrier,. In fact, while in the untreated plants the expression of this gene is present only in the two genotypes pigmentated, after UV-B exposure, it becomes not detectable in UV-B treated leaves (Figure 16). Anthocyanins are stabilized and detoxified by transporting them into the vacuole. This measurement is likely accomplished in all organisms: glutathionation of bioreactive molecules and active transport of the conjugates through a membrane by a GS-X pump requiring Mg-ATP (Alfenito et al., 1998). UV-B exposure produces an alkalinization of the cytosol and it is possible that the conjugation reaction between GSH and the anthocyanin molecules is not allowed, since the GST conjugation takes place in un acid pH. Labrou et

al. (2004) demonstrated how the GST efficiency changes during the pH change. It is possible that gst protein which demonstrated a feedback regulation, in the seven *M.truncatula* genotypes, is not transcribed and translated.

These considerations support the hypothesis that anthocyanins remain in the cytosol and play a significant role in the UV protection of plants when they occur in high amount (Solovchenko and Smitz-Eiberger, 2003; Albert *et al*., 2009). The behaviour of single mutant genotypes under UV-B radiation remain to be further investigated.

In fact, more direct physiological and molecular genetic data on anthocyanin synthesis and regulation in *M. truncatula* are essential to improve the knowledge about the role of these pigments during UV-B exposure.

Alfenito MR, Souer E, Goodman CD, Buell R, Mol J, Koes R, Walbot V (1998) Functional complementation of anthocyanin sequestration in the vacuole by widely divergent glutathione S-transferases. Plant Cell 10:1135–1149.

Labrou N.E., Rigden D.J., Clonis Y.D., 2004. Engineering the pH-dependence of kinetic parameters of maize glutathione S-transferase I by site-directed mutagenesis. Biomolecular Engineering 21 (2):61-66.

Aastrup S., Outtrup H., Erdal K., 1984. Location of the proanthocyanidins in the barley grain. Carlsberg Res Commun. 49:105–109.

Afanas'ev I. B., Dorozhko A. I., Brodskii A. V., Kostyuk V. A., Potapovitch A. I., 1989. Chelating and free radical scavenging mechanisms of inhibitory action of rutin and quercetin in lipid peroxidation. Biochem. Pharmacol. 38:1763–1769.

Androutsopoulos V.P., Mahale S., Arroo R.R., Potter G., 2009. Anticancer effects of the flavonoid diosmetin on cell cycle progression and proliferation of MDA-MB 468 breast cancer cells due to CYP1 activation. Oncol Rep. 21(6):1525-8.

Arcioni S. An Italian functional genomic resource for *Medicago truncatula*. BMC Res Notes. 15;1:129.

Baldi A., Romani A., Mulinacci N., Vincieri F.F., Casetta B., 1995. Characterization Of Anthocyanins In *Petunia Hybrida* 'Purple Wave'J. Agric Food chem. 43:2104-2109.

Caldwell M.M., Flint S.D., 1997. Uses of biological spectral weighting functions and the need of scaling for the ozone reduction problem. Plant Ecology 128: 67–76.

Castellarin S.D., Di Gaspero G., Marconi R., Nonis A., Peterlunger E., Paillard S., Adam-Blondon A.F., Testolin R., 2006. Colour variation in red grapevines (Vitis vinifera L.): genomic organisation, expression of flavonoid 3'-hydroxylase, flavonoid 3',5'-hydroxylase genes and related metabolite profiling of red cyanidin-/blue delphinidin-based anthocyanins in berry skin. BMC Genomics. 24:7-12.

Cheung F., Haas B.J., Goldberg S.M., May G.D., Xiao Y., Town C.D., 2006. Sequencing *Medicago truncatula* expressed sequenced tags using 454 Life Sciences technology. BMC Genomics 24(7):272.

Cooper J.E., 2007. Early interactions between legumes and rhizobia: disclosing complexity in a molecular dialogue. J Appl Microbiol. 103(5):1355-65.

Cos P., Ying L., Calomme M., Hu J.P., Cimanga K., Van Poel B., Pieters L., Vlietinck A.J., Vanden Berghe D., 1998. Structure-activity relationship and classification of flavonoids as inhibitors of xanthine oxidase and superoxide scavengers. J Nat Prod.61(1): 71-6.

Debeaujon I., Léon-Kloosterziel K.M., Koornneef M., 2000. Influence of the testa on seed dormancy, germination, and longevity in Arabidopsis. Plant Physiol 122: 403–413.

Deshpande S.S., Cheryan M., Salunkhe D.K., 1986. Tannin analysis of food products. Crit Rev Food Sci Nutr. 24:401–449.

Dugo P., Mondello L., Morabito D., Dugo G., 2003. Characterization of the Anthocyan Fraction of Sicilian Blood Orange Juice by Micro-HPLC-ESI/MS.

Ekambaram G., Rajendran P., Magesh V., Sakthisekaran D., 2008. Naringenin reduces tumor size and weight lost in N-methyl-N'-nitro-N-nitrosoguanidine-induced gastric carcinogenesis in rats. Nutr Res. 28(2):106-12.

Elliott A.J., Scheiber S.A., Thomas C., Pardini R.S., 1992.Inhibition of glutathione reductase by flavonoids. A structure-activity study.Biochem Pharmacol. 44(8):1603-8.

Ferrali M., Signorini C., Caciotti B., Sugherini L., Ciccoli L., Giachetti D., Comporti M.,1997. Protection against oxidative damage of erythrocyte membrane by the flavonoid quercetin and its relation to iron chelating activity. FEBS Lett. 416(2):123-9.

Galluzzo P. and Marino M., 2006. Nutritional flavonoids impact on nuclear and extranuclear estrogen receptor activities. Genes Nutr. 1(3-4):161-76.

Giuntini D., Lazzeri V., Calvenzani V., Dall'Asta C., Galaverna G., Tonelli C., Petroni K., Ranieri A., 2008. Flavonoid profiling and biosynthetic gene expression in flesh and peel of two tomato genotypes grown under UV-B-depleted conditions during ripening. J Agric Food Chem. 23;56(14):5905-15.

Grotewold E., 2004. The challenges of moving chemicals within and out of cells: insights into the transport of plant natural products. Planta. 219(5): 906-9.

Hammerstone J.F, Lazarus S.A., Schmitz H.H., 2000. Procyanidin Content and Variation in Some Commonly Consumed Foods. Journal of Nutrition.130:2086S-2092S.

Hanasaki Y., Ogawa S. S. Fukui,1994. The correlation between active oxygen scavenging and antioxidative effects of flavonoids. Free Radic. Biol. Med. 16: 845–850.

Harborne J.B and Williams C.A, 2000. Advances in flavonoid research since 1992. Phytochemistry 55:481-504.

Harrison M.J., 2005. Signaling in the arbuscular mycorrhizal symbiosis. Annu Rev Microbiol 59: 19–42.

Hirano R., Sasamoto W., Matsumoto A., Itakura H., Igarashi O., Kondo K., 2001. Antioxidant ability of various flavonoids against DPPH radicals and LDL oxidation. J Nutr Sci Vitaminol (Tokyo) 47(5):357-62.J. Agric. Food Chem. 51, 1173-1176.

Kaludjerovic J., Ward W.E., 2009. Neonatal exposure to daidzein, genistein, or the combination modulates bone development in female CD-1 mice. J Nutr. 139(3):467-73.

Kitamura S., Shikazono N,, Tanaka A,, 2004. TRANSPARENT TESTA 19 is involved in the accumulation of both anthocyanins and proanthocyanidins in Arabidopsis. Plant J. 37(1):104-14.

Krauss P., Markstädter C., Riederer M., 1997. Attenuation of UV radiation by plant cuticles from woody species. Plant, Cell and Environment 20: 1079–1085.

Kuppusamy K.T., Endre G., Prabhu R., Penmetsa R.V., Veereshlingam H., Cook D.R.,Dickstein R., Vandenbosch K.A., 2004. LIN, a *Medicago truncatula* gene Required for Nodule Differentiation and Persistence of Rhizobial Infections. Plant Physiol. 136:3682–3691.

Lepiniec L., Debeaujon I., Routaboul J.M., Baudry A., Pourcel L., Nesi N., Caboche M., 2006. Genetics and biochemistry of seed flavonoids. Annu Rev Plant Biol. 57:405-30.

Liakoura V., Bornman J.F., Karabourniotis G., 2003. The ability of abaxial and adaxial epidermis of sun and shade leaves to attenuate UV-A and UV-B radiation in relation to the UV absorbing capacity of whole leaf methanolic extracts. Physiologia Plantarum. 117:33–43.

Martinoia E., Grill E., Tommasini R., Kreuz K., Amrhein N., 1993. ATP-dependent glutathione S-conjugate export pump in the vacuolar membrane of plants. Nature. 364:247–249.

Min B.R., Pinchak W.E., Fulford J.D., Puchala R., 2005. Wheat pasture bloat dynamics, in vitro ruminal gas production, and potential bloat mitigation with condensed tannins. J Anim Sci. 83(6):1322-3.

Nielsen A.H., Olsen C.E., Møller B.L., 2005. Flavonoids in flowers of 16 Kalanchoë blossfeldiana varieties. Phytochemistry. 66(24):2829-35.

Peer W.A., Bandyopadhyay A., Blakeslee J.J., Makam S.N., Chen R.J., Masson P.H., Murphy A.S., 2004. Variation in expression and protein localization of the PIN family of auxin efflux facilitator proteins in flavonoid mutants with altered auxin transport in Arabidopsis thaliana. Plant Cell. 16: 1898–1911.

Santelia D., Henrichs S., Vincenzetti V., Sauer M., Bigler L., Klein M., Bailly A., Lee Y., Friml J., Geisler M., Martinoia E., 2008. Flavonoids redirect PIN-mediated polar auxin fluxes during root gravitropic responses. J Biol Chem. 283(45):31218-26.

Schmitz-Eiberger M., Noga G., 2001. Quantification and reduction of UV-B induced damage in *Phaseolus vulgaris* leaves and *Malus domestica* fruits. Angewandte Botanik 75: 53–58.

Schröder P., Scheer C.E., Diekmann F., Stampfl A., 2007. How plants cope with foreign compounds. Translocation of xenobiotic glutathione conjugates in roots of barley (Hordeum vulgare). Environ Sci Pollut Res Int. 14(2):114-22.

Siegelman H. W. and Hendricks S. B., 1958. Photocontrol of Alcohol, Aldehyde, and Anthocyanin Production in Apple Skin. Plant Physiol. 33: 409-413.

Smith A.P., Nourizadeh S.D., Peer W.A., Xu J., Bandyopadhyay A., Murphy A.S., Goldsbrough P.B., 2003. Arabidopsis AtGSTF2 is regulated by ethylene and auxin, and encodes a glutathione S-transferase that interacts with flavonoids. Plant J. 36(4):433-42.

Tanaka Y., Sasaki N., Ohmiya A., 2008. Biosynthesis of plant pigments: anthocyanins, betalains and carotenoids. 54(4):733-49.

Van Acker S. A. B. E., Van den Berg D.-J.,. Tromp M. N. J. L, Griffioen D. H., Van Bennekom W. P., Van der Vijgh W. J. F., Bast A., 1996. Structural aspects of antioxidant activity of flavonoids. Free Radic. Biol. Med. 20: 331–34.

Winkel-Shirley B., 2001. Flavonoid biosynthesis. A colorful model for genetics, biochemistry, cell biology, and biotechnology. Plant Physiol. 126 (2): 485-93.

Wu, X., Pittman, H.E., Prior, R.L. 2006. Fate of anthocyanins and antioxidant capacity in contents of the gastrointestinal tract of weanling pigs following black raspberry consumption. Journal of Agricultural and Food Chemistry. 54(1):583-589.

Xie D. Y., Jackson L. A., Cooper J. D., Ferreira D., Paiva N. L., 2004. Molecular and biochemical analysis of two cDNA clones encoding dihydroflavonol-4-reductase from *Medicago truncatula*. Plant Physiol. 134:979-994.

Yan H.H., Mudge J., Kim D.J., Shoemaker R.C., Cook D.R., Young N.D., 2004. Comparative physical mapping reveals features of microsynteny between Glycine max, Medicago truncatula, and Arabidopsis thaliana. Genome. 47(1):141-55.

Yao L.H., Jiang Y.M., Shi J., Tomás-Barberán F.A., Datta N., Singanusong R., Chen S.S., 2004. Flavonoids in food and their health benefits. Plant Foods Hum Nutr. 59(3):113-22.

4. ISOLATION AND MOLECULAR CHARACTERIZATION OF A *M. truncatula* MYB GENE INVOLVED IN ANTHOCYANIN BIOSYNTHESIS

INTRODUCTION

Myb genes in anthocyanin regulation pathway

Myb structure

Regulation of gene expression at the level of transcription controls many crucial biological processes. A number of different factors are required for the process of transcription. These include factors required for chromatin remodelling and DNA unwinding, as well as proteins of the pre-initiation complex and the RNA polymerase II complex. In addition to this general inventory, other factors control promoter strength. These factors are referred to as 'transcription factors', a term usually used to describe proteins that recognise DNA in a sequence-specific manner and that regulate the frequency of initiation of transcription upon binding to specific sites in the promoter of target genes. Transcription factors—which can be activators, repressors, or both—display a modular structure. On the basis of similarities in one of the modules, namely the DNA-binding domain, transcription factors have been classified into families (Pabo and Sauer, 1992). In plants, MYB factors comprise one of the largest of these families (Romero *et al*., 1998; Riechmann *et al*., 2000).

The first MYB gene identified was the 'oncogene' v-Myb derived from the avian myeloblastosis virus (Klempnauer *et al*., 1982). Evidence obtained from sequence comparisons indicates that v-Myb may have originated from a vertebrate gene, which mutated once it became part of the virus. Many vertebrates contain three genes related to v-Myb—c-Myb, A-Myb and B-Myb (Weston, 1998)—and other similar genes have been identified in insects, plants, fungi and slime moulds (Lipsick, 1996). The encoded proteins are crucial to the control of proliferation and differentiation in a number of cell types, and share the conserved MYB DNA-binding domain. This domain generally comprises up to three imperfect repeats, each forming a helix-turn-helix structure of about 53 amino acids. Three regularly spaced tryptophan residues, which form a tryptophan cluster in the three-dimensional helix-turn-helix structure, are characteristic of a MYB repeat (König *et al*.,

1998; Ogata *et al.*, 1992). The three repeats in c-Myb are referred to as R1, R2 and R3; and repeats from other MYB proteins are categorised according to their similarity to either R1, R2 or R3.

MYB proteins can be classified into three subfamilies depending on the number of adjacent repeats in the MYB domain (one, two or three) (Jin and Martin, 1999). The MYB-like proteins with a single repeat (or sometimes just a partial one) are fairly divergent and include factors that bind the consensus sequence of plant telomeric DNA (TTTAGGG) (Yu *et al.*, 2000). In contrast to animals, in plants MYB genes containing two repeats (i.e. R2R3-MYB) constitute the largest MYB gene family. The large size of this gene family was apparent from the work of Romero *et al.* in *A. thaliana* and was also confirmed in *Zea mays* (Rabinowicz *et al.*, 1999).

The R2R3-type MYB factors encoded by the Atmyb genes have been categorised into 22 subgroups on the basis of conserved amino-acid sequence motifs present carboxy-terminal to the MYB domain (Kranz *et al.*, 1998). Despite the divergence of the amino-acid sequence outside of the MYB domain, there are some conserved motifs that may contribute to function. The conserved motifs may facilitate the identification of functional domains outside of the DNA-binding domain of R2R3-type MYB factors.

Primarily through genome sequencing, genes encoding three Myb repeats have been detected in A. thaliana *(Braun and Grotewold, 1999).*

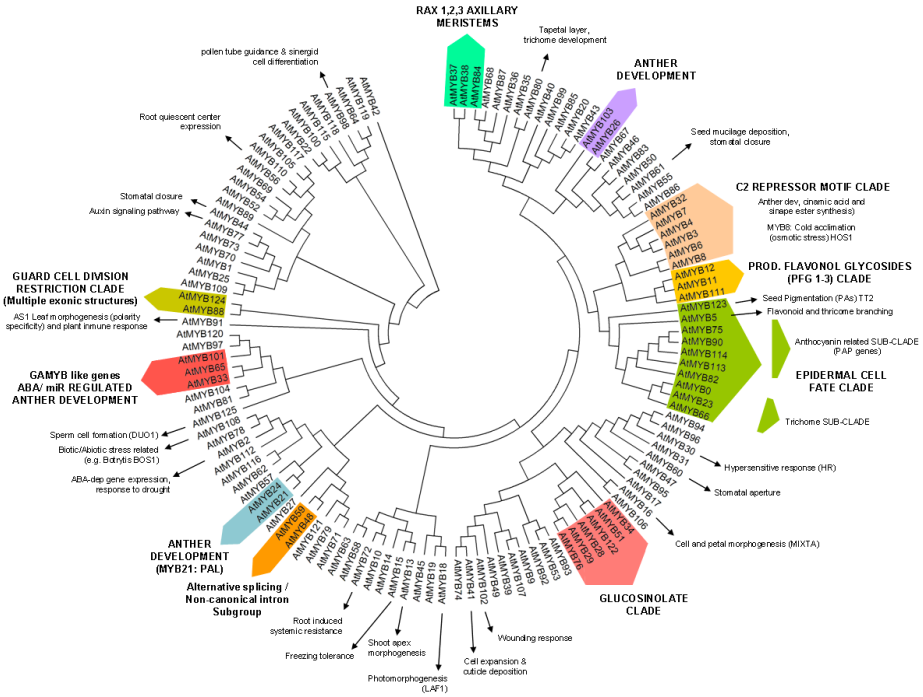

Matus *et al.*, 2008. BMC Plant Biology 8:83

Figure 1. Integrated evolutionary relationships of the 126 *Arabidopsis* R2R3 MYB proteins.

What is the role of MYB genes in anthocyanin pathway?

Recent studies especially in *Petunia hybrida*, *Zea mays*, and *Arabidopsis thaliana* have revealed the complexity of the regulatory networks which, in addition to anthocyanin and proanthocyanidin production, control multiple developmental processes including the development of trichomes, root hairs, and seed coat mucilage in Arabidopsis (Schiefelbein, 2003; Serna and Martin, 2006) as well as the morphology of seed coat epidermal cells and the vacuolar pH of petals in Petunia (Quattrocchio *et al*., 2006). Regulatory complexes in these processes have been shown to involve WD40, bHLH, and MYB proteins. The WD40 proteins and bHLH factors are more ubiquitously expressed while the regulation of these distinct developmental processes are determined by physical interaction of WD40 and bHLH proteins with different and functionally more specific MYB proteins (Koes *et al*., 2005; Ramsay and Glover, 2005).

R2R3-type myb genes have been shown to regulate phenylpropanoid metabolism in *A. thaliana* and other plants. Overexpression of AtMYB75/PAP1 (production of anthocyanin pigment1) and AtMYB90/PAP2 (Borevitz *et al*., 2000) results in accumulation of anthocyanins, and AtMYB4 represses the synthesis of sinapoyl malate (Jin *et al*., 2000). The analysis of AtMYB4 also demonstrated that R2R3-type MYB proteins can act as transcriptional activators as well as repressors. The transparent testa2 (TT2) gene has been shown to encode an R2R3-type MYB factor (Nesi *et al*., 2001). This is not a surprise as several R2R3-type myb genes, such as ZmMYBc1 from *Zea mays* (Paz Ares *et al*., 1986) or PhMYBan2 from *Petunia hybrida* (Quattrocchio *et al*., 1999) (which also control phenylpropanoid metabolism), are known to be derived from other plant species. AtMYB34/ATR1 (altered tryptophan regulation1) is a regulator of tryptophan biosynthesis, which demonstrates that pathway control by such factors is not limited to secondary metabolism (Bender and Fink, 1998).

MATERIAL AND METHODS

RNA extraction and reverse transcription

The RNA isolation was performed using TRIZOL® Reagent (Invitrogen, USA) and according to the specific protocol. The yields and concentration of the isolated RNA was determined by measuring the optical density in a biophotometer (Biophotometer, Eppendorf, Germany) at 260 nm. RNA purity was evaluated by the absorbance *ratio* A260/A280 nm while RNA integrity by 1% agarose (Seakem® LE Agarose, CAMBREX, USA) gel electrophoresis. Reverse transcription (RT) was performed using BIO-RAD iScript™ cDNA Synthesis Kit starting from 1μg of total RNA and following the manufacturer's instruction.

Primer design

The MtMYBA gene-specific primers were obtained from MWG-Biotech AG, Germany.
For PCR assays (RT-PCR and qPCR) primers have been desined using Primer3 Input 0.4.0 software.

RT-PCR amplification

The RT-PCR reaction has been conducted in a final reaction volume of 20 μL containing 30 ng of cDNA, 0.3μM of primer forward and 0.3μM of primer reverse (MWG-Biotech AG, Germany), 1X Buffer containing 1.5mM of $MgCl_2$ (GeneSpin, Italy), 0.2mM of dNTPs and 0.3U/ul of Taq Polymerase (GeneSpin, Italy). The PCR amplification profile was: 3 minutes initial denaturation at 94°C, followed by 35 cycles of 94°C for 40 sec, 57°C for 40 sec, 72°C for 50 seconds, and a 7 min final extension at 72°C. The amplified PCR products have been separated in 1% agarose gel (Seakem® LE Agarose, CAMBREX, USA) and stained with ethidium bromide (0,5μg/ml). The length of PCR products was determined by comparison with the gene marker Superladder-Low 100bp Ladder (Thermo Scientific, USA).

qPCR assay

The qPCR assay (RealTime-PCR reactions) has been performed with real-time PCR (Mini-Opticon; Bio-Rad Laboratories, CA) thermal cycler and all the operations during

amplification reaction has been controlled by MJOpticon Monitor, Version 3.1 software. Real-Time PCR reaction has been performed using iQ™ SYBR® Green Supermix (containing *Taq* DNA polymerase, dNTPs, $MgCl_2$, and SYBR Green I dye; BIO-RAD). Each reaction mix (25 □l) contained 20 ng of cDNA, 0.4 □mol/L of primers. The amplification profile was: 1 cycle of 3' at 95°C followed by 44 cycles of 10 seconds at 95°C, 25 second of annealing temperature and 72°C for 7 minutes.

A negative control has been added to each assay to assess the overall specificity. The expression of gene has been tested through three biological repetition and each sample has been repeated three times to performed technical repetition. The □-actin gene, a stable housekeeping gene, has been used for signal normalization.

Cloning Gateway technology

Fragments amplification

Gateway technology has been conducted following the manual pENTR™ Directional TOPO® Cloning Kit (Invitrogen). The amplification of MtMYBA cDNA and promoter has been performing using Platinum® *Pfx* DNA Polymerase (Invitrogen).

The PCR reaction has been conducted in a final reaction volume of 50 µL containing 10 ng of cDNA, 1,5µl of primer forward and reverse 10µM (MWG-Biotech AG, Germany), 10µl of 10X Buffer (Invitrogen), 1,5µl of dNTPs 10mM, 0,5 µl of MgSO4 and 0,5 µl of Platinum® *Pfx* DNA Polymerase (5U/µl).

The PCR amplification profile has been: 2 minutes initial denaturation at 94°C, followed by 35 cycles of 94°C for 30 sec, 57°C for 35 sec, 68°C for 60 seconds. The extension phase is not present. The amplified PCR products have been separated in 1% agarose gel (Seakem® LE Agarose, CAMBREX, USA) and stained with ethidium bromide (0,5ug/ml). The length of PCR products was determined by comparison with the gene marker Superladder-Low 100bp Ladder (Thermo Scientific, USA). The gel slice corresponding to the promoter and MYBA sequence have been excise and purifyed using kit *Wizard SV Gel and PCR Clean-up System* (Promega).

Cloning reaction and E.Coli cells transformation

To insert the PCR fragments in the pENTR™/SD/D-TOPO® (Invitrogen) vector (2601bp), the following reaction has been prepared: 20ng of PCR products have been added to 1µl of salt solution, 3µl of sterile water and 20ng of TOPO® vector. The reaction has been mixed

gently and incubate for 5 minutes at room temperature (22-23°C) and then the reaction has been placed on ice and proceed to Transforming One Shot® Competent *E. coli*, using kit *One Shot® Chemical Transformation* (Invitrogen). E.Coli colonies have been plated on LB and kanamicyn (50mg/l).

Plasmids extraction and sequencing

The recombinant plasmids have been extracted from E.Coli colonies using Wizard® *Plus* SV Minipreps DNA Purification System (Promega). The plasmids have been sequenced with *BigDye Terminator v3.1 Cycle Sequencing Kit* (AppliedBiosystems,http://www.appliedbiosystems.com) and the reaction have been prepared using: 200ng of plasmid, 8pmol of primers (10uM) and 0,3ul for each reaction of BigDye v3.1. To sequence the specific region investigated in this thesis, the following condition of reaction have been performed: 1' at 96°C and 25 cycles of 10'' at 95°C, 5' at 50°C, 4' at 60°C.

Recombination reaction between pENTR™/SD/D-TOPO® and pH2GW7,0 and pHGWFS7,0

The pENTR™/SD/D-TOPO® containing the promoter and the sequence of MtMYBA gene, has been recombined with pH2GW7,0 and pHGWFS7,0 (www.psb.ugent.be), binary vectors used in Gateway technology. Those vectors are able to reply in *Agrobacterium tumefaciens* and useful for that for genetic transformation of plants.

The reaction has been performed using the kit *Gateway® LR CLONASE™ Enzyme Mix* (Invitrogen™) and adding: 160ng of transformed *pENTR™/SD/D-TOPO®,* 160ng of destination vector, 2ul of reaction buffer, 4ul of sterile water and 2ul of LR Clonase™ Enzyme Mix. Overnight at room temperature.E. Coli cells have been transformed and plasmids have been extracted.

***Agrobacterium tumefaciens* transformation** (Hofgen *at al*., 1988)

The resulting binary vector has been sequenced to verify the correct insertion and introduced into *Agrobacterium tumefaciens* strain LBA4404 (for *Arabidopsis thaliana* ecotype Columbia transformation) and strain EHA105 (for *Medicago truncatula* ecotype M910a). Recombinant strain LBA4404 *A. tumefaciens* has been selected on yeast extract beef (YEB)

medium, containing 50 µg/ml streptomycin, 25 µg/ml rifampicin, and 50 µg/ml kanamycin. Instead, transformant strain EHA105 *A. tumefaciens* has been selected on Luria Bertani (LB) medium, containing ,25 µg/ml rifampicin, and 50 µg/ml kanamycin. 2 µg DNA per 200 µl of frozen Agrobacterium competent cells. They remained on ice for 10–15 min., then have been frozen in liquid nitrogen for 2 minutes and put in heat shock in a water bath at 37 °C for exactly 5 min directly from the liquid nitrogen. At the end, it has been added 1 ml of YEB medium (for LBA4404 strain) or LB medium (for EHA105 strain) and incubated in an orbital shaker at 200 rpm, 28 °C for 2–4 h. After that, they have been centrifuged at 3,000 rpm at room temperature for 3 min, the supernatant has been discarded and the pellet has been resuspended in 200 µl YEB/LB medium. The transformed bacteria have been spread on YEB/LB 1.5% agar plates that contain the appropriate antibiotics and incubated at 28 °C for 36–48 h until colonies appear.

Arabidopsis thaliana transformation

Arabidopsis plants were grown until they were flowering. They were grown under long days in pots in soil covered with bridal veil. The first bolts have been clipped to encourage proliferation of many secondary bolts. Optimal plants have many immature flower clusters and not many fertilized siliques, although a range of plant stages can be successfully transformed. *Agrobacterium tumefaciens* strain carrying gene of interest on a binary vector were grown in a large liquid culture at 28 °C in YEB with antibiotics to select for the binary plasmid. When the culture achieve OD600 = 0.8, it was resuspended in 5% Sucrose solution. Before dipping, Silwet L-77 was added to a concentration of 0.05% (500 µl/L) and mix well. Above-ground parts of plant in Agrobacterium solution for 2 to 3 seconds was dipped, with gentle agitation. Dipped plants were placed under a dome or cover for 16 to 24 hours to maintain high humidity (plants can be laid on their side if necessary). Dry seeds were harvested. The selection of transformants was done seeding obtained seeds on agar plates with MS and 15 µg/ml hygromicin. They were subjected to cold treatment (4°C for 2 days) and they were put in a growth chamber under continuous light (50-100 microEinsteins) for 7-10 days. Then putative transgenic plants were transplant to soil.

Medicago truncatula genetic transformation (Araújo *et al.*, 2004)

Plant material

Plants of *M. truncatula* Gaertn. cv Jemalong (M9-10a genotype) were used in this study. This genotype was selected by Neves (2000) for its high embryogenic potential. To provide leaf explants for transformation/regeneration experiments, M9-10a plants were grown and micropropagated in vitro on a growth regulator-free MS030A medium (Murashige and Skoog, 1962) salts and vitamins, 3% (v/v) sucrose and 0.7% (w/v) agar medium, as described by Neves *et al.* (2001). In vitro cultures were kept in a climate chamber at 22-24°C, with a 16-h photoperiod of 65-75 nmol/m^2/s under a cool white fluorescent lamp.

Transformation vector and *Agrobacterium tumefaciens* strains

Plasmids pH2GW7,0 and pHGWFS7,0, are two derivatives of the pBI121 binary vector (Karimi *et al.*, 2002). The schematic map of the 35S:::MtMYBA::Nos and pMYBA::GUS-GFP::Nos constructs is shown in Figure 10 and 11. The constructs were transferred into the *A. tumefaciens* strain EHA105, a non-oncogenic derivative of strain A281 which harbours the hypervirulent helper Ti plasmid pTiBo542 (Hood *et al.* 1993). The *A. tumefaciens* strain EHA105 35S:::MtMYBA::Nos and pMYBA::GUS-GFP::Nos were inoculated in 25 ml of LB liquid medium supplemented with rifampicin (100 mg l^{-1}) and kanamycin (100 mg l^{-1}) and the resulting bacterial culture was incubated at 26 °C at 120 rpm on an orbital shaker. After 48 h, the bacteria were transferred to Falcon tubes and centrifuged at 3000 rpm for 1 min. The pellets were finally resuspended with EIM (Murashige and Skoog (1962) basal salts and vitamins, 3% (v/v) sucrose, 0.45 µM 2,4-dichlorophenoxyacetic acid, 0.91 µM zeatin and 100 µM acetosyringone) liquid medium (Araujo *et al.*, 2004) to a final OD_{600} of 1.6. When transformation was carried out, bacterial cells were incubated for 30 min in the dark, in order to activate the Agrobacterium virulence mechanisms.

Agrobacterium tumefaciens-mediated transformation and *in vitro* selection/regeneration

Transformation of M9-10a leaf explants and plant regeneration were performed as described by Araujo *et al.* (2004). Leaflets from in vitro-grown plants were wounded using a surgical blade previously dipped into the Agrobacterium suspension, and transferred to EIM solid (0.2% (w/v) gerlite) medium for five days in the dark. Subsequently, infected explants were transferred on the same medium containing

carbenicillin (500 mg l^{-1}) to remove Agrobacterium and kanamycin (100 mg l^{-1}) as selective agent for transformed cells and maintained under a 16 h photoperiod of 65-75 mmol m^{-2} s^{-1} applied as cool white fluorescent light and a day/night temperature of 24/22 °C. After two weeks, explants with embryogenic calli were transferred on EPM medium (identical to EIM but without growth regulators) maintaining the same selective pressure. The explants were cultured on this medium for four weeks. During this period, somatic embryos at torpedo/dicotyledonar stage were collected from embryogenic calli and placed on MS010A medium (Murashige and Skoog (1962) salts and vitamins, 1% (v/v) sucrose and 0.7% (w/v) agar) supplemented with carbenicillin (250 mg l^{-1}) and kanamycin (100 mg l^{-1}) to develop into shoots. Embryos were maintained under the same light/temperature conditions above described. Every three weeks, green somatic embryos resistant to kanamycin were transferred to fresh selective medium until conversion into shoots occurred. When the shoot pole moved upward, both carbenicillin and kanamycin concentrations were reduced (100 mg l^{-1} and 50 g l^{-1}, respectively). Subsequently, shoots were elongated on a modified MS010A medium (vitamins: 4.5 mg l^{-1} nicotinic acid, 0.05 mg l^{-1} biotin, 0.5 mg l^{-1} folic acid, 0.4 mg l^{-1} thiamine HCl and 100 mg l^{-1} myo inositol) supplemented with carbenicillin (100 mg l^{-1}). Shoots with normal and ipt-shooty phenotype were further assayed in vitro for kanamycin resistance on MS010A medium containing carbenicillin (100 mg l^{-1}) and kanamycin (50 mg l^{-1}). After three-four weeks of incubation on this medium, only well-rooted plantlets with normal phenotype and well-developed shoots with ipt-shooty phenotype were selected as putative transgenic lines. Leaf explants of M9-10a not subjected to co-cultivation were used as control and underwent the same treatments used for the co-cultivated explants. Transformation efficiency was defined as the frequency of co-cultivated leaf explants producing independent kanamycin-resistant lines. The frequency of backbone transfer events was assessed by calculating the percentage of kanamycin-resistant lines with backbone sequences on the total number of kanamycin-resistant lines.

RESULTS AND DISCUSSION

Medicago truncatula MYBA gene isolation and analysis.

On the basis of the gene expression results in reported in chapter 3, the gene expression of MtPAP2 was investigated in details.

Blasting the entire amino acid sequence of AtPAP2 against the whole genebank data (BLASTP program http://www.ncbi.nlm.nih.gov/ the *M. truncatula* homologous sequences was retrieved. The most significant match was chosen ranking the E-value number. The best sequence showed an E value of1.2 e-42 Hereafter this sequence will be named MYBA. Afterword, MYBA has been aligned with the most important well known myb genes involved in anthocyanin biosynthesis: AtMYB113, AtPAP1, AtPAP2, LeANT1, PhAN2, MtLAP1 (Figure 2).

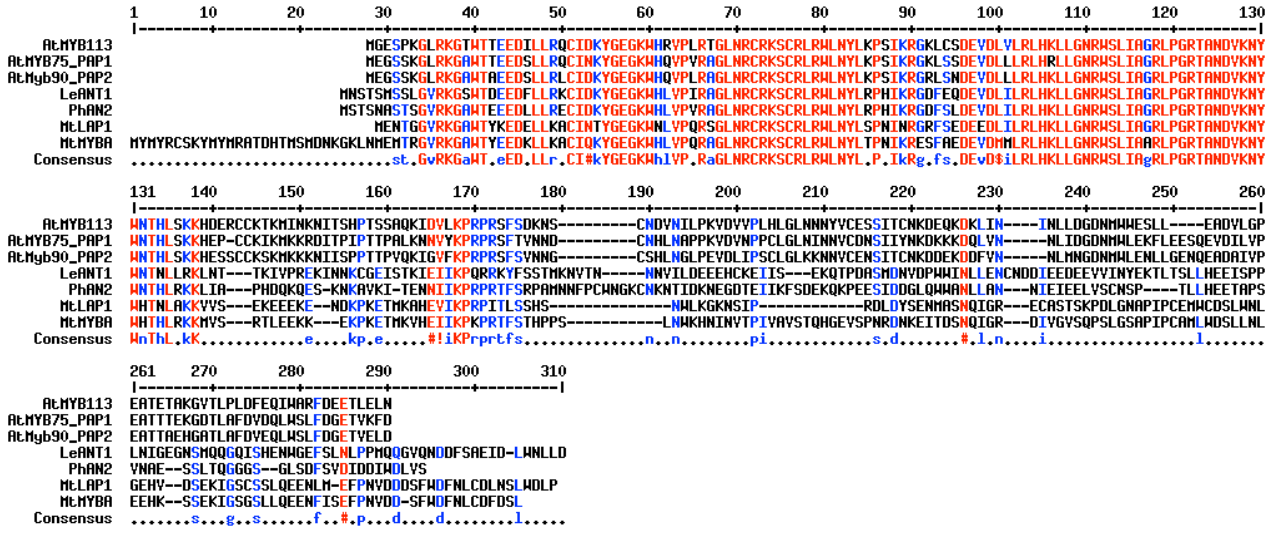

Figure 2. Amino acid sequence alignment among AtMYB113(AT1G66370), AtPAP1(AT1G56650), AtPAP2 (AT1G66390), LeANT1 (AAQ55181), PhAN2 (AAF66727), MtLAP1 (AC152405) and MtMYBA. The conserved region, shown in red, represents the typical R2R3 myb domain.

Recently Peel *et al.* (2009) described a new *M. truncatula myb* gene involved in anthocyanin biosynthesis: Legume Anthocyanin Production 1 (LAP1). In Figure 3 is shown an amino acid sequence alignment between MtLAP1 and MtMYBA.

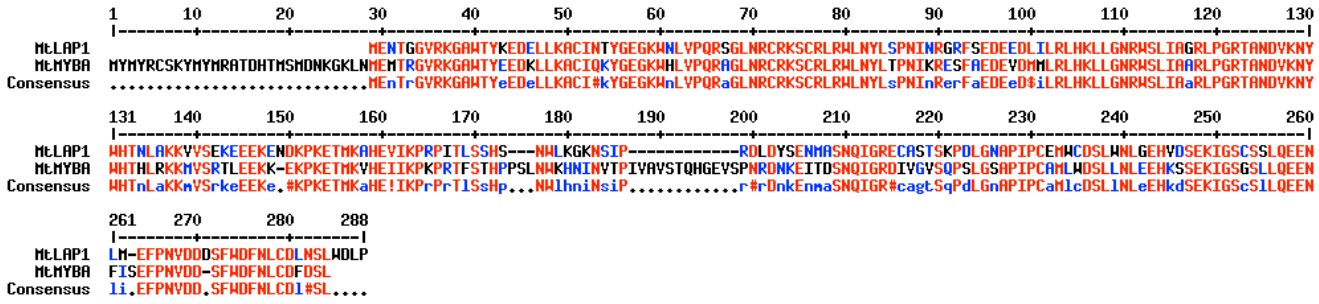

Figure 3. Amino acid sequence alignment among MtMYBA and MtLAP1. The conserved region, shown in red, represents the typical R2R3 myb domain

To highlight the role of MtMYBA in anthocyanin pathway, the R2R3 MYBA domain was uploaded in a R2R3 database to obtain a phylogenetic tree and investigate the phylogenetic relationships between the *myb* transcription factors involved in anthocyanin pathway and the new *M. truncatula myb* gene. As shown in Figure 4, MtMYBA falls in the same cluster of the most important anthocyanin transcription factors. Considering together the evidence obtained: 1) a significant amino acid homology between MYBA and MtPAP2; 2) a significant amino acid sequence alignment between MYBA and the R2 and R3 domains of MYB genes involved in anthocyanin pathway; 3) the topology of the phylogenetic tree, the potential function of that gene was confirmed.

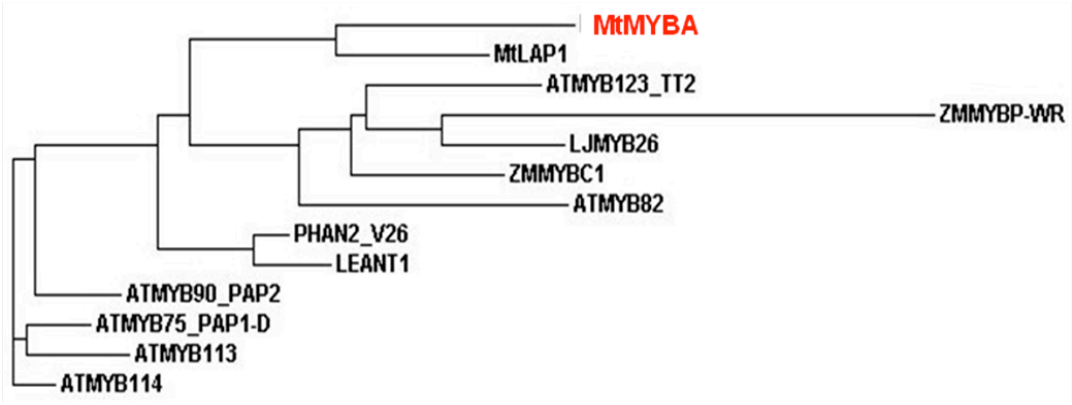

Figure 4. A phylogenetic tree with plant R2R3-type myb domain. We obtained it by neighbor-joinong methods using R2R3 full-lenght amino acid sequences. The MtMYBA (highlight in red) shows the R2R3-type myb transcription factor isolated from *M. truncatula* and described in this work

To confirm the potential implication of Mt*MYBA* in anthocyanin pathway, the gene expression was tested by RT-PCR on the leaves of the five mutants described in chapter 3 . The assay reveals that MYBA is expressed when red pigmentations on the leaves are presents (Figure 5).

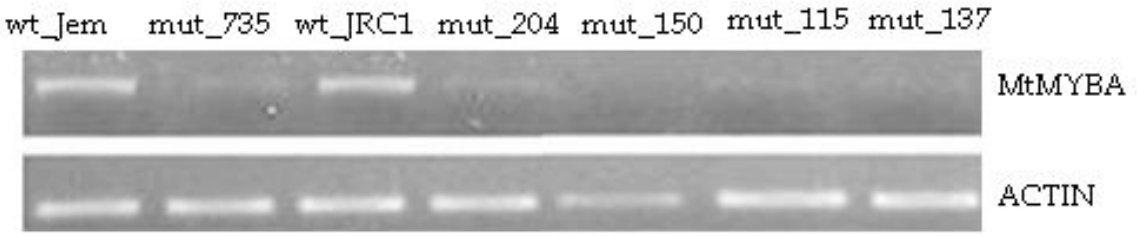

Figure 5. The expression profiles of MtMYBA gene were analysed by RT-PCR in the two wild-type genotypes and in the five mutant genotypes, using the housekeeping □-actin gene as endogenous reference.

As described in Chapter 3, wt_Jem and wt_JRC1 are the two genotypes with the typical red pigmentations on the leaves (anthocyanin accumulation).
Looking at Figure 5, it is clear how the expression of MtMYBA is high in the two wild-types and almost absent in the mutants. Adding this evidence to the sequence information showed before, we can assert that there is a link between MtMYBA gene and the anthocyanin metabolic pathway.
Considering these evidences, a follow up in the gene characterization has been planned trough:

a) Gene expression analysis
b) Functional analysis

A literature survey suggests the use of *M9-10a Medicago truncatula* genotype that showed a genetic transformation efficiency higher than Jemalong genotype.

a) MtMYBA gene expression analysis

The study of gene expression has been performed targeting six tissues: leaf, petiole, stem, flower, root, nodule, immature seeds, at three different development stages (15-60-80 days after germination (DAG)).

At 15 DAG M9-10a *M. truncatula* plants are in a young development phase. They achieve the mature stage (flowering time) at 60 DAG and since 80 DAG this genotype start to enter the senescence phase. At phenotypic level in the young phase M910a genotype does not show the characteristic red pigmentations on the leaves, visible in Jemalong ecotype.

Only few leaves has a visible anthocyanin accumulation, while the stems are heavy pigmented. At flowering time (60 DAG), all leaves show the presence of red pigmentations in the middle of their upper page and the stems appear less pigmentated than young stage. At the same developmental stage, the roots show evidence of abundant nodulation (as typical in legume plants) among which numerous pink nodules are present.

Looking at M910a *M. truncatula* plants at 80 DAG, leaves have lost anthocyanin accumulation and also the stems appear dark green coloured with no more traces of anthocyanin.

Gene expression has been tested by a qPCR assay MtMYBA (Figure 6). In leaves at 15 and 60 DAG, the MYBA gene is expressed at high levels compared to those found in leaves harvested at 80 DAG.

It is interesting to notice the no perfect correspondence between the phenotype and the gene expression level. In fact, at 60 DAG the middle of the leaves is characterized by red spots and, accordingly, qPCR shows the MYBA expression. At 80 DAG, leaves do not accumulate anthocyanins and, as expected, MYBA expression decreases 10 times. Conversely, at 15 DAG leaves do not show red pigmentation, while MYBA gene expression has almost the same level than at 60 DAG.

In petiole and stem, the link between phenotype and the molecular analyse of MYBA gene, is conserved. The gene expression is proportional to anthocyanin accumulation. Finally in roots the gene expression levels did not change during the three stages. In flowers with dark pigmentation on the sepals, the expression of MYBA gene occurred, as expected. Also in nodules, no As general conclusion it is possible to assert hat the

expression of MYBA gene varied in the different tissues according to *M. truncatula* developmental stage.

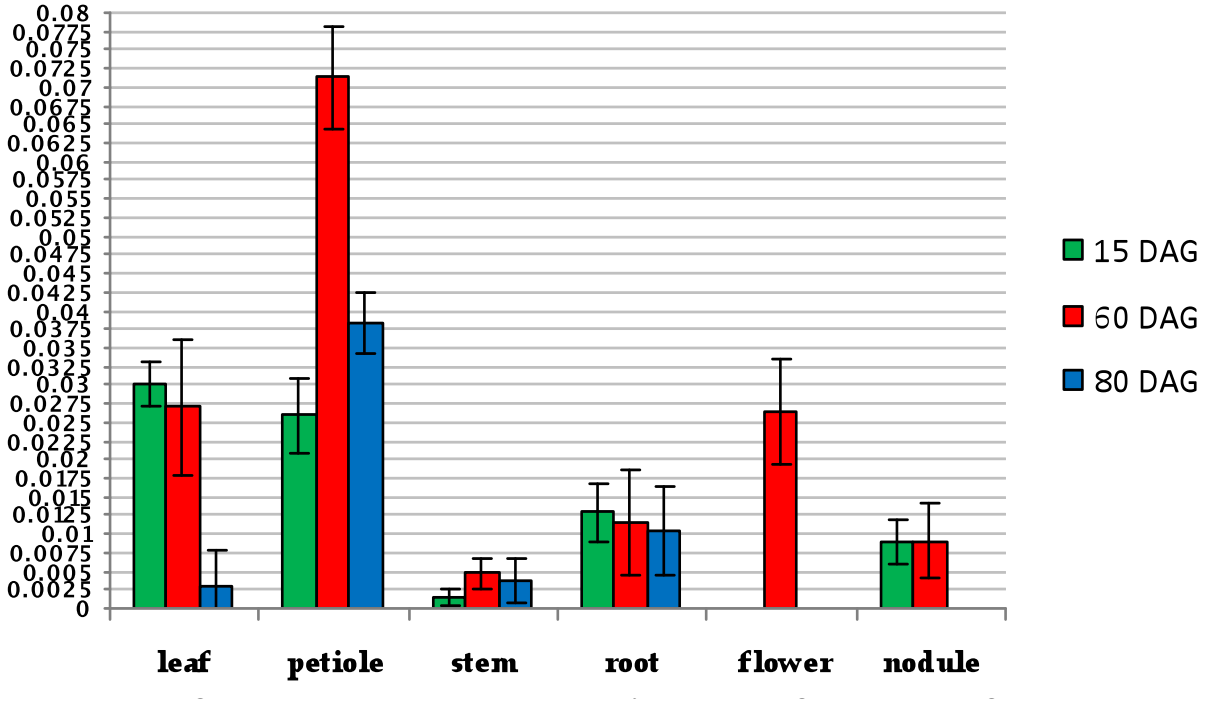

level in leaf, petiole, stem, root, flower and nodule. The assay has been performed in these tissues during three development stages :at 15 days (blue bar) - 60 days (red bar) - 80 days (yellow bar) after germination.

b) Functional analysis

The functional analysis of MtMYBA gene has been investigated with two approaches:

- Overexpression (MtMYBA cloning under 35S promoter) in *M. truncatula* and *A. thaliana*
- Promoter analysis through GFP and GUS assay in *M. truncatula* and *A. thaliana.*

MtMYBA overexpression

MtMYBA cDNA sequence has been amplified and cloning using Gateway ™ (Invitrogen) method in a plasmid under the control of 35S promoter (Figure 7).

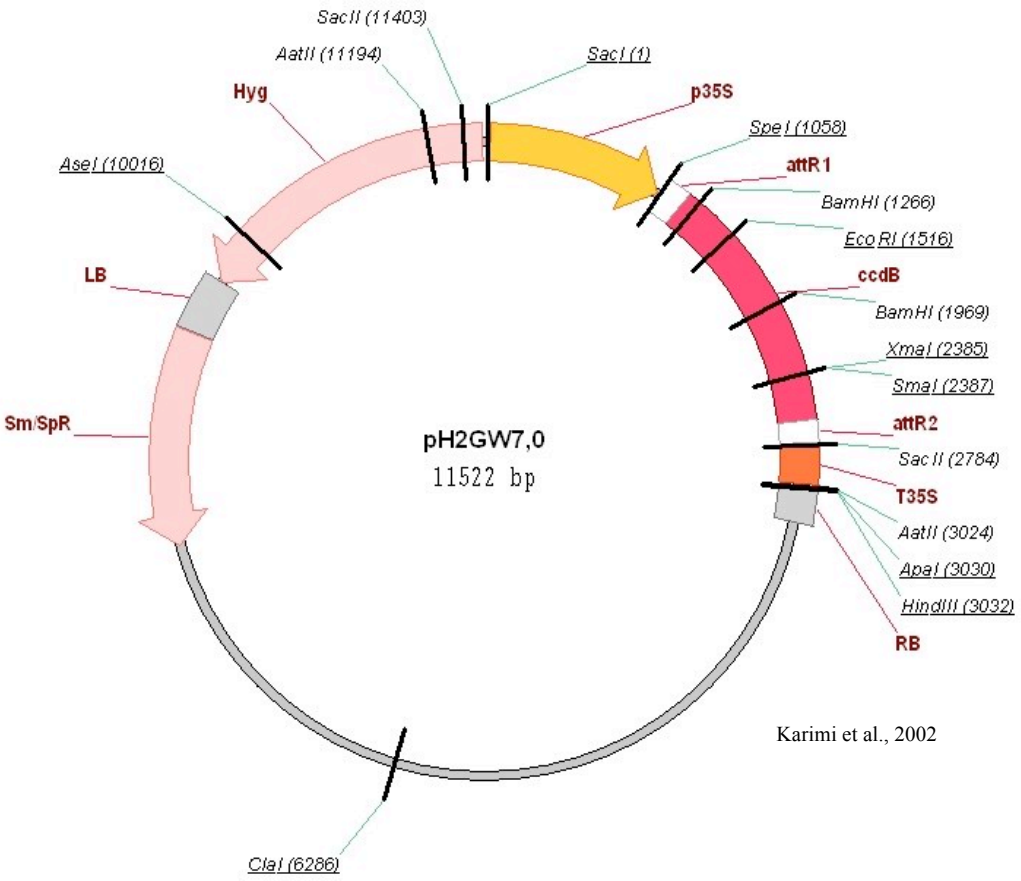

Figure 7. Binary vector pH2GW7,0 used for for the over-expression of MYBA gene gene over-expression

For this work, pH2GW7,0 binary vector has been used. Streptomycin is used to select the transformed *A. tumefaciens* cells while hygromycin is the selective agent for the transformed plant cells.

In the red portion of plasmid (Figure 10) the MtMYBA sequence is inserted. The contruct has then been used to transform *A.thaliana* ecotype Columbia and *M. truncatula* genotype M9-10a.

Among the 20 plant transformed, only one Arabidopsis plant has grown on selective MS medium (with 15µg/ml of Hygromicin). After ten days it has been moved in a pot with universal soil. A single leaf has been collected for DNA extraction and 35S promoter amplification. This assay is fundamental to establish if the genetic transformation takes place correctly. Here below (Figure 8) the amplification of 35S promoter is reported.

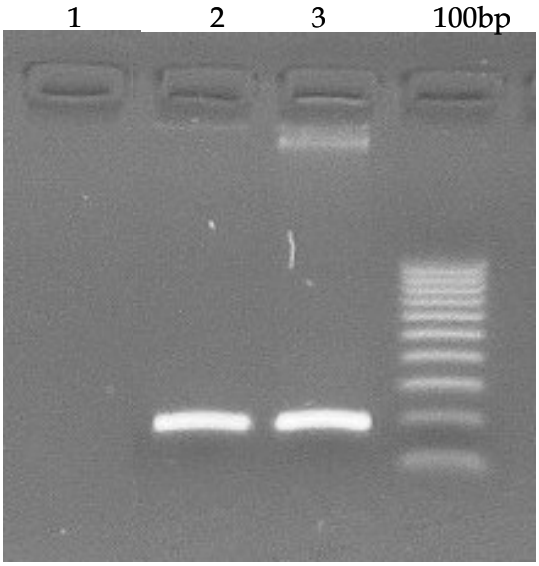

Figure 8**.** The presence of 35S promoter in the Arabidopsis line *mybA*, has been detected by PCR assays (lane 2). Control plasmid (pH2GW7,0) and the non transformed line are shown (lane 3 and 1).

Subsequently, the MtMYBA coding sequence was amplified using specific primers. Results from this analysis are shown in Figure 9. In lane 1 is reported the negative control (Arabidopsis plant DNA not transformed), in lane 2 is reported the positive control (pH2GW7,0 binary vector including MtMYBA sequence), in lane 3 the amplification of MtMYBA gene in Arabidopsis transformed plant DNA is shown.

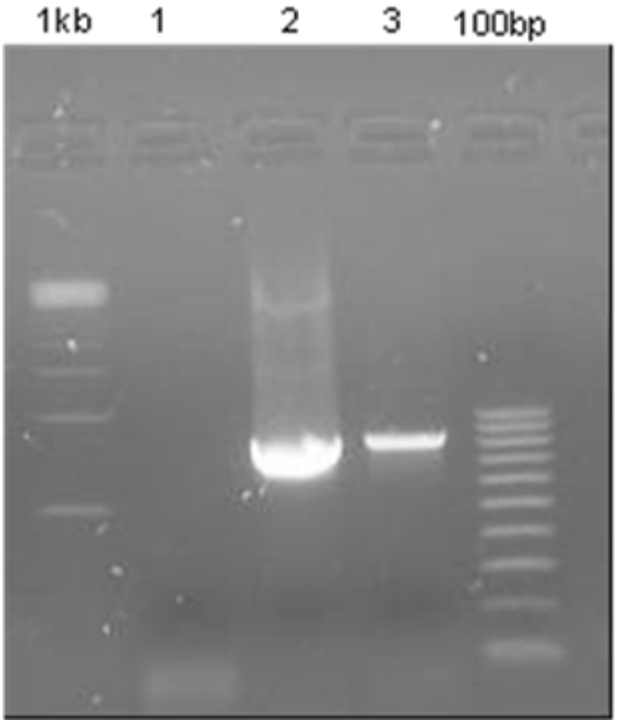

Figure 9. MtMYBA gene sequence amplification in T1 plant. The presence of MtMYBA gene sequence in the Arabidopsis line MYBA has been detected by PCR assays (lane 3). Control plasmid (pH2GW7,0) and the non transformed line are shown (lane 2 and 1).

Promoter analysis through GFP and GUS assay in *M. truncatula* and *A. thaliana*

The MtMYBA gene is localised on chromosome 5 and using TRANSFAC® 7.0 Public 2005 software (www.biobase-international.com) it has been possible to trace back the associated promoter sequence. This sequence has been amplified and inserted in a Gateway ™ (Invitrogen) binary vector containing GUS and GFP reporter genes (Figure 10).

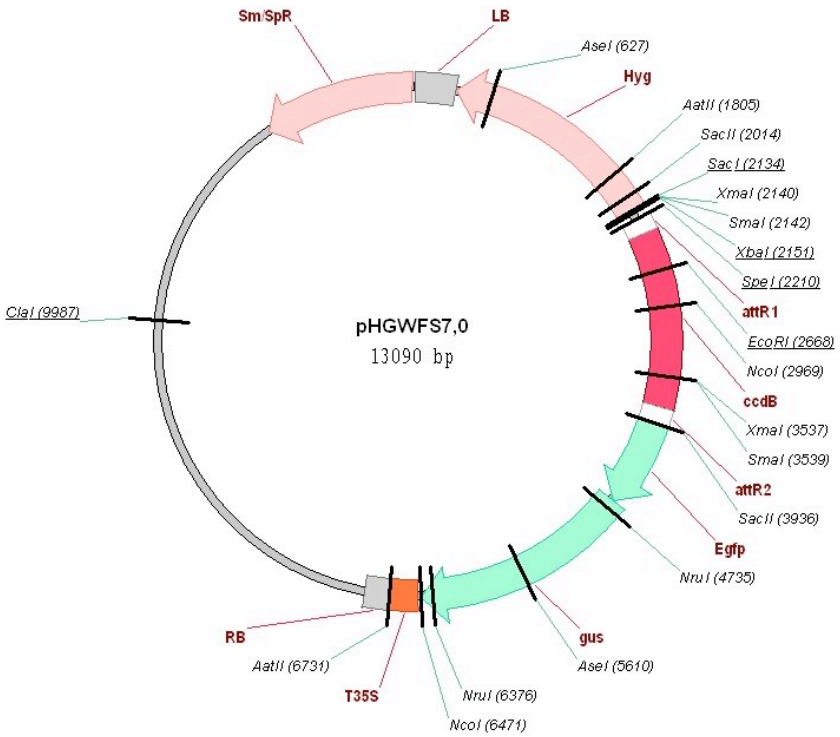

Karimi et al., 2002

Figure 10. Binary vector pHGWFS7,0 used for promoter analysis

Again, the pHGWFS7,0 construct, has been used to transform *A. thaliana* ecotype Columbia and *M. truncatula* M9-10a.

When this thesis is written, the *M. truncatula* transformations and the *A. thaliana* transformation with the construct pMYBA::GUS-GFP::Nos were in progress and the data about the transformation were not available.

The results reported in this chapter although preliminary, show that MTMYBA, a cDNA encoding a putative R2R3-MYB protein, potentially regulates the anthocyanin biosynthesis in *M.truncatula*. Peel *et al*. (2009) isolated a MYB gene (LAP1), showing an amino acidic sequence highest similar to MtMYBA (Figure 3). Also the phylogenetic tree reported in Figure 4, support the link between MtMYBA and the most known MYB genes involved in flavonoid pathway.

The expression profile of this novel MYB gene reveal a relationship between the anthocyanin accumulation in the tissues and the gene expression. In the leaf, petiole and flower (tissues highly pigmentated) the gene expression is high in all developmental stage considered, as expected. The functional analysis of *MtMYBA* in transgenic *A. thaliana* and

M. truncatula is still in progress. One line of *A. thaliana* transformed with 35S::*MtMYBA*:Nos has been obtained, but the analysis of transgenic plant is in progress.

MYB transcription factors are a strong candidate for such a regulatory factor in the upstream cascade because the expression of anthocyanin biosynthetic genes is believed to be under the control of MYB transcription factors (Stracke *et al*., 2000). Several PAP1-like MYB genes have been found in various species including tomato, grape, strawberry and petunia; all of which have shown to regulate anthocyanin synthesis in the respective species (Quattrocchio *et al*., 1999; Mathews et al., 2003). Although all of these transcription factors share the conserved R2R3 MYB domain, the C-terminal regions of the open reading frames (ORF) appear to exhibit marginal cross-species similarity. This aspect could explain why the same PAP1-like MYB gene does not produce in all species the anthocyanin accumulation. In fact, Arabidopsis PAP1 transcription factor, which induce anthocyanin levels in tobacco leaves, fails to induce anthocyanins in *M. truncatula*. For this reason, it is necessary to characterize specific MYB genes in barrel medic to understand the anthocyanin metabolism and improve the production of these pigments in the model legume plant.

Bender J. and Fink G.R., 1998. A Myb homologue, ATR1, activates tryptophan gene expression in Arabidopsis. Proc Natl Acad Sci USA 95:5655–5660.

Borevitz J.O., Xia Y.J., Blount J., Dixon R.A., Lamb C., 2000. Activation tagging identifies a conserved MYB regulator of phenylpropanoid biosynthesis. Plant Cell 12:2383–2393.

Braun E.L. and Grotewold E., 1999. Newly discovered plant c-myb-like genes rewrite the evolution of the plant myb gene family. Plant Physiol 121:21–24.

Hofgen R. and Willmitzer L., 1988. Storage of competent cells for Agrobacterium transformation. Nucleic Acids Res. 16: 9877.

Jin H. and Martin C., 1999. Multifunctionality and diversity within the plant MYB-gene family. Plant Mol Biol 41:577–585.

Jin H., Cominelli E., Bailey P., Parr A., Mehrtens F., Jones J., Tonelli C., Weisshaar B., Martin C., 2000. Transcriptional repression by AtMYB4 controls production of UV-protecting sunscreens in Arabidopsis. EMBO J 19:6150–6161.

Karimi, M., Inze, D., Depicker, A., Gateway vectors for Agrobacterium-mediated plant transformation. Trends Plant Sci. 2002 May;7(5): 193-195.

Klempnauer K.H., Gonda T.J., Bishop J.M., 1982. Nucleotide sequence of the retroviral leukemia gene v-myb and its cellular progenitor c-myb: the architecture of a transduced oncogene. Cell 31.453–463.

Koes R., Verweij W., Quattrocchio F., 2005. Flavonoids, a colorful model for the regulation and evolution of biochemical pathways. Trends in Plant Science10:236–242.

König P., Giraldo R., Chapman L., Rhodes D., 1996. The crystal structure of the DNA-binding domain of yeast RAP1 in complex with telomeric DNA. Cell 85:125–136.

Kranz H.D., Denekamp M., Greco R., Jin H., Leyva A., Meissner R.C., Petroni K., Urzainqui A., Bevan M., Martin C. et al., 1998. Towards functional characterisation of the members of the R2R3-MYB gene family from Arabidopsis thaliana. Plant J 16:263–276.

Lipsick J.S., 1996. One billion years of Myb. Oncogene 13:223–235.

Mathews H., Clendennen S.K., Caldwell C.G. et al., 2003. Activation tagging in tomato identifies a transcriptional regulator of anthocyanin biosynthesis, modification, and transport. Plant Cell, 15, 1689–1703.

Nesi N., Jond C., Debeaujon I., Caboche M., Lepiniec L., 2001. The Arabidopsis TT2 gene encodes an R2R3 MYB domain protein that acts as a key determinant for proanthocyanidin accumulation in developing seed, Plant Cell 13:2099–2114.

Ogata K., Hojo H., Aimoto S., Nakai T., Nakamura H., Sarai A., Ishii S., Nishimura Y., 1992. Solution structure of a DNA-binding unit of Myb: a helix-turn-helix-related motif with conserved tryptophans forming a hydrophobic core. Proc Natl Acad Sci USA 89:6428–6432.

Pabo C.O. and Sauer R.T., 1992. Transcription factors: structural families and principles of DNA recognition. Annu Rev Biochem. 61:1053–1095.

Paz-Ares J., Wienand U., Peterson P.A., Saedler H.,1986. Molecular cloning of the c1 locus of Zea mays: a locus regulating the anthocyanin pathway. EMBO J 5:829–834.

Quattrocchio F., Verweij W., Kroon A., Spelt C., Mol J., Koes R., 2006. PH4 of Petunia is an R2R3 MYB protein that activates vacuolar acidification through interactions with basic-helix-loop-helix transcription factors of the anthocyanin pathway. The Plant Cell 18:1274–1291.

Quattrocchio F., Wing J., van der Woude K., Souer E., de Vetten N., Mol J., Koes R., 1999. Molecular analysis of the anthocyanin2 gene of petunia and its role in the evolution of flower color. Plant Cel.l 11:1433–1444.

Rabinowicz P., Braun E., Wolfe A., Bowen B., Grotewold E., 1999. Maize R2R3 Myb genes: sequence analysis reveals amplification in the higher plants. Genetics 153:427–444.

Ramsay N.A., Glover B.J., 2005. MYB-bHLH-WD40 protein complex and the evolution of cellular diversity. Trends in Plant Science 10:1360–1385.

Riechmann J.L., Heard J., Martin G., Reuber L., Jiang C.Z., Keddie J., Adam L., Pineda O., Ratcliffe O.J., Samaha R.R. et al., 2000. Arabidopsis transcription factors: genome-wide comparative analysis among eukaryotes. Science 290**:**2105–2110.

Romero I., Fuertes A., Benito M.J., Malpical J.M., Leyva A., Paz-Ares J., 1998. More than 80 R2R3-MYB regulatory genes in the genome of Arabidopsis thaliana. Plant J 14:273–284.

Schiefelbein J., 2003. Cell-fate specification in the epidermis, a common patterning mechanism in the root and shoot. Current Opinion in Plant Biology 6:74–78.

Serna L., Martin C.,2006. Trichomes. Different regulatory networks lead to convergent structures. Trends in Plant Science 11:274–280.

Weston K., 1998. Myb proteins in life, death and differentiation. Curr Opin Genet Dev 8:76–81.

Yu E.Y., Kim S.E., Kim J.H., Ko J.H., Cho M.H., Chung I.K., 2000.Sequence-specific DNA recognition by the Myb-like domain of plant telomeric protein RTBP1. J Biol Chem 275:24208–24214.

Papers published on International peer reviewed journals

Other papers and meeting communications

Other papers and meeting participation

Carletti,G., Mazza R., Pasini L., Marocco A. Identification of a novel chilling-induced mutant in Arabidopsis. XV FESPB Congress, Lyon 2006

Pasini L., Carletti G., Marocco A. 2008. Mapping, positional cloning and profiling of mutants affecting endosperm development. Maize Genetics Cooperation Newsletter 82:25-26.

Carletti G. MaroccoA., 2008, La medica si rinnova grazie ai tannini. L'Informatore Agrario, 3.

Carletti G., Debeaujon I., Routaboul JM., Marocco A., 2008. Characterization of barrel medic mutants affected in flavonoid biosynthesis. XVI FESPB Congress, Tampere, Finland.

Carletti G., Debeaujon I., Routaboul JM., Marocco A., 2008. Characterization of Medicago truncatula mutants affected in flavonoid biosynthesis. XLVII SIFV Congress, Pisa, Italy.

Oral Communications

Carletti G., Debeaujon I., Routaboul JM., Marocco A. 2008. Characterization of Medicago truncatula mutants affected in flavonoid biosynthesis.. 52° Annual Congress SIGA, Padova, Italy.